ROLE OF GRM1 IN EXOSOME PRODUCTION AND MELANOMA METASTASIS

By

ALLISON L. ISOLA

A Dissertation submitted to the

School of Graduate Studies

Rutgers, The State University of New Jersey

In partial fulfillment of the requirements

For the degree of

Doctor of Philosophy

Graduate Program in Toxicology

Written under the direction of

Dr. Suzie Chen

And approved by

_____

_____

_____

_____

_____

New Brunswick, New Jersey

October 2017

ABSTRACT OF THE DISSERTATION

Role of GRM1 in Exosome Production and Melanoma Metastasis

By Allison L. Isola

Dissertation Director:

Suzie Chen

Exosomes are naturally occurring membrane-bound nanovesicles generated constitutively and released by various cell types, and often in higher quantities by tumor cells. Exosomes have been postulated to facilitate communication between the primary tumor and its local microenvironment, supporting cell invasion and other early events in metastasis. A neuronal receptor, metabotropic glutamate receptor 1 (GRM1), when ectopically expressed in melanocytes, induces *in vitro* melanocytic transformation and spontaneous malignant melanoma development *in vivo* in a transgenic mouse model. Earlier studies showed that genetic modulation in GRM1 expression by siRNA or disruption of GRM1-mediated glutamate signaling by pharmacological inhibitors interfering with downstream effectors resulting in a decrease in both cell proliferation *in vitro* and tumor progression *in vivo*, suggesting that active GRM1 may participate in melanomagenesis in our system. The overall goal of this dissertation is to determine whether the presence and activation of GRM1 plays a role in exosome formation, and subsequent tumor development and progression. To test this, the first aim utilized *in vitro* cultured cells in which GRM1 expression

and function were modulated by pharmacological and genetic means and consequences on exosome production by such manipulations were evaluated *in vitro*. We also assessed if exosomes derived from GRM1 expressing melanoma cells promote cell growth, migration, invasion as well as colony formation under anchorage-independent growth condition of GRM1 negative cells. Results showed that GRM1 expression in cells, per se, did not modulate exosome quantity, however, modified the qualities and functions of these exosomes. In Aim 2 we used riluzole, a glutamate signaling blockade, in a melanoma prone mouse model (TGS) for the *in vivo* assessment of exosomal quantity and quality. Daily treatment of TGS mice with riluzole had no detectable effect on the quantity of exosomes in circulation, however riluzole treatment influenced the effects of the circulating exosomes on metastatic behavior of recipient cells.

Acknowledgements

I would like to express my tremendous gratitude to my mentor, Dr. Suzie Chen, who has guided me through my dissertation, and has helped to mold me into a creative scientist and an independent thinker. Her support, guidance and intelligence have been essential to my success as a scientist. Thank you for believing in me.

I would like to thank Dr. Lori White for her mentorship and support throughout my entire scientific career as an undergraduate, technician and graduate student. She has been an essential part of my success.

I would also like to thank my committee members, and Philip Furmanski, James Goydos and Helmut Zarbl who have given me great advice and insight, contributing to my understanding of cancer biology, and helping my advancement through my studies.

Additionally, I want to express my gratitude to Kevinn Eddy, who has been a tremendous help to this project. I hope that I have contributed to your growth as a scientist as much as you have mine.

Dedication

This thesis is dedicated to the memory of my grandmother, Catherine Wedel; her strength and passion I could only dream to have. And to my parents, whose love and support has made this dream possible.

Table of Contents

List of Tables

List of Figures

Introduction

*Sections of this introduction were adapted from two review articles by the author:

Isola AL, Chen S. Exosomes: The Link between GPCR Activation and Metastatic Potential? Front Genet. 2016 Apr 8;7:56.
and
Isola AL, Eddy K, Chen S. Biology, Therapy and Implications of Tumor Exosomes in the Progression of Melanoma. Cancers. 2016 Dec 9;8(12).

Melanoma

Cancer is defined as the uncontrolled growth of cells; these cells are physiologically and often genetically different from their normal counterparts. Cancer arises from many cell types, one of the more prevalent being skin cancer. Melanoma patients only account for about 5% amongst all of the skin cancer cases, but it is responsible for the majority of deaths of skin cancer patients. One in 34 men and 1 in 53 women will develop invasive melanoma in their lifetimes with a 7% 5-year relative death rate, and patients with advanced melanoma survive an average of 2 to 8 months (*1*). In the United States, it is estimated by the American Cancer Society that approximately 87,110 new cases of invasive melanoma will be diagnosed, and about 9,730 deaths will be attributed to melanoma in 2017 (*2*). If detected early, primary melanoma tumors are surgically removed, resulting in a five-year survival rate of 92% and a ten-year survival rate of 89% (*3*). In late stage melanoma cases that have metastasized, the one-year survival rate drops to 35-62% (*4*), with the most common sites of metastasis being the lungs and the brain (*5*).

Melanocytes

Melanoma cells are derived from melanocytes, the pigment-forming cells of the skin, hair follicles, uvea, inner ear, nervous system and heart (*6*). Melanocytes originate from neural crest cells and are unique in their ability to produce melanin through a specialized membrane bound organelle known as a melanosome (*6, 7*). Phenotypically, melanocytes are oval shaped, have dendritic arms and are approximately 7 μm in diameter (*6*). Dendritic arms found on melanocytes allow for cell-cell interaction with keratinocytes, enabling the transfer of melanin-containing melanosomes from the melanocytes to the keratinocytes, which determines pigmentation of the skin and hair (*6, 7*). Melanin protects against harmful ultraviolet (UV) radiation in keratinocytes, stores ions, scavenges free radicals, and couples oxidation-reduction reactions (*6, 7*). Interestingly, melanin was demonstrated *in vitro* to have detrimental effects in normal human melanocytes, where it was shown to enhance single stranded DNA breaks, which may result from the formation of reactive oxygen species (ROS) during photo-oxidation of melanin in experimental settings (*7*). Results from these studies suggest that the complex functions of melanin may be cell type dependent.

Melanoma types

Melanoma can be divided into two categories: non-cutaneous and cutaneous. Cutaneous melanoma is the most common type of melanoma, accounting for up to 91.2% of all melanoma cases, thought to be caused by genetic predisposition or

unrepaired DNA damage due to environmental factors including UV radiation exposure. Non-cutaneous melanomas are rare (less than 10% of all melanomas) and arise from transformed melanocytes located near the eyes (5.2%) and the mucosal tissues (1.3%) such as the genital, anal, esophageal, nasal and oral cavities (*8, 9*).

There are 4 sub-types of cutaneous melanoma: acral melanoma, mucosal melanoma, chronic sun-induced damaged (CSID) and non-chronic sun-induced damage (NCSID) (*10*). Acral and mucosal melanomas have significantly more chromosomal aberrations, including increases or decreases in copy number of specific chromosomal regions when compared to other subtypes of cutaneous melanomas (*9, 10*). Acral melanoma is commonly found in individuals with darker skin such as Africans, Asians and Hispanics and is commonly associated with melanocytes of the palms, soles and mucosal surfaces (*8, 9*).

Genetic mutations associated with melanoma development

Numerous molecular pathways are frequently dysregulated in melanoma, the most common ones being the MAPK and PI3K/AKT pathways. When these pathways are activated by upstream signaling cascades, [such as growth factor receptors and G-protein coupled receptors (GPCRs)] activation leads to cell proliferation, differentiation and migration. Aberrant activation of this pathway by mutations in genes comprising the pathway, such as RAS and RAF, are frequently seen in melanoma. An example of this is a single-base missense transversion, causing the replacement of valine with glutamic acid at amino acid

residue 600 in BRAF that is detected in about 85% of nevi and melanoma (*11, 12*). BRAF is a serine/threonine kinase that is part of the MAPK signaling cascade found downstream of RAS; it activates MEK by phosphorylation, which in turn activates ERK also by phosphorylation. Mutated BRAF not only upregulates its own kinase activity, but also that of MEK and ERK, and promotes cell proliferation (*13*). In addition to mutated BRAF, mutated NRAS accounts for about 20% of melanoma cases (*14*).

The PI3K/AKT pathway also plays a critical role in melanoma pathogenesis as a consequence of mutations or loss in PTEN and dysregulation of expression of AKT, which positively regulates the G1/S phase progression in the cell cycle, suppresses apoptosis and promotes cellular survival. In a mutated BRAF mouse model, ablation of PTEN was absolutely required for melanoma development (*15*), supporting the notion that the PI3K/AKT signaling cascade is one of the key players in melanomagenesis. Mutations or deletions of PTEN are frequently concurrent with mutations in BRAF but not in N-RAS (*10*). Curtin and colleagues postulated that since N-RAS activates both PI3K and MAPK pathways, while BRAF only activates the latter, in melanoma pathogenesis, somatic mutations activating one pathway require another event to stimulate other pathways (*10*).

Mutations in cyclin-dependent kinase inhibitor 2A (CDKN2A) are widespread among human cancers including melanoma. CDKN2A encodes two proteins, p16INK4a and p14ARF. P16 binds to cyclin-dependent kinases 4 and 6 (CDK4 and CDK6) and inhibits phosphorylation of Rb, which remains associated

with the transcription factor, E2F. The Rb/E2F complex prevents the G1/S transition in the cell cycle due to lack of the transcription of E2F targeted genes necessary for cell cycle progression. P14ARF complexes with MDM2, an E3 ubiquitin ligase that regulates the stability of p53, and therefore suppressing tumor growth. P14ARF is also involved in the immune response, by modulating the tumor environment (*16*). Therefore, mutation(s) in p14ARF dysregulate p53 function and play a role in tumor immune evasion. CDK4 gene amplification, which is hypothesized to act as an independent oncogene, is more common in acral and mucosal melanoma than the CSID and NCSID cutaneous melanomas (*9, 10*). A mutation in the GTP binding region of the Gα subunit (Q209L) blocks the cleavage of GTP to GDP and deregulates both MAPK and PI3K/AKT pathways in uveal melanoma (*17*) (Figure 1). Transgenic mice harboring this mutated Gα subunit have increased skin lesions (*17*).

In addition to various mutations in key component of signaling cascades, miRNAs and lncRNAs are involved in melanoma pathogenesis (*18, 19*). Various miRNAs were implicated in the processes of carcinogenesis leading to melanoma, including miR-101, -182, -221, -222, -106-363, -106a, -92, -196, -21, -156, -214, -30b, -30d and -532-5p. Those downregulated or lost in melanoma include Let7a and b, miR-31, -125b, -148a, -211, -193b, -196a-1, -196a-2, and -203 (*20*).

Human melanoma cells were shown to have higher levels of the long non-coding RNA (lncRNA), SPRINGTLY, compared to normal human melanocytes (*18*). Zhao and co-workers showed that stable clones isolated from the expression

of exogenous SPRINGTLY into human melanocytes show increased cell proliferation, colony formation, invasion, reduction in apoptosis, and development of a multinucleated dendritic-like phenotype. When siRNA was used to knockdown SPRINGTLY, the cells showed a decrease in cell proliferation, invasion and increase in pro-apoptotic signals (*18*).

G-Protein Coupled Receptors

Our laboratory has been studying one of the upstream components involved in the stimulation of the MAPK signaling cascade, a GPCR. We demonstrated that the ectopic expression of metabotropic glutamate receptor 1 (GRM1) in melanocytes induces spontaneous melanoma development *in vivo* and transformation *in vitro* (*21, 22*).

Guanine nucleotide binding-protein coupled receptors (GPCRs) make up the largest family of proteins found within the mammalian genome (*23, 24*). The GPCR superfamily contains over 800 different seven trans-membrane receptors. Two requirements must be met in order to be classified as a GPCR; the first is that the receptor contains seven stretches of about 30 highly hydrophobic residues that represent trans-membrane locations, which provide the protein with both intracellular domains and an extracellular domain that has the ability to interact with its ligand. The second requirement that defines a GPCR is the interaction with guanine nucleotide binding proteins (G-proteins). GPCR classification within the superfamily is based on the ligand, physiological and structural features of the receptor, as well as phylogenetics. The most frequently

used classification system is A, B, C, D, E and F (*25, 26*) which represent GPCRs from all living beings from humans to bacteria. The majority of human GPCRs are separated into 5 different families; glutamate, rhodopsin, adhesion, frizzled/taste2 and secretin (GRAFS nomenclature) (*27, 28*).

The natural ligands for GPCRs vary from ions, proteins, lipids, hormones, neurotransmitters, amines, nucleotides, odorant molecules to photons. GPCRs are associated with heterotrimeric G-protein subunits consisting of G_{α}, G_{β} and G_{γ}, that function as dimers at the intracellular domain of the GPCR. Once the ligand binds to the receptor, it causes a conformational change, activating the receptor and initiating intracellular signaling cascades. The inactive form of the receptor is bound to guanine diphosphate (GDP), and this ligand-induced conformational change results in the exchange of GDP with guanine triphosphate (GTP) of the G-protein associated with the intracellular domain of the GPCR. This nucleotide exchange alters the affinity of the G-protein with the GPCR and results in the dissociation of the G-protein (*29, 30*). GPCRs can then interact with a multitude of different targets including ion channels, tyrosine kinases, adenylyl cyclases, phosphodiesterases, and others (*31, 32*). Disruption of GPCR functions are associated with many prevalent human diseases, including nephrogenic diabetes insipidus (*33*), cardiovascular disease (*34*), endocrine diseases (*31, 32, 35*) and others.

Glutamate is the predominant excitatory neurotransmitter in the central nervous system, and is the natural ligand for the glutamate receptor family. This

receptor family consists of two different types of receptors; ligand-gated ion channels (ionotropic) and G-protein coupled receptors (metabotropic)(*36-38*). It was previously believed that signaling involving glutamate was limited to the central nervous system, however, increasing evidence indicates this signaling mechanism present in peripheral tissues are required for numerous normal functions (*39*).

The GPCRs whose natural ligands are neurotransmitters, specifically glutamate, are classified under class C receptors (*40*), and are classified as metabotropic glutamate receptors (GRM), GABA receptors, calcium sensing receptors, taste receptors and some orphan receptors (*41*). The GRMs can be further divided into groups I through III, based on their sequence homology, pharmacologic responses, and intracellular second messengers. Group I consists of GRM1 and GRM5, group II contains GRM2 and GRM3, and group III contains GRM4, GRM6, GRM7 and GRM8 (*42*). Binding of the ligand, glutamate, to group I GRMs results in the exchange of GTP for GDP on $G_{\alpha.}$ Specifically, groups II and III GRMs are coupled to $G_{\alpha i/o}$. Group I GRM activation via the G-protein subunits $G_{\alpha q}/G_{\alpha 11}$ results in the stimulation of phospholipase C β (PLCβ) (*43*), which cleaves phosphatidylinositol 4,5-bisphosphate (PIP_2) into two second messengers: inositol triphosphate (IP_3). These signaling molecules are released into the cytoplasm, and Diacylgycerol (DAG) remains associated with the plasma membrane (*44*) while IP_3 diffuses into the cytosol and initiates the activation of protein kinase C (PKC), which is involved in phosphorylation of various proteins

affecting numerous cellular functions including MAPK (*44*). The hydrolysis to the second messenger, IP_3, results in the mobilization of calcium from the endoplasmic reticulum, increasing the cytosolic calcium concentration and subsequently activates calcium dependent kinases (*45*). The group II and III GRMs associated $G_{\alpha i/o}$, once activated, prevent the formation of cAMP by inhibiting adenylyl cyclase activity (*43, 44*).

Metabotropic Glutamate Receptor 1 (GRM1)

Metabotropic glutamate receptor 1 (GRM1), is a seven transmembrane-domain G-protein coupled receptor (GPCR) that is a member of the Group I GRM receptors. As with GPCRs in general, activation of Group 1 GRMs initiates signaling cascades which results in the downstream activation of PKC (*46, 47*), which then activates the MAPK signaling cascade that is involved in cell proliferation and inhibition of apoptosis (*48, 49*). PKC also activates PI3K/AKT pathway (*45, 50-52*), which is involved in tumor cell survival, epithelial-mesenchymal transition and angiogenesis (*53, 54*). These pathways are summarized in Figure 1.

Aberrant expression of GPCRs and the availability of abundant ligand in the surrounding environment was shown to induce transformation of normal cells (*55*). The first report identifying a GPCR as an oncogene was in 1986 by Wigler and co-workers, who demonstrated the transforming activity of a rat protein, MAS (*56*). Unlike most oncogenes identified at that time, MAS did not have activating mutations. Subsequent studies showed that the ability of GPCRs

to possess oncogenic potential is a result of aberrant protein expression or the excessive local production of ligands by tumor cells themselves (autocrine) or stromal counterparts (paracrine) and increasing the available ligand and subsequent receptor activation (*56*). Mutations have subsequently been detected in GPCRs, including a gain of function mutation causing amino-acid changes in G-proteins where GTP is bound. These mutations can initiate signaling cascades independent of GPCR activation (*57*).

Our laboratory was the first to suggest the role of dysregulated glutamatergic signaling in melanoma pathogenesis, subsequently confirmed by other investigators (*58*). We discovered that a gain-of-function of the murine form of GRM1, when ectopically expressed in melanocytes, induces *in vitro* melanocytic transformation and spontaneous malignant melanoma development *in vivo* in transgenic mouse models, TG-3 and Tg(Grm1)EPv (*58-60*), with 100% penetrance (*21, 22*).

Subsequent investigation revealed that GRM1 expression was also detected in 80% of human melanoma cell lines, 50% of nevus lines and 65% of human melanoma biopsy samples at levels of protein and mRNA (*59*). These biopsies include superficial spreading, nodular, lentigo maligna, cacral lentiginous and metastatic melanomas and common blue spitz nevi. GRM1 expression was not seen in normal melanocytes (*61*).

Earlier studies showed the aberrant protein expression of GPCRs and the availability of abundant ligand in the surrounding environment are involved in

cell transformation (*55*). We assessed levels of extra-cellular glutamate in several melanoma cell lines and found elevated glutamate levels only in GRM1-expressing melanoma cells (*62*). Inclusion of GRM1 antagonists led to reduced melanoma cell growth *in vitro* and tumorigenicity *in vivo* (*60, 62*). Inclusion of a reagent such as riluzole, which inhibits the release of glutamate, the natural ligand of GRM1, also led to a decrease in melanoma cell growth *in vitro* and tumor progression *in vivo*. Similar observations were made in breast (*63*) and prostate cancer cells (*59, 62*) that were shown to express GRM1. Subsequent studies by others showed the ability of GPCR to promote oncogenesis via modifications at the receptor expression level (*64, 65*). We introduced exogenous GRM1 into human melanoma cell lines with either modest GRM1 expression or absence of detectable GRM1 expression. We showed that enhanced GRM1 expression levels led to upregulated angiogenesis and increased tumorigenesis *in vitro* and *in vivo* (*66*). Interestingly, the ectopic expression of GRM1-mediated melanomagenesis is independent of the genotype of BRAF or NRAS (*62*), two of the most commonly mutated genes in melanoma.

Unlike many mouse models of cancer, TG-3 displays metastasis to several distal organs as the disease progresses (*22*). Consequently, activation of ectopically expressed GRM1 initiates signaling cascades important for melanoma pathogenesis, which could include activation of the exosomal production pathway, paving the way for metastasis. In addition to GRM1, other GRMs have been implicated in numerous cancers. Table 1 summarizes various cancers

associated with GRM misregulation.

Melanoma Treatments

Chemotherapies

The treatment for patients with primary melanoma is surgical removal of the tumor(s). Treatment options for late stage melanoma patients include targeted drug therapies with or without radiation or immunotherapies. Many of the targeted therapies involve components of the MAPK/ERK pathway. A well-known target is the mutated BRAF protein against which small molecule inhibitors have been developed as chemotherapy (*43*). The well-known BRAF inhibitors, Vemurafenib / Zelboraf (PLX4720 / PLX4032), were shown to improve survival rates for many melanoma patients (*43, 67*), however many of these patients develop resistance to the inhibitor (*3, 43*), likely due to the reactivation of the MAPK pathway or other mutations (*3, 43, 67*).

There have been various inhibitors developed against other components of the MAPK pathway. *In vivo,* the MEK inhibitor, selumetinib, has shown to reduce melanoma xenograft tumor growth (*67, 68*). Inhibitors of ERK have been shown to successfully inhibit the MAPK pathway in MEK-inhibitor resistant cells, since ERK is downstream of MEK (*69*). Efforts to date have failed to develop clinically effective inhibitor of RAS (*70*), which has led to the development of other targets to inhibit the effector molecules of RAS. These include the RAF-ERK-MEK pathway such as farnesyltransferase, Rce1, lcmt1, and components of the PI3K-AKT-mTOR and RalGEF-Ral pathways (*70*).

Malignant melanoma cells were shown to have higher levels of NOTCH signaling when compared to normal melanocytes, suggesting a role in melanoma pathogenesis (*71*). Under normal conditions, NOTCH signaling is required for the maintenance of the melanoblast and melanocyte stem cells; in mature melanocytes, NOTCH expression is low or undetectable (*71*). The gamma secretase inhibitor, GSI, was developed to target NOTCH signaling and successfully suppresses NOTCH activation. However in phase 2 trials, only a modest responsiveness to GSI was observed in metastatic melanoma patients (*71*).

Combinatorial Chemotherapies

Melanomas frequently adapt and become resistant against monotherapies. In order to increase the efficacy of therapeutic treatments and prevent emergence of resistant clones, combination therapies are commonly administered. In preclinical studies, BRAF inhibitor-resistant melanoma cells were treated with a combination of GSI and a BRAF inhibitor, cell growth was reduced and senescence increased. However, when GSI was removed, cell growth reinitiated (*71*). These pre-clinical findings suggest that a combination therapy which inhibits both MAPK and NOTCH pathways may be efficacious in melanoma patients who develop BRAF inhibitor-resistance but both inhibitors must be present to sustain the anti-tumor progression responses.

Immunotherapies

One of the important recent advances in cancer treatment has been the advent of the immune checkpoint inhibitors. These immunomodulating antibodies have been particularly effective in treatment of advanced melanoma, with some particularly striking responses. For stage IV melanoma patients, heretofore without effective treatment, they can undergo immunotherapy in conjunction with targeted drug chemotherapy, and in some cases radiotherapy has proven useful and is now a standard of care (*3*).

Immunotherapies utilize the host's immune system to elicit a tumor-specific immune response to combat cancer malignancies. One focus for immunotherapies has been on dendritic cell (DC)-based cancer vaccinations. DCs are of great interest in cancer because of their ability to uptake, process, and present antigens, which stimulates development of an immune response. Dendritic derived-exosomes (DEXO), which are nanovesicles released from DCs, have shown promise for stimulating anticancer immunity, as they contain the machinery required to activate potent antigen-specific immune response (*72*). Damo et al., incubated DEXOs from DCs with both a ligand for TLR-3, to stimulate the cytotoxic natural killer cells as well as the CD8+ cytotoxic T cells, and melanoma antigens from necrotic mouse melanoma B16F10 cells. The DEXOs were then injected into mice bearing B16F10 tumors, and resulted in a significant reduction in growth of the tumors (*72*).

More recently, the focus of immunotherapy has been on targeting immune checkpoints that function as regulators of T-cell activation through receptor/ligand complexes (*73*). Clinical trials have demonstrated that blockade of cytotoxic T lymphocyte antigen-4 (CTLA-4) with the human monoclonal ipilimumab led to an increase in survival rates, a reduction of 34% of death in a subset of advanced stage melanoma patients (*73*). Another checkpoint target is the receptor/ligand, program death-1 (PD-1) and program death ligand-1 (PD-L1). Targeting this checkpoint pair was shown to have anti-tumor activity in melanoma patients (*73*). PD-1 receptors interact with its ligands, PD-L1 and PD-L2 in peripheral tissues, which induces a reduction in proliferation of $CD8^+$ cytotoxic T cells (*73-75*). In metastatic melanoma, PD-L1 is upregulated along with tumor-invading lymphocytes and IFN-γ production, suggesting a process by which melanoma tumors evade immune system attack (*73, 74*). A phase I trial with the monoclonal anti-PD-1 antibody, nivolaumab, showed that 28% of the patients with advanced melanoma had a partial or complete response to treatment and out of those, 72% who received nivolaumab for more than a year had lasting responsive to treatment for a year or more (*73, 76*).

An interesting new approach uses immunotherapies in conjunction with natural compounds. Curcumin, a plant based chemical present in high amounts in the spice turmeric, has been shown to have anti-cancer effects including anti-angiogenic and pro-apoptotic activity and the ability to modify the immune system (*77*). Because the bioavailability in the body of curcumin is low, several

groups are developing novel delivery systems such as nanoparticles, liposomes, micelles and phospholipid complex to increase its bioavailability (*77*). Curcumin has been shown to mediate its anti-cancer effects by modulating the MST1, JNK, BIM-1, FOXO3, BCL-2, JAK-2/STAT-2, and BAX pathways in *in vitro* models (*77*). In melanoma cells, curcumin was shown to induce apoptosis in a dose and time dependent manner (*78*). In an advanced melanoma murine model, it was shown that treatment with amphiphilic curcumin–based micelles led to remodeled tumor microenvironment and enhanced vaccine efficacy. A combination therapy using amphiphilic curcumin with vaccine therapy resulted in a downregulation of immunosuppressive factors as well as an increase in the efficacy of the vaccine treatment, including a 7-fold increase in INF-y and cytotoxic T-cell responses (*79*).

Riluzole

Riluzole, 2-amino-6-(trifluoromethoxy) benzothiazole ($C_8H_5F_3N_2OS$), an FDA-approved drug for the treatment of Amyotrophic Lateral Sclerosis (ALS), acts as a glutamate release inhibitor. In ALS, the major excitatory neurotransmitter accumulates in the synaptic cleft, becoming neurotoxic and causing degeneration of motor neurons. This degeneration manifests as weakness, muscle atrophy and fasciculation. Riluzole functions to reduce the release of glutamate by the presynapse, causing a lower concentration of glutamate and slowing the progression of the disease (*80*). Riluzole acts as an

anti-glutamatergic drug, which reduces the release of glutamate, and increases the uptake of glutamate by specific transporters (*81-83*).

One of the mechanisms of action of riluzole is as a sodium channel blocker. Glutamate release is stimulated by the increased influx of sodium and calcium into presynaptic neurons. Riluzole blocks sodium channels, which prevents the excessive influx of these ions and inhibits extracellular release of glutamate from presynaptic neurons. In the postsynaptic neuron, sodium and calcium influx through N-methyl-D-aspartic acid receptor (NMDAR) and Alpha-amino-3-hydroxy-5-methyl-4-isoxazole propionic acid receptor (AMPAR) lead to cellular death and axonal edema. In addition to functioning as a sodium channel blocker, riluzole also acts as a neuroprotective anti-glutamatergic agent by its ability to inhibit glutamate release by blocking the isoxazolepropionic acid receptors: N-methyl-D-aspartic acid receptor (NMDAR), and alpha-amino-3-hydroxy-5-methyl-4-isoxazole propionic acid receptor (AMPAR) (*84*). At concentrations of 10-30uM, riluzole reduces the K^+-induced glutamate release from hippocampal sections, and at higher concentrations, GABA release was also reduced (*85*).

Riluzole Pharmacokinetics

Riluzole is rapidly absorbed in the gastrointestinal tract, reaching the maximum serum concentration (C_{max}) in about 1 hour of administration. A dose of 50mg twice daily reached C_{max} at 0.75-0.9 hours, and then rapidly declined (*86, 87*). At this dosage the elimination half-life of riluzole was 14.7 hours (*87*).

Riluzole undergoes first-pass metabolism in the liver by the cytochrome P450 enzyme CYP1A2 (*88*) and is highly bound (96%) to albumin and lipoproteins in the serum (*84*).

Riluzole and Melanoma

In order to interrogate the underlying mechanisms of ectopic expression and activation of GRM1 in melanocytes, and subsequent cell transformation and tumor formation, we used riluzole as a functional inhibitor of GRM1 activation through the reduction of available ligand and thus interfering with intracellular signaling cascades. *In vitro*, the amount of glutamate present in the medium was reduced when melanoma cells were treated with riluzole. Additionally, *in vitro*, cells treated by riluzole underwent cell cycle arrest followed by apoptosis. Using a xenograft model with human melanoma cells, tumor sizes were reduced by daily treatment of the drug. In the clinical setting, a phase 0 trial (lasting 14 days) with stages III or IV melanoma patients (all with GRM1-positive melanoma) showed a response rate of 34% of the patients plus a reduction of signaling in both the MAPK and PI3K/AKT pathways, which correlated with preclinical data (*54, 62*). Several patients saw complete resolution of several tumors, and only 2 out of 11 patients in the trial had progression of the disease (*89*).

Metastasis

Dissemination of primary tumor cells to distant vital tissues, metastasis, is the major life threatening complication, and the major cause of death in most types of cancers, including melanoma (*90*). Metastasis occurs in a stepwise

fashion relying on a number of host-tumor interactions (*91, 92*). In order for a metastatic tumor to form, a cell from the primary tumor must have the ability to survive on its own, dissociate from the tumor, occupy the surrounding tissue (*93*), enter circulation, survive the environment of the circulatory system, invade the distant parenchyma and proliferate on its own (*93*).

Hanahan and Weinberg were the first to review the six biological hallmarks of cancer and they recently added four additional new hallmarks as necessary traits during the development and progression of cancer (*94*). These hallmarks are: unregulated cell growth, anti-apoptosis signals, induction of angiogenesis, unresponsive to growth suppressors, metastatic capabilities, replicative immortality, genomic instability, immune system evasion, tumor-specific inflammatory response and transformation of cellular metabolism.

Circulating tumor cells (CTCs) can be found in the vasculature of various organs, but only in some organs will a secondary tumor survive and develop into sites of metastasis (*95*). Different primary tumors preferentially home to particular organs. For example, melanoma preferentially metastasizes to the lung and brain (*96*), suggesting that metastatic growth is dependent on a microenvironment that is receptive of that particular cancer cell type (*96*). Aberrant expression of GPCR proteins has been suggested to play a role in the organ-specific metastasis of cancer cells by enhancing mobilization, promoting angiogenesis and proliferation (*32*). To develop therapies focused on treating metastatic diseases, understanding the molecular mechanisms of metastasis is

vital. Although the disseminated primary tumor cells are essential to metastasis, the cells from the surrounding tumor microenvironment are equally critical in prompting metastatic ability.

Gene expression signatures have been determined that relate to the metastatic ability of tumors (*97*). Interestingly, these signatures have also been able to predict the organ sites of metastases will grow (*98*, *99*). Although the cells from the primary tumor are what make metastasis a threat, the cells from the surrounding tumor microenvironment play important roles in prompting metastatic ability. Successful metastatic growth is dependent on a microenvironment that is receptive of that particular cancer cell (*96*). Normal cell types such as fibroblasts, endothelial cells and bone marrow derived cells (*100*) all are recruited to, and involved in, the formation of the future site of secondary tumor formation, or the pre-metastatic niche (*101, 102*), to which the tumor cells metastasize. In addition to these different cell types, circulating tumor vesicles, exosomes, have the ability to hone towards and accumulate at common sites of metastasis (*103*).

Formation of the pre-metastatic niche

The formation of the pre-metastatic niche is an essential step in successful metastatic growth. The primary tumor initiates this formation by releasing factors into circulation that initiate changes within the niche.

One of the initial changes that occur is that the resident fibroblasts and cells from the primary tumor stimulate fibronectin deposition (*100, 104*). The

deposition of fibronectin within the organs determines the location of the metastatic niche formation (*100*). Fibronectin deposited within the tissue causes the attachment of bone marrow derived cells (BMDC), specifically macrophages and neutrophils, within the deposits (*104*).

In addition to fibronectin, fibroblasts express Tenascin-C (TN-C) glycoprotein within the premetastatic site, which may protect the cancer cells from apoptosis by cooperative interaction with TGF- β receptor II (*105*). Several cytokines, as well as Wnt and Ras/MAPK signaling, may induce TN-C glycoprotein expression. TN-C is not found in normal tissues. However, under pathological conditions, such as inflammation and cancer, its expression is strikingly increased, resulting in induction of and induces the production of angiogenic protein factors such as MMP-9. TN-C also has been implicated in other steps in cancer progression including proliferation, migration, invasion and angiogenesis Tse and Kalluri (*106*).

Periostin, a secretory protein also deposited within the extracellular matrix (ECM) by fibroblasts, acts as a bridge that binds to TN-C as well as fibronectin and collagen (*107, 108*). Studies showed that periostin does not have a direct effect on tumor cell growth. However, knocking out periostin leads to a significant reduction in the metastatic potential (*108*). Versican is an extracellular matrix (ECM) proteoglycan that is expressed by myeloid cells present in the pre-metastatic niche. It promotes mesenchymal to epithelial transition by decreasing phospho-Smad2 levels, which increases proliferation and metastasis. However,

versican does not play a role in the recruitment of immune cells or the manipulation of the immune environment (*109*).

In addition, remodeling the extracellular matrix to create greater permeability within the surrounding vasculature is necessary to form a pre-metastatic niche that is receptive of CTCs. Vascular remodeling occurs to allow for the extravasation of CTCs out of circulation, into the pre-metastatic environment. This process is dependent on angiopoietin 2 (Angpt2), matrix metalloproteinase 3 (MMP-3) and MMP-10. Huang et al., showed that knocking down these proteins reduces the vascular permeability and decreases the infiltration of myeloid cells and inhibits spontaneous lung metastasis in an in-vivo model (*110*).

Recruitment of Immune Cells

Within the metastatic niche, immune cells, including bone marrow progenitor cells are recruited to and play an important role in the formation. BMDCs express vascular endothelial growth receptor 1 (VEGFR1), which may be responsible for the homing of tumor cells to the pre-metastatic niche. Erler et al., showed accumulation of VEGFR1^{+} BMDCs in common sites of metastasis in the lung, within 9 days post-accumulation, micrometastases formed and BMDCs remained within the site (*104*). As indicated above, fibronectin deposition within the pre-metastatic environment will result in the arrest of bone marrow derived cells. When the BMDCs arrive, they form clusters of cells in the tissue parenchyma at putative sites of metastasis before evidence of tumor cells (*111*).

VEGFR1$^+$ hematopoietic cells (HPCs) express VLA-4, which allows them to adhere to the newly synthesized fibronectin to initiate the cellular clustering (*111*). Interaction of VLA-4 with fibronectin is responsible for the ability of HPCs to move within the bone marrow (*112*). After fibronectin binding to HPCs, MMP protein expression is enhanced with the presence of integrin signaling (*113, 114*). MMP-9 functions to breakdown basement membranes and the release of Kit-ligand and VEGF-A, presumably to support bone marrow migrating cells that express c-Kit (*115, 116*).

Myeloid cell recruitment is influenced by the expression of several inflammatory chemoattractant proteins, which are influenced by the primary tumor. These chemoattractants recruit Mac1$^+$ (macrophage antigen 1) myeloid cells to the lung. Furthermore, Hiratsuka et al., found these chemoattractants were involved in the ability of the tumor cells to migrate, using pseudopodia for invasion. When the expression of these inflammatory chemoattractant proteins was abolished, migration of both tumor cells and Mac1$^+$ myeloid cells was prevented (*117*).

Exosomes

Exosomes are small membrane-bound nanovesicles with the characteristic size of 30-120nm in diameter that are derived from endosomal origins. These vesicles are generated constitutively and released by various cell types, more frequently by tumor cells (*118, 119*). Exosomes can be found in the blood (*120*), urine (*121*), saliva (*122*) plasma (*123*), breast milk (*124*) as well as other bodily fluids (*125-*

128). They are actively secreted from cells by an exocytosis pathway used for receptor removal and crosstalk between cells (*118, 129, 130*). Exosomes are released from healthy cells, and take with them membrane proteins and cytoplasmic contents of the cells from which they are released, including miRNAs, mRNAs, siRNAs, and proteins (*118*). Studies of exosomes from various cell types show several common proteins common to all exosomes (*131-135*). Under normal cellular conditions, the release of exosomes accompanies normal cell growth and activation of cellular functions, such as stimulation of T cell growth *in vitro* and induction of anti-tumor immune responses depending on specific cell types (*136-138*). These vesicles contain various DNAs (*139*), miRNA (*140, 141*), mRNA (*142, 143*), and protein (*144*) and have the ability to enter circulation and act as messengers between cells (*118*).

Composition of Exosomes

Exosomes also contain a unique composition of proteins and nucleic acids that vary depending on the cell type of origin, and the content generally reflects the function of those cells. Studies of exosomes from immature dendritic cells (DCs) (*131, 132*), B lymphocytes (*133, 134*), intestinal epithelial cells (*135*) and other cell types show that there are common, as well as cell-type specific proteins residing within exosomes. Cell-type specific proteins within exosomes include Major Histocompatibility Complex (MHC) class I and II proteins, which have been detected in B lymphocyte, DCs, mast cells and intestinal epithelial cell exosomes. Von Willebrand factor (*145*), perforin and granzymes (*146*) were

found in platelet and cytotoxic T cell exosomes, respectively. The proteins that were found consistently across all exosome types include chaperones (Hsc73 and Hsc90), subunits of trimeric G proteins, Tsg101, cytoskeletal proteins and tetraspanins such as CD9, CD63, CD81 and CD82 (*131, 132, 135*). Kahlert et al., identified double stranded genomic DNA present within exosomes (*147*).

Formation of Exosomes

The process involved in the formation of exosomes was first reported in 1983 by Harding et al., (*148*), and confirmed in 1985 by Pan et al., (*149*) Using immunoelectron microscopy, they visualized the transfer of a transferrin receptor in reticulocytes from the cell surface to an early endosome, to a multivesicular endosomes, localized at the surface of the internal vesicles, then finally, fusion of these multivesicular compartments with the plasma membrane. The smaller vesicles bearing transferrin receptors were then released into the extracellular environment as characteristic exosomes (*148, 149*).

One of the defining characteristics of exosomes is their endocytic origin, which sets them apart from other cellular vesicles such as apoptotic bodies that are budded off of the plasma membrane. The initial step in the formation of exosomes is endocytosis. Invagination of the plasma membrane is initiated by the deformation of the lipid bilayer, which can be influenced extrinsically or by internal membrane structural modification. Specific membrane manipulating proteins interact with and bend the membrane surface to initiate tubulation. Membranes that are tubulated experience an external force, which causes the

inward curvature, or invagination of the membrane (*150*). The proteins involved in this process include endocytosis proteins such as epsin (*151*), N-BAR proteins, such as amphiphysin (*152, 153*) and endophilin, (*154*) or F-BAR proteins, such as syndapins (*155*) and its associated protein, dynamin. Dynamin is a GTPase that connects with both actin and F-BAR to successfully form and cut membrane tubules to create a successful invagination of the membrane (*150*). Once the invaginated membrane forms and becomes severed from the plasma membrane, it is released into the cytosol of the cell as an endosome.

The Endosomal Sorting Complex Required for Transport (ESCRT) functions on the newly formed endosome to initiate the internal budding of the multivesicular body (MVB) membrane to form smaller intraluminal vesicles within the MVB. These vesicles are exosomes. Ceramide, a sphingolipid, was found to trigger budding of exosome vesicles into the multivesicular body (*156*). ESCRT is made up of four different complexes (ESCRT-0, -I, -II and -III) and associated accessory proteins. The primary function of the ESCRT proteins is to constrict the membrane, create budding within the endosome and cause severing of the budded vesicle neck to separate the vesicle from the MVB membrane. The precise mechanism of the severing is unknown (*157-160*). The proteins in the ESCRT pathway are divided into four different complexes: ESCRT-0, -I, -II and –III. ESCRT-0 is involved in collecting ubiquitinated proteins on the membrane of the endosome. ESCRT-I and –II initiate the inward budding of the endosomal membrane and ESCRT-III severs the budding membrane from the endosome,

creating a separate smaller vesicle within the endosome: an exosome (*161*). ESCRTIII is recruited for scission by ALIX, an adaptor protein. Syndecans are proteins involved in sulfate-presentation on the membrane surface, and are found on exosomes. These proteins are sorted into exosomes by an adapter protein, syntenin, which binds to ALIX, recruiting ESCRTIII to finalize the formation of the exosome (*161, 162*).

The specificity of cargo sorting into these exosome vesicles is still unclear. However, it has been shown that ubiquitination serves as a signal for sorting cargo into the vesicles formed within the MVB. Additionally, evidence has shown that ESCRT-I recognizes ubiquitinated cargo, suggesting that this protein and its associated protein, Vps23, initiate MVB sorting, or packaging, by binding cargo and directing it to MVB for loading in a ubiquitin-binding manner (*163*).

Exosome release

Once the MVB is formed and contains exosomes within its membrane, it has one of two fates; targeted degradation by the lysosome or plasma membrane fusion resulting in exosome release.

If the MVB is targeted for lysosomal degradation, it fuses with the lysosome and results in the release of the internal exosomes and the macromolecules contained within them, into the lumen of the lysosome. These components are then exposed to the hydrolytic enzymes within the lumen of the lysosome and are degraded (*164*).

Alternatively, the MVB will travel to the plasma membrane. In this case, a GTPase, RAL-1, has recently been identified to mediate the fusion of the MVB membrane with the plasma membrane of the cell to allow the release of the exosomes into the extracellular space. Syx-5 is a t-SNARE that is recruited by RAL-1 to the plasma membrane to stimulate MVB fusion. Hyenne et al., showed that without Syx-5, the MVB is unable to fuse with the plasma membrane (*165*). Ostrowski et al., identified Rab27a, Rab27b, and their effectors (SYTL4 and Slac2b, respectively) to be involved in the exosomal pathway in HeLa cells (*166*). Specifically, Rab27a was shown to be involved in the size of the MVB, while Rab27b regulated localization of the MVB to the plasma membrane. Another Rab-GTPase, Rab35, was identified as a regulator in the docking or tethering of the MVB to the plasma membrane (*167*). In addition to enzymatic involvement of exosome regulation, intracellular levels of Ca^{2+} have been shown to be proportional to exosome release (*168*). In addition, low pH within the microenvironment influences the release of exosomes as well as the uptake (*169*).

Oncogenes have been shown to play a role in exosome secretion, including a p53-regulated pathway, TSAP6, both *in vitro* (*170*) and *in vivo* using a TSAP/Steap3-null mouse (*171*). As tumors become more aggressive, the expression and activation of the enzyme heparanase becomes upregulated. The activation of heparanase increases the release of exosomes, as well as the cargo levels found within the exosomes (*172*).

Exosome uptake

Once the exosomes are released from the plasma membrane, they have the ability to travel to distant sites of the body, and/or interact with the cells in the surrounding microenvironment. Exosomes involved in intracellular communication contain phosphatidylserine on their outer membrane, which interacts with T-cell immunoglobulin and mucin-domain-containing molecule 1 (Tim1), a transmembrane protein present on recipient cells (*118*). This interaction initiates engulfment of the exosomes by the recipient cell (*173*). In ovarian cancer cells, exosome uptake was shown to occur by clathrin-dependent endocytosis. Both proteins and specific glycoproteins present on exosomes and the cell surface were shown to be important for exosome uptake (*174*). The transfer of Major Histocompatibility Complex (MHC)-peptide complexes between dendritic cells was shown to be dependent on the presence of intercellular adhesion molecule 1 (ICAM-1) on exosomes. Exosomes from immature dendritic cells (DCs) were unable to transfer MHC to other DCs, however, exosomes from mature DCs contained ICAM-1 on the surface of the exosomes, and resulted in transfer of MHC from the exosomes (*175*). Additionally, heparin sulfate proteoglycans (HSPGs) have been shown to act as receptors of tumor derived exosomes (*176*). Parolini et al., were the first to demonstrate that endocytosis is not the sole route of exosome uptake. Under certain conditions, exosomes will undergo lipid-dependent membrane fusion with the recipient cell independent of energy-dependent exocytosis and protein-protein interaction (*169*).

Once the exosomes enter the recipient cell, the cargo has the potential to interact with and alter the physiology of the cell. Exosomes are also known to modulate gene expression: Valadi and colleagues demonstrated that RNAs in mast cell exosomes could be delivered to human and mouse mast cells leading to new protein production in recipient cells (*177*).

Interestingly, differentiation status seems to have an effect on how efficiently monocytes uptake exosomes; the more differentiated the monocyte, the greater the efficiency (*178*).

Exosomes and Cancer

Many articles have reviewed the characteristics and the formation of exosomes and their role in various diseases (*179*), including infection (*180*), neurodegenerative diseases (*181*), liver disease (*182*), heart failure (*183*) and cancer (*184*). Exosomes are more frequently released by tumor cells and may facilitate communication between the local microenvironment and the primary tumor (*142, 177, 185, 186*) to enhancing tumor cell dissemination and early events in metastasis (*187, 188*).

The hallmarks of cancer proposed by Hanahan and Weinberg include the capability acquired by cancer cells that allow them to proliferate and survive (*189*). Exosomes have been proposed as one of the critical components that contribute to these essential cancer hallmarks, namely; sustaining proliferative signaling, evading growth suppressors, resisting cell death, enabling replicative immortality, inducing angiogenesis, genome instability and mutations, tumor-

promoting inflammation and especially activating invasion and metastasis (*189*). This may occur because exosomes can mediate horizontal transfer of proteins, miRNAs and other molecules (*190-192*). For example, exosomes derived from gastrointestinal stromal tumor (GIST) cells are enriched with oncogenic protein tyrosine kinase, KIT. These exosomes can be taken up by normal human myometrial smooth muscle cells (SMCs). Uptake of KIT-enriched exosomes causes intercellular KIT pathway activation, which results in a more adhesive phenotype in these recipient cells, and the secretion of matrix metalloproteinase 1 (MMP1). The secretion of MMP1 by SMCs increases the invasiveness of GIST cells (*193*). Additionally, exosomes from hypoxic glioblastoma multiforme (GBM) cells contain hypoxia-regulated mRNAs and proteins, which are taken up by normoxic GBM cells and increase autocrine pro-migratory activation in the recipient cells. These exosomes also interact with surrounding endothelial cells and pericytes causing paracrine induction of angiogenesis and resulting in tumor growth (*194*). Melo et al., demonstrated that exosomes from cancer cell lines contain not only siRNAs, but also pre-siRNAs and the machinery required for the processing them into siRNAs, which are then introduced into the target cells and silence endogenous mRNAs and promote tumorigenesis (*195*).

Exosomes from cells within the surrounding environment also can be involved in tumor progression by transferring macromolecules to target cells. For example, exosomes derived from fibroblasts were shown to influence the invasiveness of breast cancer cells. Fibroblast-derived exosomes deliver Wnt11

protein, and cause the mobilization of the Wnt-planar cell polarity autocrine signaling, which results in increased invasive and metastatic characteristics of breast cancer cells (*196*). Furthermore, glial exosomes have been shown to transfer siRNA, and induce specific PTEN loss in breast cancer brain metastases resulting in enhanced tumor growth (*141*).

Recently, Peinedo et al., described the involvement of melanoma exosomes in tumor progression and the preparation of the pre-metastatic niche of future secondary tumor sites (*103*). The pre-metastatic niche is created even before the tumor cell arrives at the site; cells from the immune system and the resident stromal cells all participate in the formation of a supportive environment for secondary tumor growth. Earlier studies demonstrated the ability of melanoma exosomes to "educate" bone marrow progenitor cells to be receptive of and support tumor cell growth and metastasis (*103*). Once in circulation, exosomes have the capability to home towards the most common sites of metastasis and accumulate, which results in the leakiness of the vasculature, as well as recruitment of immune cells, two events involved in pre-metastatic niche formation (*103*).

Exosomes were shown to directly modulate function(s) of the immune system, which is critical in the progression of various cancers. Breast cancer cell exosomes contain prostaglandin E2 (PGE2) and transforming growth factor beta (TGFβ), which induces myeloid cells in the bone marrow to become myeloid-derived suppressor cells (MDSCs) that promote tumor progression. MDSCs

accumulate in the secondary lymphoid organs, blood and tumor tissues to provide supporting stroma and immune evasion (*197*). Exosomes from both squamous cell carcinoma of the head and neck and dendritic cells activated human T-lymphocytes and induced immunosuppression by interacting with the cell surface rather than internalization (*198*).

Unique Composition of Exosomes

The composition of exosomes often reflects the contents of the membrane and cytoplasm of the cells they are released from, suggesting that the contents of melanoma-derived exosomes are unique when compared to other tumor types, or the normal cell counterpart. A study exploring this utilized 2D-gel electrophoresis analysis of both melanoma-derived exosomes and lysates of their cells of origin; strikingly different proteomic profiles were observed. The exosomes contained drastically less or were devoid of lysosomal and mitochondrial proteins were present in the cell lysates. In contrast, several proteins that were enriched in the exosomes of SK-MEL-28 and MeWo melanoma cell lines, including p120 catenin, radixin, and immunoglobulin superfamily member 8 (PGRL) (*199*). Similarly, other groups identified other melanoma-specific exosome proteins, including prominin-1/CD133 (*200*), a transmembrane protein marker of both neural stem cells and hematopoietic progenitor cells, that is present in both melanoma cell lines and melanoma patient samples (*201*). Exposure of mesenchymal stem cells to exosomes from Prominin-1-positive melanoma cells led to more invasive characteristics in

mesenchymal stem cells. Multiple additional pro-metastatic proteins, including CD44, MAPK4K, GTP-binding proteins, ADAM10 and Annexin A2 were also detected in these melanoma-derived exosomes. In addition, these exosomes were found to be composed of lipid bilayers that contained a high concentration of sphingomyelin and high levels of tetraspanin proteins, which is hypothesized to be the determinant in the release of the exosomes (*201*).

Exosomes isolated from clinical samples from melanoma patients were found to contain higher concentrations of Melanoma Inhibitory Activity (MIA), a small protein secreted by malignant melanoma cells and S100B, a calcium binding protein involved in cell cycle progression and differentiation, when compared to healthy volunteers. Patients with an increased concentration of MIA in their circulating exosomes correlated with a shorter median survival time (*202*). Profiling of exosomes from liver perfusates of patients with metastatic uveal melanoma showed the protein melan-A and different miRNAs when compared to the primary tumor (*203*). Additional studies by others revealed a common miRNA, miR-146a, in the exosomes within the vitreous humor, as well as those circulating through the body, in uveal melanoma patients (*204*). Another miRNA in exosomes, miR-126b, was down-regulated only in patients with advanced melanoma compared to healthy donors (*205*). In another study, Felicetti et al., demonstrated a correlation between the metastatic ability of melanoma cells and miR-222 levels within the exosomes. Furthermore, miR-222 was transferred from

the exosomes to the recipient cell and subsequent induction of PI3K/AKT signaling cascade (*206*).

In clinical settings, exosomes derived from the plasma of sporadic metastatic melanoma patients often displayed elevated levels of miR-17, -19a, -21, -126 and -149 compared to those with familial melanoma or healthy controls (*207*). Additionally, there was no differential expression of miRNAs seen in familial melanoma patients and healthy controls (*207*). These results indicated that in familial melanoma, genetic predisposition, instead of miRNAs, plays a critical component in the onset and progression of the disease, suggesting that exosomal miRNAs could be used as prognostic and diagnostic tools in patients with non-familial metastatic melanoma (*207*).

Promotion of aggressive behavior in cancer cells by exosomes

Along with the potential for using these vesicles to diagnose and treat cancers, tumor exosomes have been shown to play a role in the aggressiveness of cancer. These microvesicles are more frequently released by tumor cells and may facilitate communication within the local microenvironment and the primary tumor (*142, 177, 185, 186*). Patient-derived cancer-associated fibroblast exosomes were shown to alter the cellular metabolism of prostate and pancreatic tumor cells *in vitro,* redirecting from oxidative phosphorylation to a glycolysis and glutamine-dependent reductive carboxylation (*208*). The same study illustrates the impact exosomes released by cells within the tumor microenvironment have on the cellular function of the tumor cells. Communication between the tumor

microenvironment and the cancer cells supports tumor cell dissemination and early events in metastasis (*187, 188*). Exosomes may have the ability to promote metastasis via the horizontal transfer of proteins, miRNAs and other molecules to recipient cells (*103, 191, 209, 210*). Exosomes containing the RNA-binding protein LIN28 (which is a known marker of poor outcome for ovarian cancer) were shown to be taken up by recipient cells and to significantly increase transcription of genes involved in Epithelial-to-Mesenchymal Transition (EMT), cell migration and invasion in the recipient cells (*211*).

Nieto and colleagues identified several unique proteins only in exosomes from highly metastatic melanoma cell lines. These proteins are known to be involved in cell motility, angiogenesis and immune responses, suggesting that pro-migratory proteins can be transferred from the highly metastatic exosomes to less aggressive ones (*212*).

In addition to the ability of exosomes to promote the pro-metastatic behavior of migration, Xiao et al., found that normal melanocytes could gain the ability to invade when incubated with exosomes from melanoma cells (*213*). Exosomes isolated from the highly metastatic clone of B16 melanoma cells (B16-F10) express the pro-metastatic protein, Met72. These exosomes can be taken up by the poorly metastatic clone of B16, B16-F1, which then begins to express Met72 and exhibit metastatic activity similar to B16-F10 cells (*214*). Another example of a pro-metastatic phenotype transferred to another cell via exosomes involves WNT5A. In malignant melanoma cells, WNT5A induces a calcium-dependent

release of exosomes that contain immuno-modulatory and pro-angiogenic factors involved in metastasis that have the ability to induce immune suppression and angiogenesis (*215*). It is hypothesized that melanoma exosomes induce the release of vascular endothelial cell derived tumor necrosis factor alpha (TNF-α), which causes the lymphatic endothelial cells to tolerate tumor growth within the nodes (*216*). Interestingly, exosomes from other normal cell types such as adipocytes have the ability, through exosome release, to increase pro-metastatic phenotypes. Exosomes released by adipocytes contain proteins involved in fatty acid oxidation (FAO), which are only found in these exosomes. They can be taken up by melanoma cells and induce elevated FAO levels and increased in migration and invasion (*217*). In another report, neural cell exosomes were shown to have the ability to affect the morphology and physiology of melanoma cells including activation of MAPK pathway within the cell, modulating melanogenesis and dendrite-like outgrowths of the cells, supporting the notion that exosomes from one cell type are able to influence the differentiation and cell signaling of another (*218*).

Exosomes manipulate primary tumor microenvironment

Melanoma cell-derived exosomes have been shown to manipulate the primary tumor microenvironment by: 1) supporting the epithelial-to-mesenchymal transition (EMT) of the cells in the melanocytic microenvironment, promoting metastasis, through autocrine/paracrine signaling activating the MAPK pathway. miRNAs involved in this transition, let-7i, miR191 and let-7a,

were detected in circulating exosomes from stage 1 melanoma patients but not in exosomes from non-melanoma patients (*219*). 2) Affecting the differentiation of immune cells by enhancing the maturation of dendritic cells and T-cell proliferation. 3) Activating macrophages when treated with melanoma-derived exosomes to exhibit a different cytokine and chemokine profile than when exposed by other activators such as LPS or IL-4 (*220*). 4) Increasing migration of endothelial cells and inducing angiogenesis, perhaps by transfer of miR-9 from the melanoma cells to endothelial cells via exosomes (*221*).

Cancer derived exosomes manipulate the pre-metastatic niche

In addition to the ability of melanoma-derived exosomes to affect the local cellular environment, these exosomes also shown to travel throughout the body and accumulate in distant organs. As mentioned earlier, the pre-metastatic niche is the site of a possible secondary metastasis. This microenvironment is made up of multiple different cell types, including fibroblasts, infiltrating immune cells, endothelial cells, and other cells that comprise the blood and lymph vessels. These cells and the extracellular matrix must create a supportive microenvironment for the arrival, growth and establishment of a secondary tumor from the circulating tumor cell destined to arrive there (*222*). Exosomes released from the primary tumor have been implicated in the process of pre-metastatic niche formation. Peinedo et al., described the involvement of exosomes in tumor progression and in the preparation of the pre-metastatic niche of future secondary tumor sites in a melanoma model system (*103*). They

provided evidence that exosomes are released by the primary tumor into the circulation, which results in the leakiness of the vasculature, as well as recruitment of immune cells, both events are involved in pre-metastatic niche formation (*103*).

As described earlier, the deposition of fibronectin determines the location of the metastatic niche formation. Exosomes released by tumor cells contain factors such as macrophage migration inhibitory factor (MIF) that influence the physiology of the recipient cells. The engulfment of MIF-containing exosomes promotes the release of transforming growth factor beta (TGFβ) by Kupffer cells, which then initiates the production of fibronectin by the hepatic stellate cells (hStCs) (*223*).

In a breast cancer exosome model, the macrophages within the lung and brain contain phagocytosed exosomes, which results in the activation of NF-kB and subsequent release of pro-inflammatory cytokines such as IL-6, TNFα, GCSF, and CCL2, which promote metastasis development (*224*). Hypoxic breast cancer cells release an amine oxidase, lysyl oxidase (LOX), that accumulates at sites of pre-metastatic niche formation. LOX co-localizes with metastases and crosslinks collagen within the basement membrane and is essential for the recruitment and adherence of myeloid cells. This crosslinking is critical for $CD11b^{+}$ myeloid cell recruitment, which leads to interactions with the collagen and production of MMP-2, breaking down collagen into peptides that act as chemoattractants for bone marrow derived cells (BMDCs) and circulating tumor cells (CTCs) (*104*).

Peinado et al., examined the distribution and metastatic potential of B16-derived melanoma exosomes in the lung (*103*). Together with results reported by Morishita and colleagues (*225*), they demonstrated that radio-labeled B16BL6 murine melanoma-derived exosomes first distributed throughout the body, and that after a very short period circulation, these radio-labeled exosomes accumulated in the lung, spleen and liver. Similar observations were made earlier with the gLuc-LA-coupled B16BL6 exosomes (*226*).

Melanoma exosomes have been shown to induce vascular leakiness at pre-metastatic sites. Exosomes injected into xenograft tumor bearing mice showed changes in mRNA profiling of the lungs, mainly in those that are involved in various steps in pre-metastatic niche formation. Bone marrow progenitor cells also accumulated in pre-metastatic niches (*103*); exosomes derived from these cells are thought to induce molecular signals that help melanoma cells to prepare sentinel lymph nodes for metastasis, recruit other critical molecules, and induce ECM deposition and vascular proliferation within the lymph nodes (*188*).

Tumor-derived exosomes are hypothesized to also be involved in manipulating interactions between tumor cells and their surrounding tissue stroma to promote malignancy. Specifically, these exosomes have the ability to interact with immune cells, which then help manipulate the microenvironment to be conducive for metastatic growth. For example, human melanoma and colorectal carcinoma-derived microvesicles have been shown to promote the differentiation of monocytes to myeloid-derived suppressor cells that support

the growth of the tumor and the ability to escape immune surveillance (*130*). Other immune cells were shown to interact with melanoma exosomes; RNA from either melanoma cells or Lewis lung carcinoma cell-derived exosomes is taken up by lung epithelial cells and result in activation of Toll-like receptor-3 (TLR3) in these cells and causes the infiltration of neutrophils. This infiltration promotes pre-metastatic niche (PMN) formation in the lung. TLR3-deficient mice do not form lung metastases and have a reduction in PMN formation due to a decrease in neutrophil infiltration (*227*).

Exosomes are hypothesized to ~~also~~ be involved in modulating interactions between tumor cells and the surrounding tissue stroma to promote malignancy. For example, human melanoma or colorectal carcinoma-derived microvesicles have been shown to promote the differentiation of monocytes to myeloid-derived suppressor cells that support the growth of the tumor and the ability to escape immune surveillance (*130*). Melanoma exosomes have also been implicated in the promotion of angiogenesis by regulating endothelial cells from a distance, and manipulate cytokine expression profiles to establish an immunosuppressive environment (*187*).

Additionally, the formation of the pre-metastatic niche is dependent on the infiltration of immune cells into the site. An illustration of the role of cancer derived exosomes in the infiltration of immune cells, melanoma exosomes were shown to have the ability to travel to the bone marrow, “educate” bone

progenitor cells to be receptive of and support tumor cell growth and metastasis (*103*).

Cancer derived exosomes induce resistance to treatment

Often, when patients are undergoing various treatment regimens, the tumor initially shrinks, then develops resistance and begins to resume growth, regardless of continuation of treatment. There have been several recent studies suggesting the involvement of cancer-derived exosomes in treatment resistance. In one example, melanoma cells were shown to have the ability to create a local acidic microenvironment, which can contribute to resistance to cisplatin treatment. When the cells are co-treated with proton pump inhibitors (PPI) and cisplatin, exosomal levels are reduced, local pH increases (due to the inhibition of H^+ release by the PPIs), and cytotoxic uptake activity of cisplatin is enhanced (*228*). Melanoma cells also promote the accumulation of chemotherapeutic agents within vesicular compartments and release them in exosomes, as shown by Chen et al. They found that melanosome release is enhanced in the presence of cisplatin and are exploited by the cell for cisplatin removal from the cytoplasm (*229*).

Exosomes have also been shown to promote cancer progression by enhancing multiple mechanisms of treatment resistance. Stromal cell exosomes (especially from fibroblasts) increase the expression, in breast cancer cells, of pattern recognition receptors such as RIG-1, which cause the upregulation of genes involved in treatment resistance (*230*). Exosomal miRNAs from

neuroblastoma cells mediate cellular crosstalk with co-cultured monocytes, downregulating a target gene, TERF1, an inhibitor of telomerase, and increasing telomerase activity, which is involved in chemoresistance (*231*).

Use of exosomes as biomarkers and treatment of cancer

Circulating tumor cells (CTCs) are potential biomarkers for cancer; however, depending on the stage of cancer, there can be as few as 1-10 CTCs per mL of blood. Exosomes, in contrast, are found in abundance within the blood (typically, $1x10^{12}$ exosomes per mL of blood), making them a non-invasive and ideal marker for diagnostics, cancer progression and targeted therapy (*232*).

Although these vesicles play important roles in the progression of cancer, many investigators have suggested using them as a promising non-invasive biomarker for cancer. Interestingly, increased exosome plasma levels are observed only in patients with advanced stage disease (*103, 233*). Melo and colleagues identified proteins exclusively present on exosomes derived from malignant cells. They found that Glypican-1 (GPC1) is overexpressed in breast and pancreatic cancers and is found solely on exosomes derived from those malignant cells (*234*). Recently, an assay was developed to detect GPC1 on circulating extracellular vesicles in patients with late-stage pancreatic cancer with 100% confidence. This method is more reliable than a more common assay looking for a tumor antigen in whole blood (*235*). Additionally, the level of $GPC1^{+}$ exosomes in circulation correlates well with outcome after resection of pancreatic lesions (*234*). As well as using exosomes as diagnostic tool for cancer,

Fujita et al., proposed the possibility of using exosomes as biomarkers for asthma (*236*).

In addition to use as a minimally invasive biomarker, there have been efforts in using exosomes to develop a new method of drug delivery to target drug-resistant cancer. Exosome-encapsulated Paclitaxel (exoPTX) increases the cytotoxic effects on prostate cancer cells when compared to drug alone, and holds significant potential for the delivery of various chemotherapeutics to treat cancers that have became resistant to the regimen (*237*). In addition to drug delivery, dendritic cell-derived exosomes are being explored for their potential in cancer immunotherapy (*238*). The different roles of exosomes in tumor development and progression are summarized in Figure 2.

GRM1 and Exosomes

Increasing evidence links the aberrant expression of G-protein coupled receptors with numerous pathologies, including cancer. Accumulating evidence supports the potential relationship between GPCRs and MVB formation, exosome endocytosis or exosome release has been suggested. For example, the G protein-coupled pheromone receptor, Ste2, is downregulated when activated by the transfer of the receptor to the lumen of the vacuole by way of MVB sorting (*239*). However, Myers et al., showed that activation of GPCRs result in growth factor shedding by way of proteolytic cleavage, and not by exosome release (*240*). Therefore, certain GPCRs~~, but not all,~~ may play a role in the MVB exocytosis. Some GPCRs, such as A_{2A} receptors, were shown transferred by

exosomes from a source cell expressing these receptors to a target cell that does not. Upon incubation with an A_{2A} receptor agonist, the target cells produced an increased amount of cAMP, suggesting that the transferred A_{2A} receptor is functionally active within the target cell (*241*). Additionally, under cellular stress responses to neuro-hormonal stimulation, cardiomyocytes are stimulated to release exosomes containing an endogenous functional GPCR, AT1R, which, upon activation with an AT1R agonist, results in phosphorylated-ERK (*242*). These studies suggest that functioning GPCRs can be transferred by exosomes, effecting physiological changes within the recipient cell. Locke et al., reported the relationship between the activation of GPR143 by its natural ligand, L-DOPA, in retinal pigment epithelial cells, and the release of exosomes for intercellular communication in the eye (*243*). Downstream exosome release is dependent on the interaction of L-DOPA with the receptor, which activates $G\alpha_q$, initiating the release of calcium storage from the cell. Calcium mobilization has been suggested to play a role in the release of exosomes (*168, 244*). Additionally, mutations in the yeast PI3K results in the dysfunction of MVB sorting (*239*). Mammalian melanoma cells treated with wortmannin, a fungal metabolite that functions as a PI3K inhibitor had larger endosomes containing a significantly reduced number of exosomes (*245*). These data suggest that the inward budding of the endosome may be in part regulated by PI3K; a downstream component in several signaling cascades including GRM1.

Given the examples of GPCR activation resulting in exosome formation, release and uptake, it seems reasonable to suggest a potential role for GPCRs in exosome biogenesis and function. Furthermore, activated group I GRMs promote the release of calcium from the endoplasmic reticulum by the second messenger, IP_3, and increased intracellular calcium levels may promote the release of exosomes, as suggested earlier (*168, 244*). Interestingly, activated phospholipase C (PLC), which hydrolyzes PIP_2 to IP_3, was detected within exosomes of a leukemia cell line, suggesting that exosomes may carry functional phospholipases to recipient cells (*246*). Modulation of calcium concentration may be a potential link between group I GRM activation and exosome release. This association between GRMs and exosome release may provide hints to elucidate the aggressive nature of cancers that ectopically express GRMs, and the role exosomes play in the metastatic potential of the tumor, and formation of the pre-metastatic niche.

Taken together, the aggressiveness and malignancy exhibited by various cancers aberrantly expressing GPCRs could be explained by the release of a high volume of exosomes not only manipulating the surrounding stroma of the tumor, but also preparing the sites of future metastasis for the arrival of circulating tumor cells. We hypothesize that stimulation of GPCR by its ligand/agonist initiates signaling cascades, activating a multitude of different downstream effectors that may regulate exosomal secretion and/or production. The precise mechanisms involved remain unknown. Calcium has been proposed

as one of the factors involved, for example, because stimulated group I GRMs activate PLC and promote hydrolytic cleavage of PIP_2 for the formation of two second messengers, IP_3 and DAG. IP_3 brings about the release of calcium from the endoplasmic reticulum, which initiates multiple diverse physiological alterations within the cell; one of them could be exosome release. Therefore it is plausible that GPCR signaling may participate in exosome production or secretion by tumor cells.

Section I: Determine the relationship between GRM1 and its subsequent signal transduction cascade and the production of exosomes.

Aim 1: Rationale

Exosomes are nanovesicles released by various cell types. Notably, they are released more frequently by transformed malignant cells when compared to their normal counterparts (*118, 119*).

Earlier data from our laboratory showed that introduction of exogenous murine GRM1 cDNA into immortalized normal non-tumorigenic mouse melanocytes derived from C57BL/6 (melanA) led to rapid, aggressive tumor formation in immunocompromised nude mice, as well as immunocompetent syngeneic C57BL/6 mice (*60*). Analysis of exosomes in the conditioned media from these $GRM1^{+}$ cells (MASS clones) showed elevated levels of exosomes when compared to empty vector melanA control cells by electron microscopy and by western immunoblots performed with exosome lysates probed with a commonly used exosomal protein marker, CD63 (data unpublished). Furthermore, Goydos and co-workers demonstrated that human melanoma cells with modest levels of GRM1 protein (UACC903), when transfected with human GRM1 cDNA led to an increased in levels of exosomes assessed by electron microscopy when compared to vector controls (data unpublished). The transfected UACC903 cells stained with FITC-conjugated-Cholera Toxin B subunit showed an increased membrane blebbing compared to empty vector controls (data unpublished), suggesting

increased cell membrane motility (*247*) and exosome formation (*248*).

In the first aim of this dissertation, isogenic human melanoma cell lines, the GRM1-negative C81-61 and its human GRM1 cDNA transfected derivative, C81-61 GRM1 were used to explore the role of GRM1 in exosome production.

Materials and Methods

Cell lines

C81-61 is a cell line derived from an early stage melanoma that is negative for GRM1 expression and nontumorigenic. Exogenous human GRM1 cDNA cloned in a mammalian expression vector was introduced into this cell line. Several stable clones were isolated and clone C81-61-GRM1-6 was selected for further characterization.

Silencing RNA to GRM1 in an inducible tetracycline regulated vector was introduced into the C81-61-GRM1-6 cell line to allow modulation of GRM1 expression. We then assessed the effects of decreased production of GRM1 on exosome production. Specifically, C81-61-GRM1-6 cells were infected overnight with TetR lentiviral particles and 7.5 mg/mL polybrene (Millipore cat#TR-1003-G). Stable C81-61-GRM1-TetR cells were selected with blasticidin at 5 μg/ml. C81-61-GRM1-TetR cells were transfected using DOTAP reagent (Roche cat#11 811 177 001) with 4 μg of siGRM1 plasmid DNA cloned into the pRNATin-H1.2/Hygro vector as described (*60*). Several C81-61-GRM1-TetR-siGRM1 clones

were generated by double selection with 5 μg/ml blasticidin and 5 μg/ml hygromycin.

Cell culture method

Cell lines were grown in RPMI 1640 medium with 10% Fetal Bovine Serum and 1% Penicillin/Streptomycin until confluent. $4x10^5$ C81-61-GRM1-6 cells were plated in serum free OptiMEM (Life Technologies cat#31985062) in 60mm cell culture dishes. Experimental groups included no treatment (NT), vehicle (DMSO), 5 μM riluzole and 5μM Bay36-7620 for 48 hours.

For induction studies using C81-61-GRM1-6-TetR-siGRM1-16, $4x10^5$ cells were plated in 60mm cell culture dishes in serum free Opti MEM, and treated with 10 μg/mL of doxycycline (concentration sufficient to induce siGRM1 production) for 48 hours after which exosomes are isolated.

To collect exosomal proteins for immunoblotting, C81-61 or C81-61-GRM1-6 cells were plated at $2.5x10^6$/plate in 4-150mm plates. After 24 hours, plates were rinsed with sterile 1X PBS, and media were changed to RPMI with 2% exosome-depleted fetal bovine serum (Gibco Ref#A25904DG), and exosomes collected after 48 hours.

Cell Lysate Protein Extraction

Culture media was aspirated and cells were washed twice with cold 1X PBS, and 600 μL of 10:1 Laemmli Sample Buffer: β-mercaptoethanol mixture was added to each 150 mm plate. The cells were then scraped and collected in a

centrifuge tube. The samples were heated for 10 minutes at 99°C and then centrifuged at 15,000 x g for 10 minutes at room temperature. The supernatant containing the cell lysate was then transferred into a new tube to be analyzed by immunoblot.

Immunoblot

Lysates were electrophoresed on 10% SDS gels after denaturation at 95°C for five minutes. A reference protein ladder (Precision Plus Protein Standards-Bio-Rad Cat# 161-0374) was used to determine the sizes of bands. Gels were electrophoresed for two hours at 120 volts; proteins on the gel were transferred onto a nitrocellulose membrane (GVS North America Cat#1215471) for three hours at 160 mA. The membrane was then blocked using 0.25% milk (nonfat dry milk and 50 mM Tris-Cl, pH 7.6, 150 mM NaCl, 0.1% Tween-20) with a SnapID 2.0 (Millipore), to reduce nonspecific binding. The membrane was incubated overnight with its respective primary antibody: CD63 primary antibody (1:1,000, 5% BSA, 0.1% NaAz, Biorbyt Cat# orb13317), monoclonal AliX primary antibody (1:1,000, Cell Signaling Technology Cat# 2171S) or monoclonal anti-α-tubulin antibody (Sigma Cat#T6074-200ul). After incubation, the membrane was washed five times on the SnapID 2.0 with wash buffer (1X TBS, 0.1% Tween-20). The blot was then incubated on a rocker for one hour at room temperature with the respective secondary antibody, either anti-rabbit (1:5,000, Dky x Rb IgG, Millipore Cat# AP182P) or anti-mouse IgG (1:5,000, Sigma Cat# A4416-1ML) in

0.25% w/v milk (1X TBS, 0.1% Tween-20). The blot was washed in the same manner as above, incubated with Forte Western HRP Substrate (Millipore Cat# WBLUF0100) for 3 minutes, and visualized using the GeneSys imager (Syngene). The band intensities were quantified using ImageJ computer software.

Exosome Isolation Method

Conditioned cell culture media were concentrated up to 80-fold using a centrifugal filter (Millipore Centricon Plus-70 Ref#UFC710008). The Invitrogen Exosome Isolation kit (for cell culture media, Cat# 4478359) was used following manufacturer's instructions. Briefly, concentrated cell culture media were centrifuged at 2,000 x g for 30 minutes at room temperature to remove cellular debris. Invitrogen Exosome Isolation Buffer for cell culture media was then added to the supernatant at a volume of 0.5 times the total cell culture media volume and incubated at 4°C overnight. The samples were then centrifuged for 1 hour at 10,000 x g creating a concentrated exosome pellet. The supernatant was aspirated and the pellet was then resuspended in sterile 1X Hank's balanced salt solution (HBSS).

Exosome Quantification

Exosomes were quantified using the Nanosight (Malvern), which utilizes a laser light scattering of Brownian Motion to visualize, quantify and analyze particles in a liquid suspension in size range of 10-2000nm. After being isolated by the above method, the exosome preparations were diluted 1:10 in sterile

HBSS. The samples were pumped into the nanosight analytic cell at a continuous flow speed value of 20 with a syringe pump. The Nanosight was set to a camera level of 10 and 5 videos at 30 seconds each were recorded. Nanoparticle Tracking analysis (NTA) software (Malvern) was then used to analyze the videos.

Cell proliferation/ viability (MTT) Assay

Cells were plated at a concentration of $5X10^3$ cells per well in a 96-well plate. Cells were treated with R10 or conditioned R10 (RPMI, 10% FBS, 1% Penicillin/streptomycin) media from either C81-61 cells or C81-61-GRM1-6 cells. 10 µl of Thiazolyl Blue Tetrazolum Bromide (Sigma Cat# M5655) in 1XPBS (MTT solution 1) was added on days 1, 3 or 5 to each well, incubated for 4-6 hours at 37°C. MTT solution 2 [(10% Sodium dodecyl sulfate (SDS) in 0.01M HCl)] at an equal volume was added and incubated overnight at 37°C. A 96-well plate reader (Infinite 200, Tecan) was used to measure the absorbance at 550 nm with a reference wavelength of 750 nm.

Wound Healing Assay

Conditioned media were collected from either C81-61 ($2X10^5$ cells) or C81-61-GRM1-6 (10^5 cells) that were plated in 60mm plates with R10 for 48 hours at 37°C. For wound healing assays, C81-61 cells ($3X10^5$) were plated in a 12-well plate. After 24 hours, the media were replaced with conditioned media, and incubated overnight. Each well was then scratched with a pipette tip, and washed drop-wise with sterile 1XPBS three times, and R10 medium then added.

Photographs of the cells (10X, Keyence BZ-X710 microscope) were taken at 0, 4, 6, 12 and 24 hours after media replacement. Area of the wound was calculated using ImageJ and normalized to hour 0.

To test the effects of exosomes on cell migration, exosomes were isolated from the conditioned media as above and resuspended in R10 medium. C81-61 cells were incubated overnight with the isolated exosomes resuspended in R10 following the same procedure as described above. In order to determine significance, student's T-test was performed at each time-point, and a p value <0.05 was considered significant.

Matrigel Invasion Assay

The matrigel invasion assay as described by Higginbotham et al. (*249*) was followed using our cell model system. C81-61 ($GRM1^-$) and C81-61-GRM1-6 ($GRM1^+$) cells were plated at $2x10^5$ and $1x10^5$ cells per plate, respectively, in 60mm plates with R10 medium. Once the cells were attached (4-5 hours), media were then replaced with OptiMEM and incubation continued for 48 hours. Media were collected, and exosomes isolated as described above. C81-61 cells were incubated with either $GRM1^+$ or $GRM1^-$ exosomes for 2 hours, in snap-cap tubes under constant rotation at 37°C. The cells were pelleted and resuspended in serum-free RPMI. A total of $6.5x10^4$ cells were plated on each Corning Matrigel Plate (Corning Cat#354481), which was rehydrated prior to cell plating per instructions from the manufacturer. Exosomes were added to the lower chamber of each well in R10 media, which was replaced every 24 hours. The cells were

incubated in the chambers for 72 hours at 37°C, 5% CO_2. Cells that remained on the top of the chamber were removed by cotton swab, and the membranes were fixed with 100% methanol for 2 minutes, stained with 1% toluidine blue in 10% borax for 2 minutes and rinsed with deionized water. The membranes were dried, detached and mounted on a microscope slide with mounting oil, and an image of the slide was captured under a Keyence BZ-X710 microscope. The stained cells were then counted in 10 random fields of the membrane. Student's t-test was performed to determine statistical significance.

Generation of tagged clones

C8161 ptdTomato-CD81 and C81-61 ptdTomato-CD81: C8161 and C81-61 melanoma cells were transfected using DOTAP reagent with 4ug commercially available ptdTomato-CD81 plasmid (Addgene Cat# 58078). These clones were generated using G418 antibiotic selection at a concentration of 125 µg/ml.

C81-61 CD63-GFP: C81-61 melanoma cells were infected using the commercially available CD63-GFP lentivirus (System Biosciences Cat# CYTO120-VA-1) and 7.5µg/ml polybrene. Stable C81-61 CD63-GPF clones were selected with 0.2µg/ml puromycin.

Microscopy

The Keyence BZ-X710 microscope was utilized to confirm the presence of either the ptdTomato or GFP fluorescent-tagged proteins when generating stable clones of C81-61 CD63-GFP, C8161 ptdTomato-CD81 and C81-61 ptdTomato-CD81.

Anchorage-independent Assay

Tissue culture 60mm plates were layered with a mixture of 4 ml final concentration of 0.5% agarose in R10. After allowing the agarose on the plates to become solidified for 1-2 hours at 4°C. 1205Lu (as a positive control) or C81-61 CD63-GFP cells were plated at $1x10^5$/plate in 4 ml of final concentration of 0.33% agarose in R10 with exosomes isolated from either C8161 ptdTomato-CD81 or C81-61 ptdTomato-CD81 at 1µl/ml. Fresh R10 medium with 0.33% agarose and exosomes were added once a week for 21 days. The number of colonies in the semi-solid agarose media was counted. The Keyence BZ-X710 microscope was utilized to obtain photographs of the colonies formed in the agarose.

Results

Comparisons between ultracentrifugation/sucrose gradient and a commercial kit in the isolation of exosomes

Many different methods are used to isolate and quantify exosomes, including ultracentrifugation through sucrose gradients and commercial kits. To determine which approach would best serve the needs of this project, , a side-by-side comparison was performed to compare the Total Exosome Isolation Kit (TEIK) with the commonly used method of ultracentrifugation (UCM). Mouse blood samples were taken from 3 different animals (SKH-1 mouse #1, 10 and 12) and exosomes were isolated from these blood plasma samples. CD63, a protein enriched in exosomes, and commonly used as an exosome marker (*123, 134, 250*), as well as an alternative exosome enriched protein, CD9, were analyzed in the

sample by immunoblots. The results show that the both markers are present in exosome isolates from both methods, and in some cases is enriched in the total exosome isolation kit samples (Figure 3A). To assess the quality of the exosome preparation, electron microscopy was performed. Intact exosomes of the characteristic size were found in both ultracentrifugation and kit methods. One difference observed in the 2 methods was a black background present in the ultracentrifugation samples, indicating a higher soluble protein contamination when compared to the exosomes isolated using the kit (Figure 3B). These data indicate that the commercial kit, in some cases, enriches for a higher quantity of CD63-protein rich exosome fractions with minimal protein contamination when compared to the commonly used ultracentrifugation isolation method.

The Zetasizer Nano (Malvern) was used to measure the size of the particles present in the exosome suspension. It utilizes Brownian motion principles to measure the diffusion of particles and their motion, converting it to a size distribution using the Stokes-Einstein relationship. Back Scatter technology is used to give the highest sensitivity with high size and concentration range. Figure 3C shows the size distribution of the particles in the exosome isolation suspension with a peak around 100nm; consistent with the characteristic size of exosomes (30-120nm).

Ectopic GRM1 expression in C81-61 cells show little effect on levels of released exosomes

To determine if GRM1 affects the levels of released exosomes, two

complementary approaches were used. The first involved the introduction of exogenous human GRM1 cDNA into an early stage melanoma cell line, C81-61, which does not express endogenous GRM1. *In vitro* and *in vivo* characterization of several GRM1-expressing C81-61 clones showed these clones were transformed and tumorigenic (*66*). We selected C81-61-GRM1-6 for further studies. Exosomal levels were compared between the parental C81-61 and C81-61 GRM1 clones.

C81-61 and C81-61-GRM1-6 cells were plated, incubated overnight, the media were then replaced with serum-free OptiMEM media and incubated for an additional 48 hours. OptiMEM media was used to avoid possible contamination from exosomes present in the serum used in standard culture media. The exosomes were isolated from conditioned cell culture media and quantified using the Nanosight. The results show no increase in number of exosomes released by C81-61-GRM1-6 cells when compared to the parental C81-61 on a per cell basis (Figure 4A). Two exosomal markers (CD63, AliX) and an internal standard (tubulin) were also used in western immunoblots to assess exosomal levels. An increase in band intensity is seen in the exosome protein samples in C81-61-GRM1-6 samples compared to the parental C81-61 cells (Figure 4B).

Alterations in size distribution of exosomes in cells with GRM1 expression

Particle size analysis was performed using the Nanoparticle Tracking Analysis (NTA) software on exosomes isolated from C81-61 and C81-61-GRM1-6 cells. A smooth unimodal distribution of exosome size secreted by C81-61 cells was detected. In contrast, exosomes isolated from C81-61-GRM1-6 cells contained a large number of smaller, more heterogeneous vesicles in addition to the exosomes of similar size distribution to C81-61 (Figure 4C).

Genetic modulation of GRM1 expression in cells did not affect release of exosomes

In order to determine if the level of GRM1 protein present within the cells affects the amounts of exosomes released by the cells, we took advantage of the inducible Tet-On silencing RNA system to modulate GRM1 expression levels in C81-61-GRM1-6 cells. C81-61-GRM1-6 cells were transfected with both TetR and siGRM1 plasmids to create several C81-61-GRM1-6-TetR-siGRM1 clones, clone 16 was selected for further characterization. In the presence of the inducer, doxycycline, the amount of GRM1 was reduced substantially as shown by the immunoblot (Figure 5A).

We then isolated exosomes from cultured cells with or without the inducer, doxycycline, and analyzed quantity with the Nanosight. No change was seen in exosome number when normalized to cell number and compared to vehicle or no treatment controls (Figure 5B).

Pharmacological modulation of GRM1 function did not affect exosome release by melanoma cells

In addition to using genetic means to modulate GRM1 expression,

pharmacological glutamate signaling blockades were used in these *in vitro* approaches. Two types of blockades were used; the first is the inhibitor of glutamate release, riluzole, an FDA approved drug for treatment of Amyotrophic Lateral Sclerosis (ALS). The ability of riluzole to block the release of glutamate and subsequently reduce levels of available ligand allows it to act functionally as an inhibitor of GRM1-mediated signaling and interferes with intracellular events that follow stimulation of the receptor. The second pharmacological reagent was the specific non-competitive inhibitor of GRM1, Bay36-7620, which binds the intracellular loops and alters the conformation of the receptor rendering it non-functional. Both blockades were shown previously by our group to reduce cell growth *in vitro* and tumor progression *in vivo (62)*.

C81-61-GRM1-6 cells were treated with riluzole (5μM) or Bay36-7620 (5μM) for 48 hours. Nanosight quantification was used to determine the number of nanovesicles secreted into the media. We found no significant change in the number of exosomes released from either riluzole or Bay36-7620 treated cells (Figure 5C) when normalized to cell number and compared to untreated and vehicle controls.

Levels of intracellular CD63 protein in melanoma cells are unaffected by GRM1 inhibitors

To determine if treatment of C81-61 GRM1-6 cells with riluzole or Bay36-7620 affects the amount of exosome marker produced within the cell,

immunoblots were performed on the C81-61 GRM1-6 cell lysates after 48 hours of treatment with either riluzole or Bay36-7620. No change in the levels of the exosome protein marker, CD63, was seen within the cells when normalized to the loading control α-tubulin (Figure 6A).

Additionally, immunoblots were performed on C81-61 GRM1-6 TetR siGRM1-16 cells that were treated with doxycycline (10μg/mL) for 48 hours. These results also showed no change in the amount of CD63 protein in comparison to no treatment and vehicle controls when normalized using the internal control, α-tubulin (Figure 6B).

Exosomes from GRM1$^+$ cells do not promote cell proliferation in GRM1$^-$ cells

C81-61 cells were treated with either C81-61 or C81-61-GRM1-6 conditioned media. Cellular proliferation was measured using a colorometric cell proliferation/cell viability assay. Comparisons were made between C81-61 incubated in the untreated control media, conditioned media from C81-61 cells and conditioned media from C81-61-GRM1-6, very similar growth rate was observed in C81-61 cells incubated in all three media. These results indicate that exosomes released from C81-61-GRM1-6 in the conditioned media did not promote cell proliferation in C81-61 cells (Figure 7).

Exosomes from GRM1$^+$ cells induce migration in GRM1$^-$ cells

Earlier reports from other investigators demonstrated that exposure to exosomes from metastatic cells altered the behavior of non-metastatic cells,

including increasing their metastatic capability (*187, 188*). We performed wound-healing assays to assess possible differential migration abilities of C81-61 incubated with media conditioned by either GRM1$^+$ (C81-61-GRM1-6) or GRM$^-$ (C81-61) cells. After a 24-hour incubation with GRM1$^+$ conditioned media, C81-61 cells exhibited a significant increase in migration into the culture wound ($p<0.05$) (Figures 8A and 8B).

We then assessed if the increased migration property is a result of exosomes released into the growth media, we isolated and purified exosomes from the conditioned media and repeated the experiment. C81-61 (GRM1$^-$) cells were incubated with exosomes from either GRM1$^+$ (C81-61-GRM1-6) or GRM$^-$ (C81-61) cells for 24 hours and the cultures were scraped. Images were captured at different time points and the wound healing analysis showed a similar increase in migration induced by GRM1$^+$ exosomes as shown in conditioned media from GRM1$^+$ (C81-61-GRM1-6) cells, although for purified exosomes this was evident only after 48 hours instead of 24 hours for conditioned ($p<0.005$) (Figure 8C).

Exosomes from GRM1$^+$ cells induce invasion in GRM1$^-$ cells

In order for tumor cells to metastasize, the cell must have the ability to invade the surrounding tissues, embed and proliferate in distant tissues in the body. We therefore determined if C81-61 cells acquire an invasive property when incubated with exosomes from GRM1$^+$ cells, using an *in vitro* invasion assay. Exosomes from C81-61-GRM1-6 and C81-61 cells were isolated from cell culture

media after 48 hours. C81-61 cells were incubated with exosomes from either C81-61 or C81-61-GRM1-6, or no exosomes for 2 hours, and then seeded on the matrigel invasion chamber plate. After a 72-hour incubation, cells that had migrated through the matrigel were stained and counted in 10 random fields. A significant increase in the number of cells migrated after incubation with $GRM1^+$ cell exosomes was seen when compared to those cells incubated with either no exosomes or exosomes from $GRM1^-$ cells (Figure 9).

Confirmation of generated cell lines

C81-61 CD63-GFP, C8161 ptdTomato-CD81 and C81-61 ptdTomato-CD81 stable clones were viewed under fluorescent microscope for the presence of the GFP or ptdTomato fluorescent tags within the cells (Figure 10).

Exosomes from $GRM1^+$ cells induce anchorage-independent colony formation in $GRM1^-$ cells

The soft agar colony formation assay is used to determine the ability of cells to form colonies without the dependence of an extracellular matrix contact. C81-61 CD63-GFP cells were grown in a layer of soft agar containing medium with either exosomes isolated from C81-61 ptdTomato-CD81 cells or C8161 ptdTomato-CD81. The tumorigenic human melanoma cell line, 1205Lu, was used as a positive control. Cells were fed with a fresh agarose containing medium and exosomes once a week, and after 21 days, the number of colonies formed were quantified. C81-61 CD63-GFP cells incubated with exosomes isolated from C8161

ptdTomato-CD81 cells formed a significantly higher number of colonies when compared to C81-61 CD63-GFP cells with exosomes isolated from C81-61 ptdTomato-CD81 cells (Figure 11).

Exosomes from GRM1^{+} cells do not transfer GRM1 protein to GRM1^{-} cells

To explore the possible mechanism of the induction of migration, invasion and colony formation abilities in C81-61 cells by C81-61 GRM1-6 exosomes, C81-61 cells were incubated with conditioned media from C81-61 GRM1-6 cells. The C81-61 cells were then washed multiple times and protein was extracted from the cells. An immunoblot for GRM1 was performed, and α-tubulin was used as a loading control. Immunoblot results indicate the absence of GRM1 in cells treated with C81-61 GRM1-6 exosomes, while a band is present in the positive control (Figure 12). These data indicate GRM1 protein is not transferred from the exosomes to the recipient cells to induce metastatic abilities.

Section II: Perform pre-clinical melanoma metastasis and metastasis prevention studies with a glutamate signaling blockade in a melanoma prone mouse model (TGS)

Aim 2: Rationale

The role of deregulated glutamatergic signaling in melanoma pathogenesis was first demonstrated by our laboratory and subsequently confirmed by work from other groups (*58*). The gain of function of the murine GRM1, when expressed ectopically by otherwise normal melanocytes induces spontaneous malignant melanoma development *in vivo* in the transgenic mouse model TG-3 (*58-60*) with 100% penetrance (*21, 22*).

To show the involvement of GRM1 in exosome production *in vivo*, a preclinical study in our transgenic mouse model, TGS, was performed. TGS is derived from crossing the melanoma-prone transgenic mouse model, TG-3, with the hairless SKH-1 strain to produce a melanoma mouse model where pigmented lesions on the skin are easily visualized in the absence of fur. Crosses between the TGS heterozygotes yield three genotypes: wild type mice that do not harbor the transgene, those that harbor only one copy of the transgene (heterozygous) and those harboring two copies of transgene (homozygous). Melanoma in heterozygous and homozygous TGS are histologically indistinguishable except for the latency of onset of the disease (6-8 weeks for homozygotes, and 7-8 months for heterozygous TGS) and tumor multiplicity (far higher in

homozygotes than heterozygotes). Metastases are detected in both genotypes, and can be found in various organs including lungs, muscle and brain.

This pre-clinical study focused on metastasis prevention. The detection of elevated levels of exosomes that correlated with an increase in GRM1 expression as seen by our collaborators, Goydos and colleagues, prompted us to hypothesize that the glutamatergic signaling cascades in GRM1 expressing melanoma cells participate in various downstream events including exosome production and secretion. Preliminary results show an increased sensitivity in cell growth and a decrease in exosome level production in the presence of a glutamate signaling blocker, riluzole. If GRM1 expression and/or function influence levels of exosomes, which may modulate the metastasis potential of a tumor as suggested (*103, 187, 188*), then daily administration of riluzole in TGS mice may prevent or delay tumor progression and metastases.

Materials and Methods

TGS Mouse Genotyping

Genomic tail DNA was isolated from a mouse tail sample (3mm in length) utilizing a commercially available DNA extraction kit [Zymo Research *Quick*-DNA Universal Kit (Zymo Research Cat#D4069)] according to the manufacturer's instructions. Briefly, the mouse tail sample was added into a tube containing 95 uL of water, 95 uL of Solid Tissue Buffer and 10 uL of 20 mg/ml Proteinase K. The sample was then mixed thoroughly and incubated at 55^{o}C for

1-3 hours or until the tissue solubilized. The lysed sample was then centrifuged at 12,000 x g for 1 minute and the supernatant was transferred into a new tube. Two volumes of Genomic Binding Buffer were added to each tube and tubes were inverted to mix. The mixture was transferred to the Zymo-Spin IIC-XL column collection tube. The column was centrifuged at 12,000xg for 1 minute and washed with 400 uL of DNA pre-wash buffer and centrifuged at 12,000xg for 1 minute. 700 uL of g-DNA wash buffer was then added to the column and centrifuged at 12,000xg for 1 minute, 200 uL of g-DNA wash buffer was again added to the column and was centrifuged at 12,000xg for 1 minute. The Zymo-Spin IIC-XL column was transferred into a new microcentrifuge tube, and 50 uL of DNA elution buffer was added into the column. It was incubated for 5 minutes at room temperature, and centrifuged at 12,000xg for 1 minute. DNA concentrations and integrities were determined on a 0.8% agarose gel with HindIII digested lambda DNA as a marker.

The DNA was then used in Polymerase Chain Reaction (PCR) to determine the genotype of the TGS animal. Qiagen Taq PCR Master Mix Kit (Qiagen Cat# 201443) protocol was followed for PCR. The PCR mix contained Qiagen Taq PCR Master Mix, RNAase free water, reverse primer and forward primer and DNA. Sequences for these primers can be found in Table 2. The reaction was as follows: denaturing at 95^{o} C for 1 minute and 15 seconds, 94^{o} for 45 seconds, annealing step at 63^{o}C for 45 seconds-1^{o}C per cycle, elongation step held at 72^{o} C for 4 minutes and this cycle is repeated thirteen times from the step

94° C at 45 seconds. After this cycle is repeated 13 times then the cycle denatures the DNA at 94° C for 45 seconds, anneals the primer at 50° C for 45 seconds, elongates at 72° C for 4 minutes and adding 5 seconds every cycle for 29 cycles. After the 29 cycles are finished the last elongation step is at 72° C for 10 minutes. The samples were electrophoresed on 1.5% agarose gels with HaeIII restricted ϕX174 DNA marker to identify the genotypes of TGS mice.

Blood Collection

Heparinized capillary tubes (Fisherbrand Heparinized Micro-Hematocrit Capillary Tubes Cat# 22-362-566) were used to retro-orbitally bleed mice. About 300ul of blood was collected per mouse at each time-point and kept on ice. The centrifuge was pre-cooled to 4°C and the samples were then spun for 8 minutes at 18,000xg. Plasma supernatant was separated from the red blood cell pellet and was stored at -20°C.

TGS Study Design

Blood was drawn from TGS heterozygous mice and wild-type littermates prior to treatment at 8 weeks old and every 6 weeks until termination after 18 weeks. Riluzole (10mg/kg) and vehicle (36.4% DMSO) was administered by oral gavage daily to both genotypes at 8 weeks of age, blood samples were acquired once every 6 weeks and exosomes were isolated from blood plasma, quantified and characterized.

Exosome Isolation from Blood Plasma

The plasma, either freshly prepared or thawed from -20°C, was transferred to a new tube, and the Total Exosome Isolation (from serum) Kit (Invitrogen Cat# 4478360) was used based on manufacturer's protocol. Briefly, a clarification step of 2,000xg centrifugation for 30min at 4°C was performed, and the clarified plasma was transferred to a new tube, 0.2 volumes of the Total Exosome Isolation Solution was added to the clarified plasma and incubated for 30min at 4°C. The samples were then centrifuged at 10,000xg for 10min at room temperature. The supernatant was aspirated, leaving an exosome pellet. The pellet was resuspended in sterile 1X phosphate buffered saline (PBS) and stored at -20°C until analysis by immunoblot or Nanosight.

Preparation of Exosomal Protein Lysates

Protein was isolated using equal parts of isolated exosomes and extraction buffer (EB) (1XPBS, 2-Mercaptoethanol (5% v/v) and Laemmli Sample Buffer). The samples were mixed thoroughly, heated to 99ºC for ten minutes and centrifuged for ten minutes at 15,000xg in a microcentrifuge. The supernatant was transferred to a new tube for analysis by Western blot.

Western Immunoblot

Immunoblot protocol was as described in Section I, with some additional changes. Exosome lysates were electrophoresed on 7.5% SDS gels after being denatured at 95º C for five minutes. Primary antibodies used in this section are

the CD63 antibody (1:1,000 (Biorbyt Cat# orb13317), AliX (1:1,000 Cell Signaling Technology Cat# 2171S), CD81 (1:1,000, Cell Signalling Cat# 10037S), CD9 (Abcam ab92726) and anti-α-tubulin (Sigma Cat#T6074-200ul). Bands were quantified using ImageJ software, with 2-way ANOVA statistical test, $p<0.05$ was significant.

Exosome Quantification

After being isolated by the above method, exosomes from plasma were diluted 1:1,000 in sterile HBSS. The samples were pumped at a continuous flow speed set at a value of 20 with a syringe pump. The Nanosight was set to a camera level of 10 and 5 videos at 30 seconds each were recorded. Nanoparticle Tracking analysis (NTA) software (Malvern) was then used to analyze the videos.

Immunohistochemistry

Lungs were excised from several mice (control and riluzole treated) at the end of the experimental period, fixed in 10% formalin for 48 hours, and stored in 70% ethanol. Immunohistochemistry was performed with the Rabbit Anti-Mouse Fibronectin polyclonal antibody (Chemicon® International, AB2033, 1:1000 dilution). Unbiased quantitative assessment of IHC staining was completed using a digital Aperio ScanScopeGL system and ImageScope software (Aperio Technologies, Inc., Vista, CA). Images were taken using Olympus BX51

microscope and camera system. Student's T-test was performed for statistical analysis of positive fibronectin staining.

Wound Healing Assay

C81-61 cells ($3X10^5$) were plated in each well of a 12-well plate. Pooled plasma exosomes from the same TGS genotypes and treatment groups were included in the media for 24 hours. An n=1 represents a pooled sample of 3 individual TGS mice. Confluent cells were then scratched with a pipette tip, and washed drop-wise with sterile 1XPBS three times, and R10 media was added. Photographs of the cells (10X) were taken at 0, 6, 12, 24 and 48 hours after media replacement. Area of the wound was calculated using ImageJ and normalized to hour 0. Statistical significance was determined using the Student's T-test.

Results

Daily oral gavage with riluzole (10mg/kg) for 18 weeks shows no apparent toxicity to TGS mice

A dose of 10mg/kg riluzole daily by oral gavage was chosen for these studies based off of efficacious doses in xenograft models (*62*). To ensure that this extended treatment regimen did not result in toxicity, body weights of the mice were monitored before every blood draw, and livers were taken at necropsy, weighed and fixed. The fixed livers were stained with hematoxylin and eosin (H&E) and analyzed for any pathologies due to potential toxicity. No statistical difference was observed in body weight or liver weight in the riluzole treated

TGS mice when compared to both no treatment and vehicle controls (Figures 13A and 13B). Liver H&E histology showed the no indication of liver toxicity, such as steatosis or fibrosis (Figure 13C).

TGS melanoma skin lesion size unchanged with treatment

To quantify the growth of skin lesions of the TGS mice throughout treatment, the mice were photographed once monthly beginning with day 0, using the IVIS small animal imaging system with an imaging camera at a fixed height. Each image was cropped and each subsequent photograph throughout riluzole or vehicle treatment of the TGS mouse was cropped the same way (Figure 14). ImageJ software was used to convert the cropped photograph into a binary image (Figure 14), five individual lesions were chosen at random from each image, and each individual lesion size was quantified and defined by the number of pixels. The data in Figure 14 represent the percent change of lesion sizes throughout the duration of treatment from the original lesion (day 0 prior to treatment). These data show no significant difference between the growth of the lesions throughout treatment with riluzole when compared to either vehicle or no treatment controls.

Treatment of heterozygous TGS with riluzole resulted in a reduction of CD63 protein in circulating exosomes

To quantify the exosomes present in the circulation of the TGS mouse with or without daily treatment with riluzole had an effect on the quantity, exosomal lysates were extracted from identical volumes of plasma at each time point. They

were then analyzed by immunoblot for the exosome protein marker, CD63 which we showed could serve as a marker for the number of exosomes present. Amount of protein was normalized to the day 0 value to take the animal variability into account. As seen in Figure 15A, no statistically significant difference was found in CD63 amounts at week 6 or 12. However, at week 18, a statistically significant decrease in CD63 intensity was seen in the riluzole treated animal samples when compared to both no treatment and vehicle controls.

Quantification of exosomes by Nanosight shows no change in number of exosomes

To validate the reduction in CD63 observed in riluzole treated TGS mice, we utilized a Nanosight NS300 to quantify the number of exosomes present in the samples. Samples were diluted 1:10 and analyzed by NTA, which showed no significant difference in the number of circulating exosomes between the treatment groups (Figure 15B).

Analysis of multiple exosome markers show no change in exosome quantity with treatment

Due to discrepancies between the commonly used protein marker, CD63, and the Nanosight data, the TGS exosome samples were further analyzed by immunoblots for levels of other commonly used exosome protein markers, AliX, CD81 and CD9. We also included data for a protein commonly used as an internal loading control, α-tubulin. In the case of all protein markers analyzed, protein quantities increased as the mice aged, however, no statistical difference

was observed in protein quantity among the treatment groups (Figures 16A-16D).

Alterations in size distribution of plasma exosomes from TGS mice after treatment

Particle size analysis was performed using the Nanoparticle Tracking Analysis (NTA) software on exosomes isolated from TGS mice treated with 10mg/kg riluzole for 18 weeks and untreated TGS mice of the same age. Comparisons in diameter changes of plasma exosomes from day 0 to day 18 of treatments were shown in Figure 17, indicating major differences between treatment groups.

Reduction in a pre-metastatic niche marker in the TGS lung after treatment

An indication of pre-metastatic niche formation is the deposition of fibronectin throughout a secondary organ. Exosomes have been shown to play an indirect role in this deposition in secondary organs. More specifically, it was demonstrated that the uptake of exosomes by Kupffer cells initiates the fibrotic pathways within the liver, and a pro-inflammatory environment. Macrophage migratory inhibitory factor (MIF) contained within exosomes induces the release of transforming growth factor B by the Kupffer cells. This release induces fibronectin production by hepatic stellate cells (*223*). Kaplan et al., (*100*) showed that VEGFR1^{+} cells express VLA-4, which upregulates fibronectin expression in resident fibroblasts, providing a permissive niche for circulating tumor cells. Additionally, deposition of fibronectin causes the arrest of bone marrow derived

macrophages and neutrophils. The establishment of fibrotic and pro-inflammatory environment, as well as the arrest of immune cells are critical processes in the establishment of the pre-metastatic niche. In order to determine possible consequences of riluzole treatment on the pre-metastatic niche formation in TGS mice, fibronectin was used as a marker for the assessment.

Lungs from the different treatment groups were collected at necropsy and fixed. Immunohistochemistry was then performed on these samples with a fibronectin antibody, a red color indicating fibronectin deposition. Riluzole treated lungs showed a significantly reduced staining intensity (Figure 18) when compared to the lungs of the untreated animals. Interestingly, the vehicle treated animals similarly showed a reduction when compared to the untreated control, but to a lesser extent. These data suggest that daily treatment with oral riluzole for 18 weeks led to a reduction of fibronectin deposition within the lung

Circulating exosomes from tumor-bearing TGS mice induce cellular migration in GRM1$^-$ cells

To explore the metastatic ability of exosomes released by GRM1$^+$ tumors *in vivo*, exosomes were isolated from both heterozygous and wild type TGS mouse blood plasma. Wound healing assays were performed on C81-61 cells to assess possible alterations in the migration abilities when incubated with exosomes isolated from blood plasma of either wild type or heterozygous TGS mice. Three TGS mouse blood plasma samples with the same genotype were pooled together and then incubated with C81-61 (GRM1$^-$) cells, and the wound

healing capabilities of the cells were assessed. After a 24-hour incubation with TGS heterozygous exosomes, a decrease in wound size ($p<0.1$) was observed, which indicates an increase in cellular migration ability. Similar measurements were made at 48 hours, there was a further decrease in the remaining unoccupied area in TGS heterozygous exosomes treated samples when compared to those incubated with wild type TGS exosomes (Figure 19A). Migration ability was calculated by the measurement of the remaining unoccupied area at a given time point after the initial scratch was made divided by the original area at time 0 using ImageJ.

Blood plasma exosomes from riluzole treated heterozygous TGS mice reduce migration in GRM1$^-$ cells

As shown above, exosomes from heterozygous mice induce migratory abilities in GRM1$^-$ cells. To test if the inhibition of GRM1 activation by an inhibitor of glutamatergic signaling, riluzole, in these mice inhibits the migration induction in these cells, TGS heterozygotes were treated daily with 10mg/kg riluzole for 18 weeks, blood was collected from each mouse and exosomes were isolated from blood plasma. The wound healing assays were performed as described above, with exosomes from both treated and untreated TGS mouse plasma exosomes. A reduction in migration ability was seen after 48 hours ($p<0.1$) in the C81-61 cells incubated with exosomes from riluzole treated heterozygote TGS when compared to those incubated with exosomes from untreated heterozygote TGS (Figure 19B).

Section IV. Discussion

The role of Metabotropic Glutamate Receptor 1 (GRM1) in the transformation of melanocytes has been clearly demonstrated and characterized by our group and others (*45, 58, 59*). However, its possible contribution to metastasis via nano-vesicles, exosomes, has not been investigated and is the overall goal of this thesis. In the first aim, we explored the role of GRM1 expression/function in levels of exosomes in melanoma. We used a pair of isogenic cell lines, C81-61 and C81-61-GRM1-6, which were derived from transfection of GRM1 cDNA into the C81-61 non-tumorigenic melanoma cell line. Transfection with GRM1 resulted in the transformation from a non-tumorigenic into an aggressive, tumorigenic cell line *in vivo* and *in vitro* (*66*). Previous reports from several groups have shown an increase in the quantity of exosomes released by aggressive, tumorigenic cell lines, when compared to their non-tumorigenic or normal counterparts (*142, 177, 185, 186*). However, our data using various methods to quantify exosomes did not detect a significant difference between the exosomes derived from non-tumorigenic C81-61 compared to those from the tumorigenic C81-61-GRM1 clone, despite the differences in phenotypes of these cells. This could be explained by insensitivity and variability of the methods used. We then altered the expression of GRM1 by inducible silencing RNA, we found no alteration in exosomal levels between control and cells with reduced GRM1 expression. We then applied inhibitors to modulate GRM1 activities, either a non-competitive inhibitor, Bay36-7620, or a functional

inhibitor, riluzole, and we observed the same results; there was no significant changes in the number of exosomes released by treated cells.

Although no alteration in the number of exosomes released was detected in cells with GRM1 expression, the sizes of the vesicles released by these cells were different with expression of the receptor. Data obtained with the Nanoparticle Tracking Analysis showed the majority of the exosomes shifted to a smaller diameter compared with the parental cells without exogenous GRM1. This shift in exosomal sizes could indicate a potential change in the cargo and/or function of the exosomes with GRM1 expression.

Tumor exosomes have been shown to play a role in the aggressive nature of cancer cells. They may accomplish these behaviors by transferring macromolecules from the originating cell to the recipient cells (*103, 191, 209, 210*). Melanoma cell derived exosomes have been shown to contain various determinants found in the cells they originated from. Several unique proteins only found in exosomes from highly metastatic melanoma cell lines have been identified; these proteins play various roles in cell motility, suggesting the exosomes have the capability of transferring pro-migratory proteins to the less aggressive cell lines (*212*). Additionally, exosomes containing a known marker of poor outcome for ovarian cancer (RNA-binding protein, LIN28) were shown to be present in recipient cells, resulting in the increase in production of proteins involved in Epithelial-to-Mesenchymal Transition (EMT), cell migration and invasion (*211*).

In addition to the ability of exosomes to promote the pro-metastatic behavior of migration, normal melanocytes become invasive when exposed to exosomes from melanoma cells (*213*). These results were very similar to earlier reports by others where the highly metastatic B16 melanoma cell (B16-F10) derived exosomes were shown to contain pro-metastatic protein, Met72, and that are taken up by the poorly metastatic clone of B16, B16-F1. Uptake of exosomes by the recipient cells results in the expression of Met72, causing cells to adopt metastatic abilities similar to the aggressive B16-F10 cells, sources of these exosomes (*214*).

The changes detected in exosomal sizes and the evidence in the literature of metastatic functions of exosomes prompted us to hypothesize that exosomal quality/function may also be altered by the expression of GRM1. In order to test this hypothesis, the non-aggressive GRM1$^-$ C81-61 cells were incubated with exosomes isolated from either GRM1$^-$ C81-61 or GRM1$^+$ C81-61-GRM1-6 cells. The increase in cell migration and cell invasion abilities, as well as colony formation in anchorage-independent condition were only detected in C81-61 treated with exosomes from GRM1$^+$ C81-61-GRM1-6 but not GRM1$^-$ C81-61 cells. The results suggested that the expression of GRM1 results in the alteration in functionality of the exosomes released by the cells.

To explore the notion that melanoma cells expressing GRM1 release exosomes that are functionally aggressive *in vivo*, we used the TGS mouse model. TGS mice aberrantly express GRM1 within their melanocytes, resulting in

spontaneous GRM1$^+$ melanoma skin lesions. If GRM1 activation by glutamate is required for the functional aggressiveness of the exosomes released by those lesions, the treatment of these animals with the GRM1 functional inhibitor, riluzole, may suppress the aggressiveness of the exosomes in circulation.

Blood was sampled from these mice throughout treatment to analyze the circulating exosome concentration. Exosome concentration was measured in a few different manners that are common methods of quantification; western blots with antibodies to specific exosome protein markers (CD63, CD9, CD81 and AliX) as well as quantification by nanoparticle tracking analysis (NTA). Interestingly, the initial measurement showed a significant reduction of the exosome protein marker CD63 in the circulating exosomes of the TGS mice treated with riluzole when compared to the vehicle and no treatment control mice. The samples were then analyzed by NTA, for confirmation of exosome reduction. However, the results using this method did not correlate with the CD63 data, and showed no change in exosome quantity. Additional exosome protein markers showed no consistent changes within the exosome quantity with treatment. The only consistency observed in this analysis was the increase in exosomes with age over all treatment groups. This increase was expected, as an increase in circulating exosome concentration with increasing age has been observed due to senescence-associated exosomal release (*251*).

Due to the inconsistencies on the measurement of exosome quantity by the different methods used, and the changes detected in mouse plasma exosome

sizes with treatment, it was hypothesized that, similar to the *in vitro* data, the composition and functionality of the exosomes are changed with GRM1 expression. To further explore this notion, exosomes from the tumor bearing heterozygous TGS blood plasma and from the non-tumor bearing wild type TGS blood plasma were isolated and incubated with GRM1$^-$ C81-61 cells. C81-61 cells that were incubated with the exosomes derived from heterozygote TGS blood plasma had an increased migratory ability when compared to those that were incubated with the wild type TGS blood plasma exosomes. Taken together, these results suggest that, similar to the *in vitro* data, functionality of the exosomes is altered when released from cells expressing GRM1. To further explore this notion, blood plasma exosomes isolated from heterozygotes TGS that have been treated daily with 10mg/kg riluzole were incubated with GRM1$^-$ C81-61 cells in migration assays. Cells that were incubated with exosomes isolated from riluzole-treated TGS had a reduced migratory ability when compared to those incubated with untreated exosomes. This suggests that the treatment with the functional inhibitor of GRM1 resulted in the reduction on GRM1 activity, thus restoring the non-aggressive phenotype observed in the wild type animals.

Melanoma metastasis occurs frequently in the lungs and brain (*5*), which are also common sites for metastasis within the aged TGS transgenic mice. Immunohistochemistry on the TGS lungs for a marker of pre-metastatic niche formation, fibronectin, indicated a significant decrease in positive-fibronectin staining in the TGS lungs of mice treated with riluzole when compared to the

untreated mice. Reduction in fibronectin, although to a lesser extent, was also seen in the vehicle treated TGS lungs. In this thesis I also assessed if there are toxicities associated with riluzole in mice *in vivo* at the concentration of 10mg/kg and long term dosing (daily for 18 weeks). There were no weight differences between treatment groups, nor abnormal liver histological pathologies. Additionally, no significant difference in pigmented lesion growth between groups was recorded, indicating that the tumor burden of the mice was consistent through the treatment groups.

Conclusion

Taken together, the results from this thesis suggest that the aggressive transformed phenotypes exhibited by cells aberrantly expressing GPCRs, such as GRM1, may be due to the release of exosomes that are functionally altered towards a more tumorigenic phenotype. This may result in effects on the physiology of the cells exposed to the exosomes, such as the surrounding stroma of the tumor, but also the cells present at sites of future metastasis, facilitating the recruitment of circulating tumor cells. Exosomes have been shown by several groups to participate in tumor progression, and little is known about the modifications that may occur within the tumor cells that results in the altered functions of exosomes released by the tumor cell. The data presented in this dissertation suggest that stimulation of GRM1 by its ligand, glutamate, initiates signaling cascades within the cell, stimulating various downstream effectors that modulate the formation and packaging. Thus the exosomes secreted from these cells, then modify the physiology of cells that come in contact with them. The precise mechanisms of alterations of the exosomal pathway due to GRM1 activation and subsequent signaling remain unknown. This association between GRM1 and the aggressiveness of the exosomes released by cells expressing GRM1 may provide hints to elucidate the aggressive nature of GRM1$^-$ expressing melanomas, and the role of exosomes in the metastatic potential.

Future Directions

In order to further explore the conclusions of this dissertation, investigating changes in functions of exosomes from GRM1$^+$ melanoma cells compared to GRM1$^-$ cells will provide knowledge towards understanding of the oncogenic activity of GRM1 in cell transformation and tumor formation. The ability of these exosomes to have such a profound influence on metastatic behavior of recipient cells suggests alterations in formation and/or packaging within the originating cell, prior to release.

Preliminary proteomic analyses by mass spectrometry of exosomes isolated from the two isogenic cell lines, C81-61 (non-tumorigenic) and C81-61 GRM1-6 (tumorigenic) show an approximate 20% difference in the number of identified proteins present in exosomes between these two lines. Exosomes from GRM1$^+$ cells contain over 500 additional proteins when compared to the exosomes derived from GRM1$^-$ cells, and exosomes isolated from GRM1$^-$ cells contain 200 proteins that are now no longer detectable in the exosomes from GRM1$^+$ cells. Based on these initial data, we suspect that the transfer of the aggressive characteristics by exosomes from GRM1$^+$ to GRM1$^-$ cells are likely the consequence of the differences in protein and/or RNA cargo delivered to the recipient cells. The differential in exosomal proteins could represent an increase in proteins that are involved in cell migration, invasion and potentially metastasis, delivered to recipient cells, while proteins involved in apoptosis or growth suppression were present in exosomes isolated from GRM1$^-$ cells. It will

be important to further analyze and prioritize these differentially expressed proteins and to validate the potential players in altered cell behavior. In addition to protein, miRNAs have been suggested to be important in regulating numerous cell functions. Potential miRNA candidates could also be confirmed and validated by genetic manipulation.

Identification, confirmation and validation of these putative candidates will provide avenues to elucidate mechanisms of exosomes in metastases. For example, horizontal transfer of proteins, RNAs, miRNAs are examples of critical components in initiating and establishing the metastatic niche for future metastases. In addition, these differentially expressed molecules could serve as noninvasive diagnostic markers in circulation to distinguish between healthy, early- and late-stage diseases, particularly for those cancers currently lacking noninvasive and reliable markers for diagnosis. For example, Glypican-1 (GPC1), a cell surface proteoglycan, was shown to be one such putative marker (*234*). GPC1 was shown to be enriched in cancer-cell-derived exosomes from the serum of patients and mice with cancer. Furthermore, GPC1-postitive exosomes were detected in the serum of pancreatic cancer patients and were shown to correlate with tumor burden and survival of patients. Detailed analyses on the differentially expressed protein identified by our preliminary proteomic profiling may identify markers that could distinguish between high and low metastatic potential in melanoma patients.

Immunohistochemistry performed with fibronectin, a marker of premetastatic niche formation, within the lung specimens of TGS mice showed differences in fibronectin deposition. The timeframe of 180 days of treatment in our study design was not long enough for a large number of metastatic lesions to occur in heterozygous TGS mice. In order to fully explore the consequences of daily treatment with riluzole, a blockade of glutamatergic signaling and formation of lung metastasis, the study design would need to be extended for a much longer time period.

As with the nature of science, many more questions arise with novel results. I conclude that GRM1 expression and activity are not sufficient to alter the quantity of exosomes but are sufficient to change the characteristics and functions of the released exosomes. Elucidation of the precise mechanisms and how this occurs will require further studies.

References

1. A. Jemal *et al.*, Cancer statistics, 2004. *CA Cancer J Clin* **54**, 8-29 (2004).
2. R. L. Siegel, K. D. Miller, A. Jemal, Cancer Statistics, 2017. *CA Cancer J Clin* **67**, 7-30 (2017).
3. R. L. Siegel, K. D. Miller, A. Jemal, Cancer statistics, 2016. *CA Cancer J Clin* **66**, 7-30 (2016).
4. C. M. Balch *et al.*, Final version of 2009 AJCC melanoma staging and classification. *J Clin Oncol* **27**, 6199-6206 (2009).
5. S. Osella-Abate *et al.*, Risk factors related to late metastases in 1,372 melanoma patients disease free more than 10 years. *Int J Cancer* **136**, 2453-2457 (2015).
6. M. Cichorek, M. Wachulska, A. Stasiewicz, A. Tyminska, Skin melanocytes: biology and development. *Postepy Dermatol Alergol* **30**, 30-41 (2013).
7. M. Brenner, V. J. Hearing, The protective role of melanin against UV damage in human skin. *Photochem Photobiol* **84**, 539-549 (2008).
8. D. Kuk *et al.*, Prognosis of Mucosal, Uveal, Acral, Nonacral Cutaneous, and Unknown Primary Melanoma From the Time of First Metastasis. *Oncologist* **21**, 848-854 (2016).
9. D. K. Wilkins, P. D. Nathan, Therapeutic opportunities in noncutaneous melanoma. *Ther Adv Med Oncol* **1**, 29-36 (2009).
10. J. A. Curtin *et al.*, Distinct sets of genetic alterations in melanoma. *N Engl J Med* **353**, 2135-2147 (2005).
11. H. Davies *et al.*, Mutations of the BRAF gene in human cancer. *Nature* **417**, 949-954 (2002).
12. P. M. Pollock *et al.*, High frequency of BRAF mutations in nevi. *Nat Genet* **33**, 19-20 (2003).
13. J. Wangari-Talbot, S. Chen, Genetics of melanoma. *Frontiers in genetics* **3**, 330 (2012).
14. J. A. Jakob *et al.*, NRAS mutation status is an independent prognostic factor in metastatic melanoma. *Cancer* **118**, 4014-4023 (2012).
15. D. Dankort *et al.*, Braf(V600E) cooperates with Pten loss to induce metastatic melanoma. *Nat Genet* **41**, 544-552 (2009).
16. L. Jimenez-Garcia, S. Herranz, M. A. Higueras, A. Luque, S. Hortelano, Tumor suppressor ARF regulates tissue microenvironment and tumor growth through modulation of macrophage polarization. *Oncotarget*, (2016).
17. C. D. Van Raamsdonk *et al.*, Frequent somatic mutations of GNAQ in uveal melanoma and blue naevi. *Nature* **457**, 599-602 (2009).
18. W. Zhao *et al.*, The Long Noncoding RNA SPRIGHTLY Regulates Cell Proliferation in Primary Human Melanocytes. *J Invest Dermatol* **136**, 819-828 (2016).
19. C. R. Gasque Schoof, A. Izzotti, M. G. Jasiulionis, R. Vasques Ldos, The Roles of miR-26, miR-29, and miR-203 in the Silencing of the Epigenetic Machinery during Melanocyte Transformation. *Biomed Res Int* **2015**, 634749 (2015).
20. A. Gajos-Michniewicz, M. Duechler, M. Czyz, MiRNA in melanoma-derived exosomes. *Cancer Lett* **347**, 29-37 (2014).
21. S. Chen, H. Zhu, W. J. Wetzel, M. A. Philbert, Spontaneous melanocytosis in transgenic mice. *J Invest Dermatol* **106**, 1145-1151 (1996).
22. H. Zhu *et al.*, Development of heritable melanoma in transgenic mice. *J Invest Dermatol* **110**, 247-252 (1998).
23. E. S. Lander *et al.*, Initial sequencing and analysis of the human genome. *Nature* **409**, 860-921 (2001).
24. J. C. Venter *et al.*, The sequence of the human genome. *Science* **291**, 1304-1351 (2001).
25. T. K. Attwood, J. B. Findlay, Fingerprinting G-protein-coupled receptors. *Protein Eng* **7**, 195-203 (1994).
26. L. F. Kolakowski, Jr., GCRDb: a G-protein-coupled receptor database. *Receptors Channels* **2**, 1-7 (1994).
27. R. Fredriksson, M. C. Lagerstrom, L. G. Lundin, H. B. Schioth, The G-protein-coupled receptors in the human genome form five main families. Phylogenetic analysis, paralogon groups, and fingerprints. *Mol Pharmacol* **63**, 1256-1272 (2003).
28. M. C. Lagerstrom, H. B. Schioth, Structural diversity of G protein-coupled receptors and significance for drug discovery. *Nat Rev Drug Discov* **7**, 339-357 (2008).

29. H. E. Hamm, The many faces of G protein signaling. *J Biol Chem* **273**, 669-672 (1998).
30. M. Bunemann, M. Frank, M. J. Lohse, Gi protein activation in intact cells involves subunit rearrangement rather than dissociation. *Proc Natl Acad Sci U S A* **100**, 16077-16082 (2003).
31. R. Lappano, M. Maggiolini, G protein-coupled receptors: novel targets for drug discovery in cancer. *Nat Rev Drug Discov* **10**, 47-60 (2011).
32. H. J. Lee, B. Wall, S. Chen, G-protein-coupled receptors and melanoma. *Pigment Cell Melanoma Res* **21**, 415-428 (2008).
33. A. M. Spiegel, Defects in G protein-coupled signal transduction in human disease. *Annu Rev Physiol* **58**, 143-170 (1996).
34. J. A. Hata, W. J. Koch, Phosphorylation of G protein-coupled receptors: GPCR kinases in heart disease. *Mol Interv* **3**, 264-272 (2003).
35. A. M. Spiegel, Mutations in G proteins and G protein-coupled receptors in endocrine disease. *J Clin Endocrinol Metab* **81**, 2434-2442 (1996).
36. S. Ozawa, H. Kamiya, K. Tsuzuki, Glutamate receptors in the mammalian central nervous system. *Prog Neurobiol* **54**, 581-618 (1998).
37. M. R. Bennett, V. J. Balcar, Forty years of amino acid transmission in the brain. *Neurochem Int* **35**, 269-280 (1999).
38. J. P. Pin, F. Acher, The metabotropic glutamate receptors: structure, activation mechanism and pharmacology. *Curr Drug Targets CNS Neurol Disord* **1**, 297-317 (2002).
39. H. S. Haas *et al.*, The non-competitive metabotropic glutamate receptor-1 antagonist CPCCOEt inhibits the in vitro growth of human melanoma. *Oncol Rep* **17**, 1399-1404 (2007).
40. T. K. Bjarnadottir, R. Fredriksson, H. B. Schioth, The gene repertoire and the common evolutionary history of glutamate, pheromone (V2R), taste(1) and other related G protein-coupled receptors. *Gene* **362**, 70-84 (2005).
41. H. Wu *et al.*, Structure of a class C GPCR metabotropic glutamate receptor 1 bound to an allosteric modulator. *Science* **344**, 58-64 (2014).
42. S. Nakanishi, Molecular diversity of glutamate receptors and implications for brain function. *Science* **258**, 597-603 (1992).
43. J. L. Teh, S. Chen, Glutamatergic signaling in cellular transformation. *Pigment Cell Melanoma Res* **25**, 331-342 (2012).
44. A. G. Gilman, G proteins: transducers of receptor-generated signals. *Annu Rev Biochem* **56**, 615-649 (1987).
45. Y. E. Marin, S. Chen, Involvement of metabotropic glutamate receptor 1, a G protein coupled receptor, in melanoma development. *Journal of molecular medicine* **82**, 735-749 (2004).
46. E. Hermans, R. A. Challiss, Structural, signalling and regulatory properties of the group I metabotropic glutamate receptors: prototypic family C G-protein-coupled receptors. *Biochem J* **359**, 465-484 (2001).
47. A. C. Newton, Protein kinase C: structural and spatial regulation by phosphorylation, cofactors, and macromolecular interactions. *Chem Rev* **101**, 2353-2364 (2001).
48. Y. Ueda *et al.*, Protein kinase C activates the MEK-ERK pathway in a manner independent of Ras and dependent on Raf. *J Biol Chem* **271**, 23512-23519 (1996).
49. L. J. Yu, B. A. Wall, J. Wangari-Talbot, S. Chen, Metabotropic glutamate receptors in cancer. *Neuropharmacology*, (2016).
50. R. Busca *et al.*, Ras mediates the cAMP-dependent activation of extracellular signal-regulated kinases (ERKs) in melanocytes. *EMBO J* **19**, 2900-2910 (2000).
51. R. Busca, R. Ballotti, Cyclic AMP a key messenger in the regulation of skin pigmentation. *Pigment Cell Res* **13**, 60-69 (2000).
52. S. Thandi, J. L. Blank, R. A. Challiss, Group-I metabotropic glutamate receptors, mGlu1a and mGlu5a, couple to extracellular signal-regulated kinase (ERK) activation via distinct, but overlapping, signalling pathways. *J Neurochem* **83**, 1139-1153 (2002).
53. A. Stepulak *et al.*, Expression of glutamate receptor subunits in human cancers. *Histochem Cell Biol* **132**, 435-445 (2009).
54. Y. E. Marin *et al.*, Stimulation of oncogenic metabotropic glutamate receptor 1 in melanoma cells activates ERK1/2 via PKCepsilon. *Cell Signal* **18**, 1279-1286 (2006).

55. D. Julius, T. J. Livelli, T. M. Jessell, R. Axel, Ectopic expression of the serotonin 1c receptor and the triggering of malignant transformation. *Science* **244**, 1057-1062 (1989).
56. D. Young, G. Waitches, C. Birchmeier, O. Fasano, M. Wigler, Isolation and characterization of a new cellular oncogene encoding a protein with multiple potential transmembrane domains. *Cell* **45**, 711-719 (1986).
57. C. D. Van Raamsdonk, K. R. Fitch, H. Fuchs, M. H. de Angelis, G. S. Barsh, Effects of G-protein mutations on skin color. *Nat Genet* **36**, 961-968 (2004).
58. Y. Ohtani *et al.*, Metabotropic glutamate receptor subtype-1 is essential for in vivo growth of melanoma. *Oncogene* **27**, 7162-7170 (2008).
59. P. M. Pollock *et al.*, Melanoma mouse model implicates metabotropic glutamate signaling in melanocytic neoplasia. *Nat Genet* **34**, 108-112 (2003).
60. S. S. Shin *et al.*, Oncogenic activities of metabotropic glutamate receptor 1 (Grm1) in melanocyte transformation. *Pigment Cell Melanoma Res* **21**, 368-378 (2008).
61. Y. Funasaka, T. Harada, A. Aiba, C. Nishigori, Expression of metabotropic glutamate receptor 1 and phosphorylated extracellular signal-regulated kinase 1/2 proteins in human melanocytic lesions. *Pigment Cell Melanoma Res* **19**, (2006).
62. J. Namkoong *et al.*, Metabotropic glutamate receptor 1 and glutamate signaling in human melanoma. *Cancer research* **67**, 2298-2305 (2007).
63. J. L. Teh *et al.*, Metabotropic glutamate receptor 1 mediates melanocyte transformation via transactivation of insulin-like growth factor 1 receptor. *Pigment Cell Melanoma Res* **27**, 621-629 (2014).
64. P. Casellas, CB2, a paradigm for a novel class of "onco-GPCRs"? *Blood* **104**, (2004).
65. N. Kuzumaki *et al.*, Multiple analyses of G-protein coupled receptor (GPCR) expression in the development of gefitinib-resistance in transforming non-small-cell lung cancer. *PloS one* **7**, e44368 (2012).
66. Y. Wen *et al.*, Activation of the glutamate receptor GRM1 enhances angiogenic signaling to drive melanoma progression. *Cancer research* **74**, 2499-2509 (2014).
67. J. A. McCubrey *et al.*, Ras/Raf/MEK/ERK and PI3K/PTEN/Akt/mTOR cascade inhibitors: how mutations can result in therapy resistance and how to overcome resistance. *Oncotarget* **3**, 1068-1111 (2012).
68. M. Beloueche-Babari *et al.*, Acute tumour response to the MEK1/2 inhibitor selumetinib (AZD6244, ARRY-142886) evaluated by non-invasive diffusion-weighted MRI. *British journal of cancer* **109**, 1562-1569 (2013).
69. G. Hatzivassiliou *et al.*, ERK inhibition overcomes acquired resistance to MEK inhibitors. *Mol Cancer Ther* **11**, 1143-1154 (2012).
70. A. T. Baines, D. Xu, C. J. Der, Inhibition of Ras for cancer treatment: the search continues. *Future Med Chem* **3**, 1787-1808 (2011).
71. G. Zhu *et al.*, Combination with gamma-secretase inhibitor prolongs treatment efficacy of BRAF inhibitor in BRAF-mutated melanoma cells. *Cancer Lett* **376**, 43-52 (2016).
72. M. Damo, D. S. Wilson, E. Simeoni, J. A. Hubbell, TLR-3 stimulation improves anti-tumor immunity elicited by dendritic cell exosome-based vaccines in a murine model of melanoma. *Sci Rep* **5**, 17622 (2015).
73. P. A. Ott, F. S. Hodi, C. Robert, CTLA-4 and PD-1/PD-L1 blockade: new immunotherapeutic modalities with durable clinical benefit in melanoma patients. *Clin Cancer Res* **19**, 5300-5309 (2013).
74. J. M. Taube *et al.*, Colocalization of inflammatory response with B7-h1 expression in human melanocytic lesions supports an adaptive resistance mechanism of immune escape. *Sci Transl Med* **4**, 127ra137 (2012).
75. M. E. Keir, M. J. Butte, G. J. Freeman, A. H. Sharpe, PD-1 and its ligands in tolerance and immunity. *Annu Rev Immunol* **26**, 677-704 (2008).
76. S. L. Topalian *et al.*, Safety, activity, and immune correlates of anti-PD-1 antibody in cancer. *N Engl J Med* **366**, 2443-2454 (2012).
77. H. Mirzaei *et al.*, Curcumin: A new candidate for melanoma therapy? *Int J Cancer* **139**, 1683-1695 (2016).

78. J. A. Bush, K. J. Cheung, Jr., G. Li, Curcumin induces apoptosis in human melanoma cells through a Fas receptor/caspase-8 pathway independent of p53. *Exp Cell Res* **271**, 305-314 (2001).
79. Y. Lu *et al.*, Curcumin Micelles Remodel Tumor Microenvironment and Enhance Vaccine Activity in an Advanced Melanoma Model. *Mol Ther* **24**, 364-374 (2016).
80. L. Van Den Bosch, P. Van Damme, E. Bogaert, W. Robberecht, The role of excitotoxicity in the pathogenesis of amyotrophic lateral sclerosis. *Biochim Biophys Acta* **1762**, 1068-1082 (2006).
81. B. D. Kretschmer, U. Kratzer, W. J. Schmidt, Riluzole, a glutamate release inhibitor, and motor behavior. *Naunyn Schmiedebergs Arch Pharmacol* **358**, 181-190 (1998).
82. E. Fumagalli, M. Funicello, T. Rauen, M. Gobbi, T. Mennini, Riluzole enhances the activity of glutamate transporters GLAST, GLT1 and EAAC1. *Eur J Pharmacol* **578**, 171-176 (2008).
83. S. J. Wang, K. Y. Wang, W. C. Wang, Mechanisms underlying the riluzole inhibition of glutamate release from rat cerebral cortex nerve terminals (synaptosomes). *Neuroscience* **125**, 191-201 (2004).
84. N. Nagoshi, H. Nakashima, M. G. Fehlings, Riluzole as a neuroprotective drug for spinal cord injury: from bench to bedside. *Molecules* **20**, 7775-7789 (2015).
85. D. Martin, M. A. Thompson, J. V. Nadler, The neuroprotective agent riluzole inhibits release of glutamate and aspartate from slices of hippocampal area CA1. *Eur J Pharmacol* **250**, 473-476 (1993).
86. A. Le Liboux *et al.*, A comparison of the pharmacokinetics and tolerability of riluzole after repeat dose administration in healthy elderly and young volunteers. *J Clin Pharmacol* **39**, 480-486 (1999).
87. A. Le Liboux *et al.*, Single- and multiple-dose pharmacokinetics of riluzole in white subjects. *J Clin Pharmacol* **37**, 820-827 (1997).
88. H. M. Bryson, B. Fulton, P. Benfield, Riluzole. A review of its pharmacodynamic and pharmacokinetic properties and therapeutic potential in amyotrophic lateral sclerosis. *Drugs* **52**, 549-563 (1996).
89. D. Yip *et al.*, A phase 0 trial of riluzole in patients with resectable stage III and IV melanoma. *Clin Cancer Res* **15**, 3896-3902 (2009).
90. P. Mehlen, A. Puisieux, Metastasis: a question of life or death. *Nat Rev Cancer* **6**, 449-458 (2006).
91. I. J. Fidler, I. R. Hart, Biological diversity in metastatic neoplasms: origins and implications. *Science* **217**, 998-1003 (1982).
92. B. U. Pauli, D. E. Schwartz, E. J. Thonar, K. E. Kuettner, Tumor invasion and host extracellular matrix. *Cancer Metastasis Rev* **2**, 129-152 (1983).
93. L. A. Liotta, W. G. Stetler-Stevenson, Tumor invasion and metastasis: an imbalance of positive and negative regulation. *Cancer research* **51**, 5054s-5059s (1991).
94. D. Hanahan, R. A. Weinberg, Hallmarks of cancer: the next generation. *Cell* **144**, 646-674 (2011).
95. G. Poste, I. J. Fidler, The pathogenesis of cancer metastasis. *Nature* **283**, 139-146 (1980).
96. I. J. Fidler, The pathogenesis of cancer metastasis: the 'seed and soil' hypothesis revisited. *Nat Rev Cancer* **3**, 453-458 (2003).
97. M. J. van de Vijver *et al.*, A gene-expression signature as a predictor of survival in breast cancer. *N Engl J Med* **347**, 1999-2009 (2002).
98. A. J. Minn *et al.*, Genes that mediate breast cancer metastasis to lung. *Nature* **436**, 518-524 (2005).
99. Y. Kang *et al.*, A multigenic program mediating breast cancer metastasis to bone. *Cancer Cell* **3**, 537-549 (2003).
100. R. N. Kaplan *et al.*, VEGFR1-positive haematopoietic bone marrow progenitors initiate the pre-metastatic niche. *Nature* **438**, 820-827 (2005).
101. J. A. Joyce, J. W. Pollard, Microenvironmental regulation of metastasis. *Nat Rev Cancer* **9**, 239-252 (2009).
102. T. Guise, Examining the metastatic niche: targeting the microenvironment. *Seminars in oncology* **37 Suppl 2**, S2-14 (2010).

103. H. Peinado *et al.*, Melanoma exosomes educate bone marrow progenitor cells toward a pro-metastatic phenotype through MET. *Nature medicine* **18**, 883-891 (2012).
104. J. T. Erler *et al.*, Hypoxia-induced lysyl oxidase is a critical mediator of bone marrow cell recruitment to form the premetastatic niche. *Cancer Cell* **15**, 35-44 (2009).
105. J. T. O'Connell *et al.*, VEGF-A and Tenascin-C produced by S100A4+ stromal cells are important for metastatic colonization. *Proc Natl Acad Sci U S A* **108**, 16002-16007 (2011).
106. J. C. Tse, R. Kalluri, Mechanisms of metastasis: epithelial-to-mesenchymal transition and contribution of tumor microenvironment. *J Cell Biochem* **101**, 816-829 (2007).
107. I. Kii *et al.*, Incorporation of tenascin-C into the extracellular matrix by periostin underlies an extracellular meshwork architecture. *J Biol Chem* **285**, 2028-2039 (2010).
108. Z. Wang, G. Ouyang, Periostin: a bridge between cancer stem cells and their metastatic niche. *Cell Stem Cell* **10**, 111-112 (2012).
109. D. Gao *et al.*, Myeloid progenitor cells in the premetastatic lung promote metastases by inducing mesenchymal to epithelial transition. *Cancer research* **72**, 1384-1394 (2012).
110. Y. Huang *et al.*, Pulmonary vascular destabilization in the premetastatic phase facilitates lung metastasis. *Cancer research* **69**, 7529-7537 (2009).
111. R. N. Kaplan, S. Rafii, D. Lyden, Preparing the "soil": the premetastatic niche. *Cancer research* **66**, 11089-11093 (2006).
112. J. A. Burger, A. Spoo, A. Dwenger, M. Burger, D. Behringer, CXCR4 chemokine receptors (CD184) and alpha4beta1 integrins mediate spontaneous migration of human CD34+ progenitors and acute myeloid leukaemia cells beneath marrow stromal cells (pseudoemperipolesis). *Br J Haematol* **122**, 579-589 (2003).
113. P. Huhtala *et al.*, Cooperative signaling by alpha 5 beta 1 and alpha 4 beta 1 integrins regulates metalloproteinase gene expression in fibroblasts adhering to fibronectin. *The Journal of cell biology* **129**, 867-879 (1995).
114. V. P. Yakubenko, R. R. Lobb, E. F. Plow, T. P. Ugarova, Differential induction of gelatinase B (MMP-9) and gelatinase A (MMP-2) in T lymphocytes upon alpha(4)beta(1)-mediated adhesion to VCAM-1 and the CS-1 peptide of fibronectin. *Exp Cell Res* **260**, 73-84 (2000).
115. B. Heissig *et al.*, Recruitment of stem and progenitor cells from the bone marrow niche requires MMP-9 mediated release of kit-ligand. *Cell* **109**, 625-637 (2002).
116. G. Bergers *et al.*, Matrix metalloproteinase-9 triggers the angiogenic switch during carcinogenesis. *Nat Cell Biol* **2**, 737-744 (2000).
117. S. Hiratsuka, A. Watanabe, H. Aburatani, Y. Maru, Tumour-mediated upregulation of chemoattractants and recruitment of myeloid cells predetermines lung metastasis. *Nat Cell Biol* **8**, 1369-1375 (2006).
118. C. Thery, L. Zitvogel, S. Amigorena, Exosomes: composition, biogenesis and function. *Nature reviews. Immunology* **2**, 569-579 (2002).
119. F. Andre *et al.*, Malignant effusions and immunogenic tumour-derived exosomes. *Lancet* **360**, 295-305 (2002).
120. D. D. Taylor, C. Gercel-Taylor, MicroRNA signatures of tumor-derived exosomes as diagnostic biomarkers of ovarian cancer. *Gynecol Oncol* **110**, 13-21 (2008).
121. T. Pisitkun, R. F. Shen, M. A. Knepper, Identification and proteomic profiling of exosomes in human urine. *Proc Natl Acad Sci U S A* **101**, 13368-13373 (2004).
122. M. Gonzalez-Begne *et al.*, Proteomic analysis of human parotid gland exosomes by multidimensional protein identification technology (MudPIT). *Journal of proteome research* **8**, 1304-1314 (2009).
123. M. P. Caby, D. Lankar, C. Vincendeau-Scherrer, G. Raposo, C. Bonnerot, Exosomal-like vesicles are present in human blood plasma. *Int Immunol* **17**, 879-887 (2005).
124. C. Admyre *et al.*, Exosomes with immune modulatory features are present in human breast milk. *Journal of immunology* **179**, 1969-1978 (2007).
125. J. L. Gatti, S. Metayer, M. Belghazi, F. Dacheux, J. L. Dacheux, Identification, proteomic profiling, and origin of ram epididymal fluid exosome-like vesicles. *Biol Reprod* **72**, 1452-1465 (2005).
126. S. Keller *et al.*, CD24 is a marker of exosomes secreted into urine and amniotic fluid. *Kidney Int* **72**, 1095-1102 (2007).

127. J. C. da Silveira, D. N. Veeramachaneni, Q. A. Winger, E. M. Carnevale, G. J. Bouma, Cell-secreted vesicles in equine ovarian follicular fluid contain miRNAs and proteins: a possible new form of cell communication within the ovarian follicle. *Biol Reprod* **86**, 71 (2012).
128. F. Andre *et al.*, Tumor-derived exosomes: a new source of tumor rejection antigens. *Vaccine* **20 Suppl 4**, A28-31 (2002).
129. W. Stoorvogel, M. J. Kleijmeer, H. J. Geuze, G. Raposo, The biogenesis and functions of exosomes. *Traffic* **3**, 321-330 (2002).
130. R. Valenti *et al.*, Tumor-released microvesicles as vehicles of immunosuppression. *Cancer research* **67**, 2912-2915 (2007).
131. C. Thery *et al.*, Molecular characterization of dendritic cell-derived exosomes. Selective accumulation of the heat shock protein hsc73. *The Journal of cell biology* **147**, 599-610 (1999).
132. C. Thery *et al.*, Proteomic analysis of dendritic cell-derived exosomes: a secreted subcellular compartment distinct from apoptotic vesicles. *Journal of immunology* **166**, 7309-7318 (2001).
133. G. Raposo *et al.*, B lymphocytes secrete antigen-presenting vesicles. *J Exp Med* **183**, 1161-1172 (1996).
134. J. M. Escola *et al.*, Selective enrichment of tetraspan proteins on the internal vesicles of multivesicular endosomes and on exosomes secreted by human B-lymphocytes. *J Biol Chem* **273**, 20121-20127 (1998).
135. G. van Niel *et al.*, Intestinal epithelial cells secrete exosome-like vesicles. *Gastroenterology* **121**, 337-349 (2001).
136. B. Fevrier, G. Raposo, Exosomes: endosomal-derived vesicles shipping extracellular messages. *Current opinion in cell biology* **16**, 415-421 (2004).
137. B. Hugel, M. C. Martinez, C. Kunzelmann, J. M. Freyssinet, Membrane microparticles: two sides of the coin. *Physiology (Bethesda)* **20**, 22-27 (2005).
138. L. L. Horstman, W. Jy, J. J. Jimenez, C. Bidot, Y. S. Ahn, New horizons in the analysis of circulating cell-derived microparticles. *Keio J Med* **53**, 210-230 (2004).
139. J. Cai, G. Wu, P. A. Jose, C. Zeng, Functional transferred DNA within extracellular vesicles. *Exp Cell Res* **349**, 179-183 (2016).
140. M. Daly, L. O'Driscoll, MicroRNA Profiling of Exosomes. *Methods in molecular biology* **1509**, 37-46 (2017).
141. L. Zhang *et al.*, Microenvironment-induced PTEN loss by exosomal microRNA primes brain metastasis outgrowth. *Nature* **527**, 100-104 (2015).
142. M. Baj-Krzyworzeka *et al.*, Tumour-derived microvesicles carry several surface determinants and mRNA of tumour cells and transfer some of these determinants to monocytes. *Cancer Immunol Immunother* **55**, 808-818 (2006).
143. A. Zomer *et al.*, In Vivo imaging reveals extracellular vesicle-mediated phenocopying of metastatic behavior. *Cell* **161**, 1046-1057 (2015).
144. J. Skog *et al.*, Glioblastoma microvesicles transport RNA and proteins that promote tumour growth and provide diagnostic biomarkers. *Nat Cell Biol* **10**, 1470-1476 (2008).
145. H. F. Heijnen, A. E. Schiel, R. Fijnheer, H. J. Geuze, J. J. Sixma, Activated platelets release two types of membrane vesicles: microvesicles by surface shedding and exosomes derived from exocytosis of multivesicular bodies and alpha-granules. *Blood* **94**, 3791-3799 (1999).
146. P. J. Peters *et al.*, Cytotoxic T lymphocyte granules are secretory lysosomes, containing both perforin and granzymes. *J Exp Med* **173**, 1099-1109 (1991).
147. C. Kahlert *et al.*, Identification of double-stranded genomic DNA spanning all chromosomes with mutated KRAS and p53 DNA in the serum exosomes of patients with pancreatic cancer. *J Biol Chem* **289**, 3869-3875 (2014).
148. C. Harding, J. Heuser, P. Stahl, Receptor-mediated endocytosis of transferrin and recycling of the transferrin receptor in rat reticulocytes. *The Journal of cell biology* **97**, 329-339 (1983).
149. B. T. Pan, K. Teng, C. Wu, M. Adam, R. M. Johnstone, Electron microscopic evidence for externalization of the transferrin receptor in vesicular form in sheep reticulocytes. *The Journal of cell biology* **101**, 942-948 (1985).

150. R. Lipowsky, Spontaneous tubulation of membranes and vesicles reveals membrane tension generated by spontaneous curvature. *Faraday Discuss* **161**, 305-331; discussion 419-359 (2013).
151. M. G. Ford *et al.*, Curvature of clathrin-coated pits driven by epsin. *Nature* **419**, 361-366 (2002).
152. K. Takei, V. I. Slepnev, V. Haucke, P. De Camilli, Functional partnership between amphiphysin and dynamin in clathrin-mediated endocytosis. *Nat Cell Biol* **1**, 33-39 (1999).
153. B. J. Peter *et al.*, BAR domains as sensors of membrane curvature: the amphiphysin BAR structure. *Science* **303**, 495-499 (2004).
154. K. Farsad *et al.*, Generation of high curvature membranes mediated by direct endophilin bilayer interactions. *The Journal of cell biology* **155**, 193-200 (2001).
155. Q. Wang *et al.*, Molecular mechanism of membrane constriction and tubulation mediated by the F-BAR protein Pacsin/Syndapin. *Proc Natl Acad Sci U S A* **106**, 12700-12705 (2009).
156. K. Trajkovic *et al.*, Ceramide triggers budding of exosome vesicles into multivesicular endosomes. *Science* **319**, 1244-1247 (2008).
157. J. H. Hurley, P. I. Hanson, Membrane budding and scission by the ESCRT machinery: it's all in the neck. *Nat Rev Mol Cell Biol* **11**, 556-566 (2010).
158. S. Peel, P. Macheboeuf, N. Martinelli, W. Weissenhorn, Divergent pathways lead to ESCRT-III-catalyzed membrane fission. *Trends Biochem Sci* **36**, 199-210 (2011).
159. W. M. Henne, H. Stenmark, S. D. Emr, Molecular mechanisms of the membrane sculpting ESCRT pathway. *Cold Spring Harb Perspect Biol* **5**, (2013).
160. J. McCullough, L. A. Colf, W. I. Sundquist, Membrane fission reactions of the mammalian ESCRT pathway. *Annu Rev Biochem* **82**, 663-692 (2013).
161. J. H. Hurley, G. Odorizzi, Get on the exosome bus with ALIX. *Nat Cell Biol* **14**, 654-655 (2012).
162. M. F. Baietti *et al.*, Syndecan-syntenin-ALIX regulates the biogenesis of exosomes. *Nat Cell Biol* **14**, 677-685 (2012).
163. D. J. Katzmann, M. Babst, S. D. Emr, Ubiquitin-dependent sorting into the multivesicular body pathway requires the function of a conserved endosomal protein sorting complex, ESCRT-I. *Cell* **106**, 145-155 (2001).
164. C. E. Futter, A. Pearse, L. J. Hewlett, C. R. Hopkins, Multivesicular endosomes containing internalized EGF-EGF receptor complexes mature and then fuse directly with lysosomes. *The Journal of cell biology* **132**, 1011-1023 (1996).
165. V. Hyenne *et al.*, RAL-1 controls multivesicular body biogenesis and exosome secretion. *The Journal of cell biology* **211**, 27-37 (2015).
166. M. Ostrowski *et al.*, Rab27a and Rab27b control different steps of the exosome secretion pathway. *Nat Cell Biol* **12**, 19-30; sup pp 11-13 (2010).
167. C. Hsu *et al.*, Regulation of exosome secretion by Rab35 and its GTPase-activating proteins TBC1D10A-C. *The Journal of cell biology* **189**, 223-232 (2010).
168. A. Savina, M. Furlan, M. Vidal, M. I. Colombo, Exosome release is regulated by a calcium-dependent mechanism in K562 cells. *J Biol Chem* **278**, 20083-20090 (2003).
169. I. Parolini *et al.*, Microenvironmental pH is a key factor for exosome traffic in tumor cells. *J Biol Chem* **284**, 34211-34222 (2009).
170. X. Yu, S. L. Harris, A. J. Levine, The regulation of exosome secretion: a novel function of the p53 protein. *Cancer research* **66**, 4795-4801 (2006).
171. A. Lespagnol *et al.*, Exosome secretion, including the DNA damage-induced p53-dependent secretory pathway, is severely compromised in TSAP6/Steap3-null mice. *Cell death and differentiation* **15**, 1723-1733 (2008).
172. C. A. Thompson, A. Purushothaman, V. C. Ramani, I. Vlodavsky, R. D. Sanderson, Heparanase regulates secretion, composition, and function of tumor cell-derived exosomes. *J Biol Chem* **288**, 10093-10099 (2013).
173. M. Miyanishi *et al.*, Identification of Tim4 as a phosphatidylserine receptor. *Nature* **450**, 435-439 (2007).
174. C. Escrevente, S. Keller, P. Altevogt, J. Costa, Interaction and uptake of exosomes by ovarian cancer cells. *BMC Cancer* **11**, 108 (2011).

175. E. Segura, S. Amigorena, C. Thery, Mature dendritic cells secrete exosomes with strong ability to induce antigen-specific effector immune responses. *Blood cells, molecules & diseases* **35**, 89-93 (2005).
176. H. C. Christianson, K. J. Svensson, T. H. van Kuppevelt, J. P. Li, M. Belting, Cancer cell exosomes depend on cell-surface heparan sulfate proteoglycans for their internalization and functional activity. *Proc Natl Acad Sci U S A* **110**, 17380-17385 (2013).
177. H. Valadi *et al.*, Exosome-mediated transfer of mRNAs and microRNAs is a novel mechanism of genetic exchange between cells. *Nat Cell Biol* **9**, 654-659 (2007).
178. L. Czernek, A. Chworos, M. Duechler, The Uptake of Extracellular Vesicles is Affected by the Differentiation Status of Myeloid Cells. *Scandinavian journal of immunology* **82**, 506-514 (2015).
179. A. L. Isola, S. Chen, Exosomes: The Messengers of Health and Disease. *Curr Neuropharmacol* **15**, 157-165 (2017).
180. I. Cestari, E. Ansa-Addo, P. Deolindo, J. M. Inal, M. I. Ramirez, Trypanosoma cruzi immune evasion mediated by host cell-derived microvesicles. *Journal of immunology* **188**, 1942-1952 (2012).
181. L. J. Vella, R. A. Sharples, R. M. Nisbet, R. Cappai, A. F. Hill, The role of exosomes in the processing of proteins associated with neurodegenerative diseases. *European biophysics journal : EBJ* **37**, 323-332 (2008).
182. A. I. Masyuk, T. V. Masyuk, N. F. Larusso, Exosomes in the pathogenesis, diagnostics and therapeutics of liver diseases. *Journal of hepatology* **59**, 621-625 (2013).
183. J. Halkein *et al.*, MicroRNA-146a is a therapeutic target and biomarker for peripartum cardiomyopathy. *The Journal of clinical investigation* **123**, 2143-2154 (2013).
184. B. N. Hannafon, W. Q. Ding, Intercellular Communication by Exosome-Derived microRNAs in Cancer. *International journal of molecular sciences* **14**, 14240-14269 (2013).
185. V. Huber, P. Filipazzi, M. Iero, S. Fais, L. Rivoltini, More insights into the immunosuppressive potential of tumor exosomes. *J Transl Med* **6**, 63 (2008).
186. M. Iero *et al.*, Tumour-released exosomes and their implications in cancer immunity. *Cell death and differentiation* **15**, 80-88 (2008).
187. J. L. Hood *et al.*, Paracrine induction of endothelium by tumor exosomes. *Laboratory investigation; a journal of technical methods and pathology* **89**, 1317-1328 (2009).
188. J. L. Hood, R. S. San, S. A. Wickline, Exosomes released by melanoma cells prepare sentinel lymph nodes for tumor metastasis. *Cancer research* **71**, 3792-3801 (2011).
189. K. Meehan, L. J. Vella, The contribution of tumour-derived exosomes to the hallmarks of cancer. *Crit Rev Clin Lab Sci* **53**, 121-131 (2016).
190. J. M. Aliotta *et al.*, Alteration of marrow cell gene expression, protein production, and engraftment into lung by lung-derived microvesicles: a novel mechanism for phenotype modulation. *Stem Cells* **25**, 2245-2256 (2007).
191. L. Balaj *et al.*, Tumour microvesicles contain retrotransposon elements and amplified oncogene sequences. *Nat Commun* **2**, 180 (2011).
192. J. Ratajczak *et al.*, Embryonic stem cell-derived microvesicles reprogram hematopoietic progenitors: evidence for horizontal transfer of mRNA and protein delivery. *Leukemia* **20**, 847-856 (2006).
193. S. Atay *et al.*, Oncogenic KIT-containing exosomes increase gastrointestinal stromal tumor cell invasion. *Proc Natl Acad Sci U S A* **111**, 711-716 (2014).
194. P. Kucharzewska *et al.*, Exosomes reflect the hypoxic status of glioma cells and mediate hypoxia-dependent activation of vascular cells during tumor development. *Proc Natl Acad Sci U S A* **110**, 7312-7317 (2013).
195. S. A. Melo *et al.*, Cancer exosomes perform cell-independent microRNA biogenesis and promote tumorigenesis. *Cancer Cell* **26**, 707-721 (2014).
196. V. Luga *et al.*, Exosomes mediate stromal mobilization of autocrine Wnt-PCP signaling in breast cancer cell migration. *Cell* **151**, 1542-1556 (2012).
197. X. Xiang *et al.*, Induction of myeloid-derived suppressor cells by tumor exosomes. *Int J Cancer* **124**, 2621-2633 (2009).

198. L. Muller, M. Mitsuhashi, P. Simms, W. E. Gooding, T. L. Whiteside, Tumor-derived exosomes regulate expression of immune function-related genes in human T cell subsets. *Sci Rep* **6**, 20254 (2016).
199. R. Mears *et al.*, Proteomic analysis of melanoma-derived exosomes by two-dimensional polyacrylamide gel electrophoresis and mass spectrometry. *Proteomics* **4**, 4019-4031 (2004).
200. G. Rappa *et al.*, Wnt interaction and extracellular release of prominin-1/CD133 in human malignant melanoma cells. *Exp Cell Res* **319**, 810-819 (2013).
201. G. Rappa, J. Mercapide, F. Anzanello, R. M. Pope, A. Lorico, Biochemical and biological characterization of exosomes containing prominin-1/CD133. *Mol Cancer* **12**, 62 (2013).
202. E. Alegre *et al.*, Circulating melanoma exosomes as diagnostic and prognosis biomarkers. *Clin Chim Acta* **454**, 28-32 (2016).
203. M. Eldh *et al.*, MicroRNA in exosomes isolated directly from the liver circulation in patients with metastatic uveal melanoma. *BMC Cancer* **14**, 962 (2014).
204. M. Ragusa *et al.*, miRNA profiling in vitreous humor, vitreal exosomes and serum from uveal melanoma patients: Pathological and diagnostic implications. *Cancer Biol Ther* **16**, 1387-1396 (2015).
205. E. Alegre *et al.*, Study of circulating microRNA-125b levels in serum exosomes in advanced melanoma. *Arch Pathol Lab Med* **138**, 828-832 (2014).
206. F. Felicetti *et al.*, Exosome-mediated transfer of miR-222 is sufficient to increase tumor malignancy in melanoma. *J Transl Med* **14**, 56 (2016).
207. S. R. Pfeffer *et al.*, Detection of Exosomal miRNAs in the Plasma of Melanoma Patients. *J Clin Med* **4**, 2012-2027 (2015).
208. H. Zhao *et al.*, Tumor microenvironment derived exosomes pleiotropically modulate cancer cell metabolism. *Elife* **5**, (2016).
209. J. Ratajczak, M. Wysoczynski, F. Hayek, A. Janowska-Wieczorek, M. Z. Ratajczak, Membrane-derived microvesicles: important and underappreciated mediators of cell-to-cell communication. *Leukemia* **20**, 1487-1495 (2006).
210. J. M. Aliotta *et al.*, Microvesicle entry into marrow cells mediates tissue-specific changes in mRNA by direct delivery of mRNA and induction of transcription. *Exp Hematol* **38**, 233-245 (2010).
211. V. A. Enriquez *et al.*, High LIN28A Expressing Ovarian Cancer Cells Secrete Exosomes That Induce Invasion and Migration in HEK293 Cells. *Biomed Res Int* **2015**, 701390 (2015).
212. I. Lazar *et al.*, Proteome characterization of melanoma exosomes reveals a specific signature for metastatic cell lines. *Pigment Cell Melanoma Res* **28**, 464-475 (2015).
213. D. Xiao *et al.*, Identifying mRNA, microRNA and protein profiles of melanoma exosomes. *PloS one* **7**, e46874 (2012).
214. S. Hao *et al.*, Epigenetic transfer of metastatic activity by uptake of highly metastatic B16 melanoma cell-released exosomes. *Exp Oncol* **28**, 126-131 (2006).
215. E. J. Ekstrom *et al.*, WNT5A induces release of exosomes containing pro-angiogenic and immunosuppressive factors from malignant melanoma cells. *Mol Cancer* **13**, 88 (2014).
216. J. L. Hood, Melanoma exosomes enable tumor tolerance in lymph nodes. *Med Hypotheses* **90**, 11-13 (2016).
217. I. Lazar *et al.*, Adipocyte Exosomes Promote Melanoma Aggressiveness through Fatty Acid Oxidation: A Novel Mechanism Linking Obesity and Cancer. *Cancer research*, (2016).
218. S. Park, E. S. Ahn, Y. Kim, Neuroblastoma SH-SY5Y cell-derived exosomes stimulate dendrite-like outgrowths and modify the differentiation of A375 melanoma cells. *Cell Biol Int* **39**, 379-387 (2015).
219. D. Xiao *et al.*, Melanoma cell-derived exosomes promote epithelial-mesenchymal transition in primary melanocytes through paracrine/autocrine signaling in the tumor microenvironment. *Cancer Lett* **376**, 318-327 (2016).
220. A. Marton *et al.*, Melanoma cell-derived exosomes alter macrophage and dendritic cell functions in vitro. *Immunol Lett* **148**, 34-38 (2012).
221. G. Zhuang *et al.*, Tumour-secreted miR-9 promotes endothelial cell migration and angiogenesis by activating the JAK-STAT pathway. *EMBO J* **31**, 3513-3523 (2012).

222. B. Psaila, R. N. Kaplan, E. R. Port, D. Lyden, Priming the 'soil' for breast cancer metastasis: the pre-metastatic niche. *Breast Dis* **26**, 65-74 (2006).
223. B. Costa-Silva *et al.*, Pancreatic cancer exosomes initiate pre-metastatic niche formation in the liver. *Nat Cell Biol* **17**, 816-826 (2015).
224. A. Chow *et al.*, Macrophage immunomodulation by breast cancer-derived exosomes requires Toll-like receptor 2-mediated activation of NF-kappaB. *Sci Rep* **4**, 5750 (2014).
225. M. Morishita *et al.*, Quantitative analysis of tissue distribution of the B16BL6-derived exosomes using a streptavidin-lactadherin fusion protein and iodine-125-labeled biotin derivative after intravenous injection in mice. *J Pharm Sci* **104**, 705-713 (2015).
226. Y. Takahashi *et al.*, Visualization and in vivo tracking of the exosomes of murine melanoma B16-BL6 cells in mice after intravenous injection. *J Biotechnol* **165**, 77-84 (2013).
227. Y. Liu *et al.*, Tumor Exosomal RNAs Promote Lung Pre-metastatic Niche Formation by Activating Alveolar Epithelial TLR3 to Recruit Neutrophils. *Cancer Cell* **30**, 243-256 (2016).
228. C. Federici *et al.*, Exosome release and low pH belong to a framework of resistance of human melanoma cells to cisplatin. *PloS one* **9**, e88193 (2014).
229. K. G. Chen *et al.*, Melanosomal sequestration of cytotoxic drugs contributes to the intractability of malignant melanomas. *Proc Natl Acad Sci U S A* **103**, 9903-9907 (2006).
230. M. C. Boelens *et al.*, Exosome transfer from stromal to breast cancer cells regulates therapy resistance pathways. *Cell* **159**, 499-513 (2014).
231. K. B. Challagundla *et al.*, Exosome-mediated transfer of microRNAs within the tumor microenvironment and neuroblastoma resistance to chemotherapy. *J Natl Cancer Inst* **107**, (2015).
232. K. A. Hyun, J. Kim, H. Gwak, H. I. Jung, Isolation and enrichment of circulating biomarkers for cancer screening, detection, and diagnostics. *Analyst* **141**, 382-392 (2016).
233. M. Logozzi *et al.*, High levels of exosomes expressing CD63 and caveolin-1 in plasma of melanoma patients. *PloS one* **4**, e5219 (2009).
234. S. A. Melo *et al.*, Glypican-1 identifies cancer exosomes and detects early pancreatic cancer. *Nature* **523**, 177-182 (2015).
235. C. Thery, Cancer: Diagnosis by extracellular vesicles. *Nature* **523**, 161-162 (2015).
236. Y. Fujita *et al.*, Intercellular communication by extracellular vesicles and their microRNAs in asthma. *Clin Ther* **36**, 873-881 (2014).
237. H. Saari *et al.*, Microvesicle- and exosome-mediated drug delivery enhances the cytotoxicity of Paclitaxel in autologous prostate cancer cells. *J Control Release* **220B**, 727-737 (2015).
238. S. Viaud *et al.*, Dendritic cell-derived exosomes for cancer immunotherapy: what's next? *Cancer research* **70**, 1281-1285 (2010).
239. G. Odorizzi, M. Babst, S. D. Emr, Fab1p PtdIns(3)P 5-kinase function essential for protein sorting in the multivesicular body. *Cell* **95**, 847-858 (1998).
240. T. J. Myers *et al.*, Mitochondrial reactive oxygen species mediate GPCR-induced TACE/ADAM17-dependent transforming growth factor-alpha shedding. *Mol Biol Cell* **20**, 5236-5249 (2009).
241. M. Guescini *et al.*, Microvesicle and tunneling nanotube mediated intercellular transfer of g-protein coupled receptors in cell cultures. *Exp Cell Res* **318**, 603-613 (2012).
242. G. Pironti *et al.*, Circulating Exosomes Induced by Cardiac Pressure Overload Contain Functional Angiotensin II Type 1 Receptors. *Circulation* **131**, 2120-2130 (2015).
243. C. J. Locke *et al.*, Controlled exosome release from the retinal pigment epithelium in situ. *Exp Eye Res* **129**, 1-4 (2014).
244. S. Pant, H. Hilton, M. E. Burczynski, The multifaceted exosome: biogenesis, role in normal and aberrant cellular function, and frontiers for pharmacological and biomarker opportunities. *Biochemical pharmacology* **83**, 1484-1494 (2012).
245. M. Fernandez-Borja *et al.*, Multivesicular body morphogenesis requires phosphatidyl-inositol 3-kinase activity. *Curr Biol* **9**, 55-58 (1999).
246. C. Subra *et al.*, Exosomes account for vesicle-mediated transcellular transport of activatable phospholipases and prostaglandins. *Journal of lipid research* **51**, 2105-2120 (2010).
247. O. T. Fackler, R. Grosse, Cell motility through plasma membrane blebbing. *The Journal of cell biology* **181**, 879-884 (2008).

248. O. M. Lucero, D. W. Dawson, R. T. Moon, A. J. Chien, A re-evaluation of the "oncogenic" nature of Wnt/beta-catenin signaling in melanoma and other cancers. *Curr Oncol Rep* **12**, 314-318 (2010).
249. J. N. Higginbotham *et al.*, Amphiregulin exosomes increase cancer cell invasion. *Curr Biol* **21**, 779-786 (2011).
250. D. G. Nguyen, A. Booth, S. J. Gould, J. E. Hildreth, Evidence that HIV budding in primary macrophages occurs through the exosome release pathway. *J Biol Chem* **278**, 52347-52354 (2003).
251. D. Xu, H. Tahara, The role of exosomes and microRNAs in senescence and aging. *Adv Drug Deliv Rev* **65**, 368-375 (2013).
252. S. P. Shah *et al.*, The clonal and mutational evolution spectrum of primary triple-negative breast cancers. *Nature* **486**, 395-399 (2012).
253. J. L. Teh *et al.*, Metabotropic glutamate receptor 1 disrupts mammary acinar architecture and initiates malignant transformation of mammary epithelial cells. *Breast Cancer Res Treat* **151**, 57-73 (2015).
254. C. L. Speyer *et al.*, Metabotropic glutamate receptor-1: a potential therapeutic target for the treatment of breast cancer. *Breast Cancer Res Treat* **132**, 565-573 (2012).
255. Z. Kan *et al.*, Diverse somatic mutation patterns and pathway alterations in human cancers. *Nature* **466**, 869-873 (2010).
256. N. Cancer Genome Atlas Research, Comprehensive genomic characterization defines human glioblastoma genes and core pathways. *Nature* **455**, 1061-1068 (2008).
257. L. D. Wood *et al.*, The genomic landscapes of human breast and colorectal cancers. *Science* **318**, 1108-1113 (2007).
258. T. Sjoblom *et al.*, The consensus coding sequences of human breast and colorectal cancers. *Science* **314**, 268-274 (2006).
259. N. Stransky *et al.*, The mutational landscape of head and neck squamous cell carcinoma. *Science* **333**, 1157-1160 (2011).
260. S. Durinck *et al.*, Temporal dissection of tumorigenesis in primary cancers. *Cancer Discov* **1**, 137-143 (2011).
261. D. W. Parsons *et al.*, An integrated genomic analysis of human glioblastoma multiforme. *Science* **321**, 1807-1812 (2008).
262. K. S. Brocke *et al.*, Glutamate receptors in pediatric tumors of the central nervous system. *Cancer Biol Ther* **9**, 455-468 (2010).
263. C. Frati *et al.*, Expression of functional mGlu5 metabotropic glutamate receptors in human melanocytes. *J Cell Physiol* **183**, 364-372 (2000).
264. K. Y. Choi, K. Chang, J. M. Pickel, J. D. Badger, 2nd, K. W. Roche, Expression of the metabotropic glutamate receptor 5 (mGluR5) induces melanoma in transgenic mice. *Proc Natl Acad Sci U S A* **108**, 15219-15224 (2011).
265. N. Pissimissis, E. Papageorgiou, P. Lembessis, A. Armakolas, M. Koutsilieris, The glutamatergic system expression in human PC-3 and LNCaP prostate cancer cells. *Anticancer Res* **29**, 371-377 (2009).
266. S. Y. Park *et al.*, Clinical significance of metabotropic glutamate receptor 5 expression in oral squamous cell carcinoma. *Oncol Rep* **17**, 81-87 (2007).
267. N. Kalariti, P. Lembessis, E. Papageorgiou, N. Pissimissis, M. Koutsilieris, Regulation of the mGluR5, EAAT1 and GS expression by glucocorticoids in MG-63 osteoblast-like osteosarcoma cells. *J Musculoskelet Neuronal Interact* **7**, 113-118 (2007).
268. M. D'Onofrio *et al.*, Pharmacological blockade of mGlu2/3 metabotropic glutamate receptors reduces cell proliferation in cultured human glioma cells. *J Neurochem* **84**, 1288-1295 (2003).
269. A. Arcella *et al.*, Pharmacological blockade of group II metabotropic glutamate receptors reduces the growth of glioma cells in vivo. *Neuro Oncol* **7**, 236-245 (2005).
270. T. D. Prickett, Y. Samuels, Molecular pathways: dysregulated glutamatergic signaling pathways in cancer. *Clin Cancer Res* **18**, 4240-4246 (2012).
271. H. J. Chang *et al.*, Metabotropic glutamate receptor 4 expression in colorectal carcinoma and its prognostic significance. *Clin Cancer Res* **11**, 3288-3295 (2005).

272. L. Iacovelli *et al.*, Pharmacological activation of mGlu4 metabotropic glutamate receptors inhibits the growth of medulloblastomas. *J Neurosci* **26**, 8388-8397 (2006).
273. J. L. Esseltine *et al.*, Somatic mutations in GRM1 in cancer alter metabotropic glutamate receptor 1 intracellular localization and signaling. *Mol Pharmacol* **83**, 770-780 (2013).

Group	GRM	Cancer	References
I	GRM1	Malignant Melanoma	(*45, 58, 59*)
		Breast Cancer	(*252-254*)
		Lung	(*255*)
		Ovary	(*256*)
		Large Intestine	(*256-258*)
		Upper Aerodigestive Tract	(*259, 260*)
		Astrocytoma	(*261*)
		Glioma	(*262*)
		Medulloblastoma	(*262*)
	GRM5	Malignant Melanoma	(*263, 264*)
		Prostate	(*265*)
		Oral Squamous Cell Carcinoma	(*266*)
		Osteosarcoma	(*267*)
		Glioma	(*262*)
		Medulloblastoma	(*262*)
II	GRM2	Glioma	(*268, 269*)
		Prostate	(*265*)
	GRM3	Glioma	(*268, 269*)
		Malignant Melanoma	(*270*)
III	GRM4	Colorectal Carcinoma	(*271*)
		Glioma	(*262*)
		Malignant Melanoma	(*271*)
		Squamous Cell Carcinoma	(*271*)
		Medulloblastoma	(*272*)
	GRM6	Glioma	(*262*)
		Medulloblastoma	(*262*)
	GRM7	N/A	
	GRM8	Malignant Melanoma	(*264, 270*)

Table 1: Metabotropic glutamate receptors (GRMs) and associated malignancies. Adapted from (*43, 270, 273*)

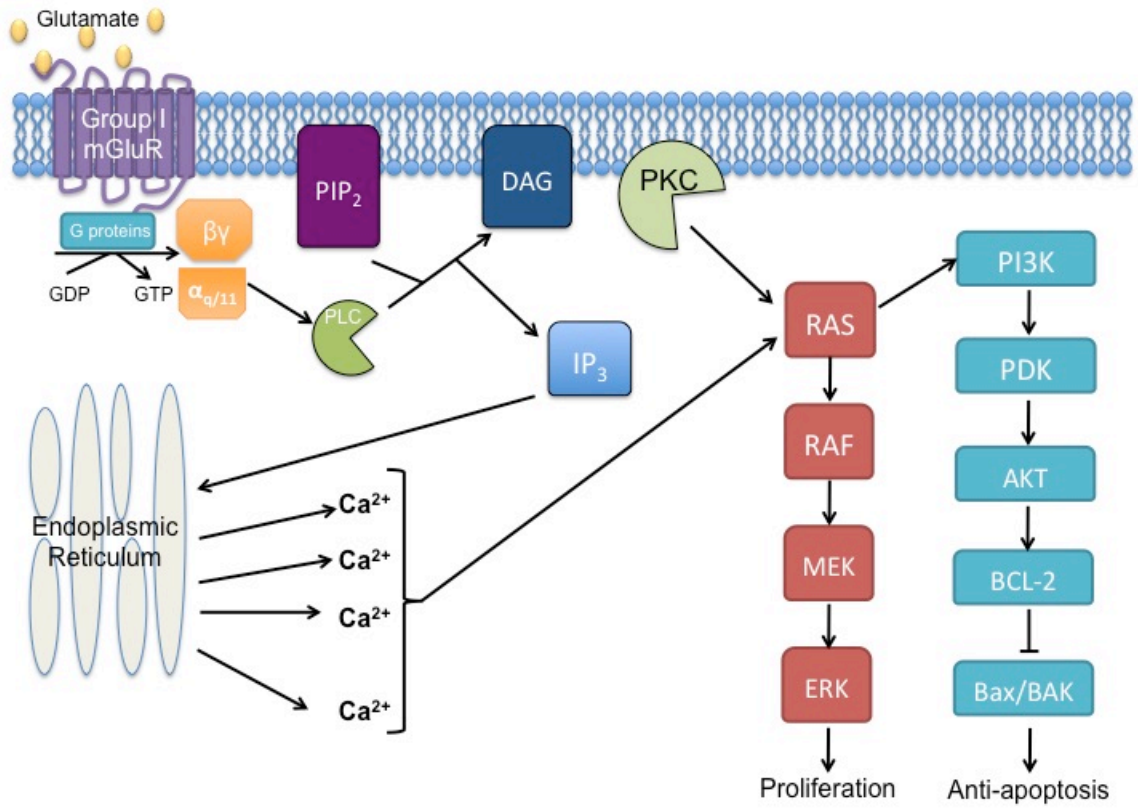

Figure 1: Proposed signal transduction cascade initiated by activated GRM1
A summary of the proposed signal cascade mediated by GRM1 in tumor development and progression

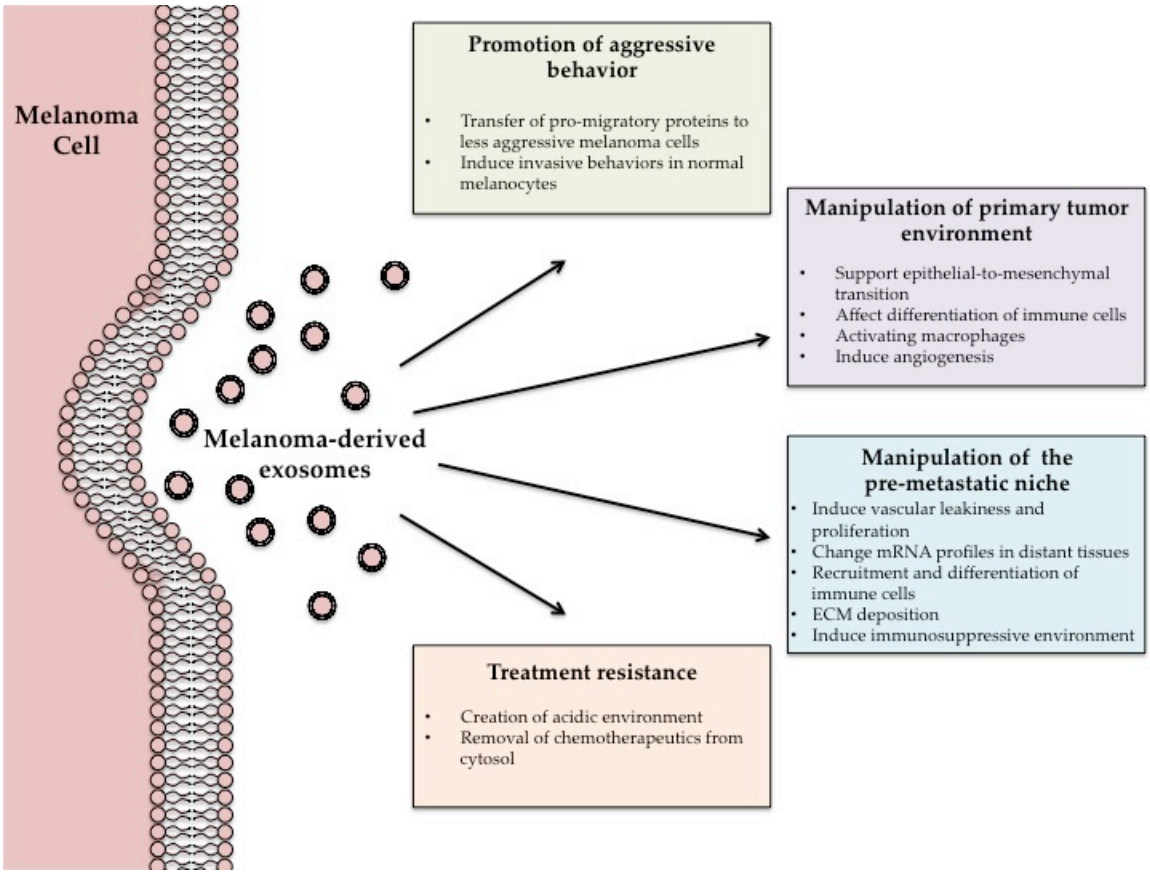

Figure 2: Roles of Exosomes in Tumor Development and Progression
A summary of the proposed roles/functions mediated by melanoma exosomes in tumor development and progression

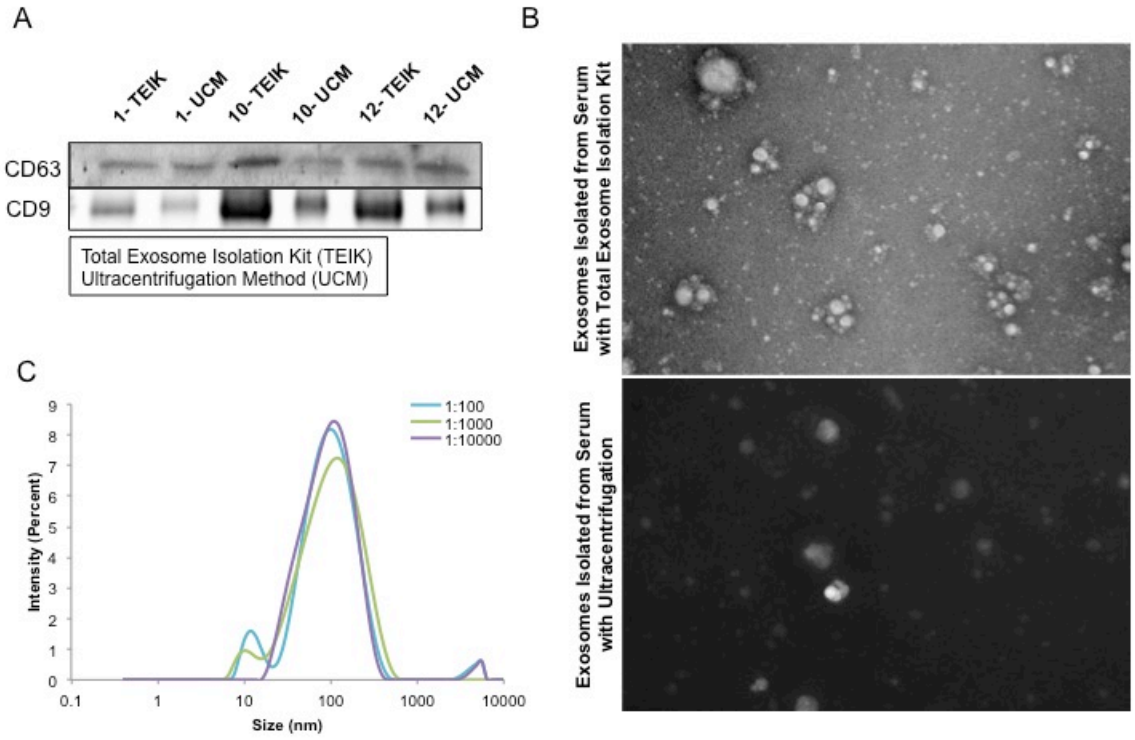

Figure 3: Exosome Isolation Method
(A) Samples are plasma exosome lysates (SEL) from identical volumes of plasma from untreated SKH-1 mice, where the Total Exosome Isolation Kit (Invitrogen) (TEIK) was compared to the Ultracentrifugation Method (UM). Number indicates mouse identification number. (B) Plasma exosome samples were run on the Zetasizer to determine the particle sizes present, each curve representing a 1:100 (red), 1:1000 (green) and a 1:10,000 (blue) dilution. (C) Electron micrographs of samples isolate by either the total exosome isolation kit or ultracentrifugation show intact exosomes of the correct size in both samples. Although, a higher level of background protein staining was observed in the samples isolated with the ultracentrifugation method, as seen here by the dark background.

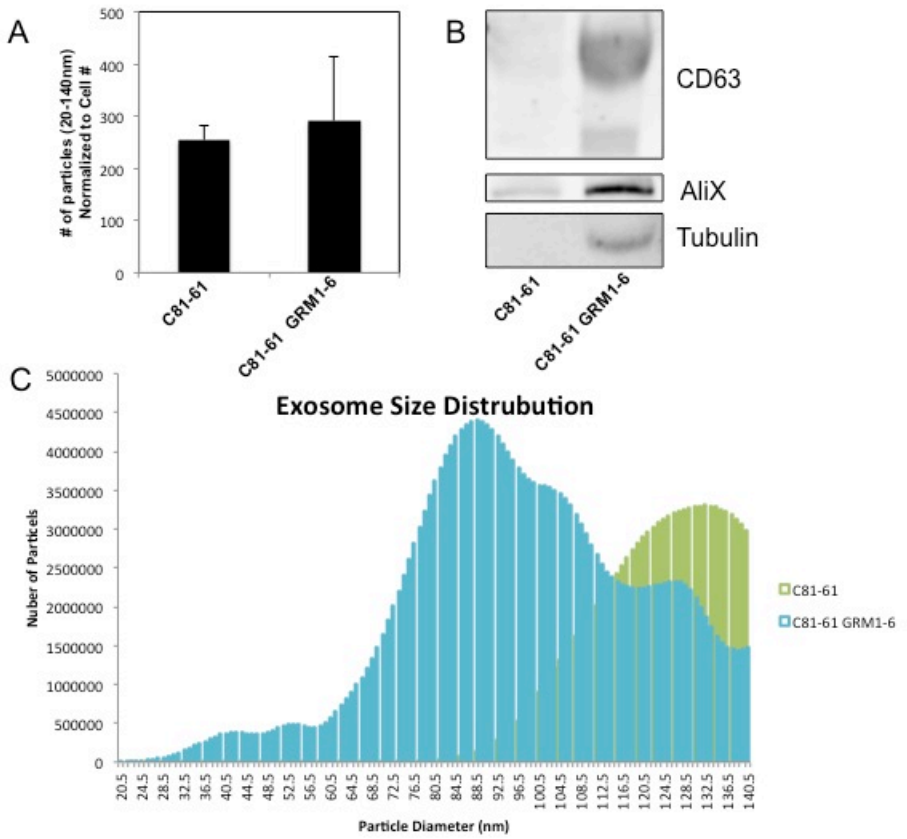

Figure 4: GRM1 expression results in exosome size distribution change
Nanosight analysis of exosomes isolated from C81-61 GRM1-6 show an increase in number when compared to C81-61, however, when normalized to cell number, the difference in exosome number is negligible (A). Immunoblots show an increase in exosome protein markers in C81-61 GRM1-6 when compared to C81-61, however, when normalized to tubulin, the increase is dampened to an insignificant amount (B). Nanosight analysis indicates a shift in size of exosomes released by cells expressing GRM1. Exosomes isolated from C81-61 GRM1-6 conditioned media show a smaller average size when compared to the parental C81-61 exosomes (C).

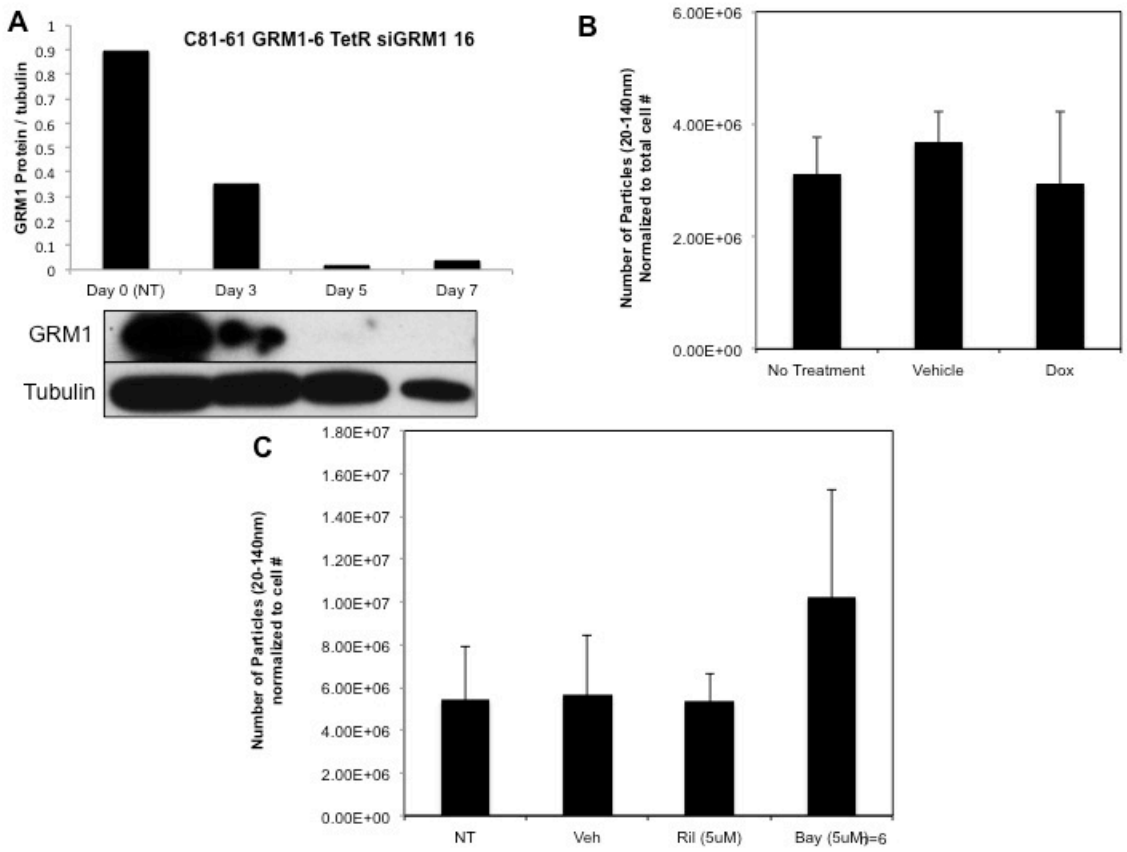

Figure 5: Exosome levels are unchanged with varying levels of GRM1 protein and when treated with GRM1 inhibitors

Western blot showing a reduction in GRM1 protein with treatment of doxycycline (10ng/ml) (A). Nanoparticle Tracking Analysis of exosomes isolated from the media conditioned by C81-61 GRM1-6 TetR siGRM1 cells after 48 hours (n=3)(B). Nanosight analysis of exosomes isolated from C81-61 GRM1-6 cells treated with either riluzole or Bay36-7620 (n=6) (C).

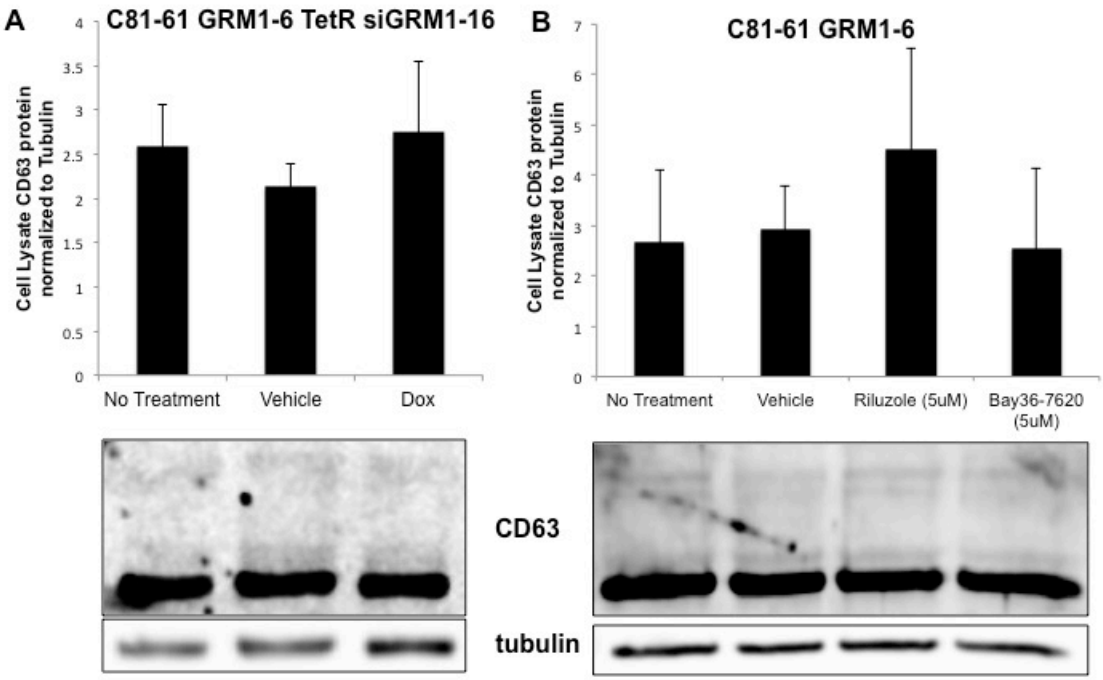

Figure 6: Levels of intracellular CD63 protein in melanoma cells are unaffected by treatment

Immunoblots for CD63 protein were performed on the cell lysates of melanoma cells with various treatments and normalized to tubulin protein levels. C81-61 GRM1-6 TetR siGRM1 – 16 cells were treated with vehicle control (DMSO) or Doxycycline and no differences were seen in the amount of CD63 protein present in the cell (n=3)(A). C81-61 GRM1-6 cells were treated with vehicle control (DMSO), 5uM riluzole or 5uM Bay36-7620, and no differences were observed in the CD63 protein levels (n=3)(B).

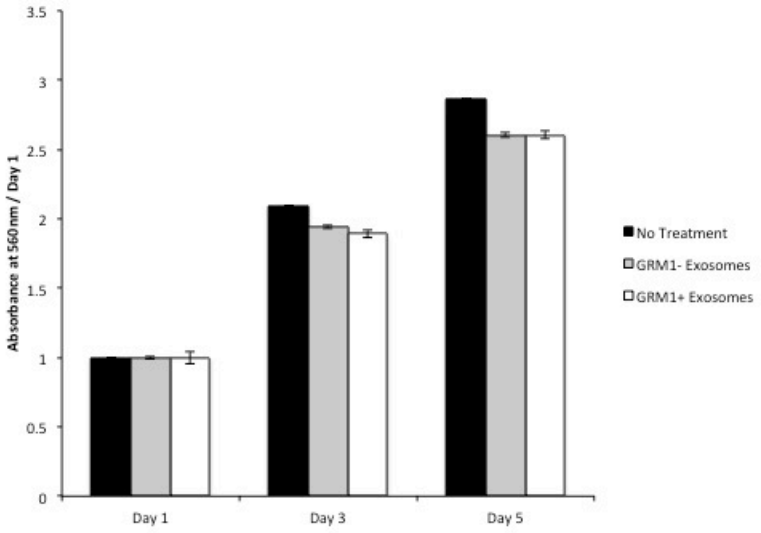

Figure 7: Cell Proliferation Assay
C81-61 cells were incubated with conditioned media from C81-61 or C81-61 GRM1-6 cells and cell proliferation was measured using the MTT cell proliferation assay. Cell proliferation was unaffected by conditioned media from the 2 cell lines on Day 1, 3 and 5 of incubation (n=3).

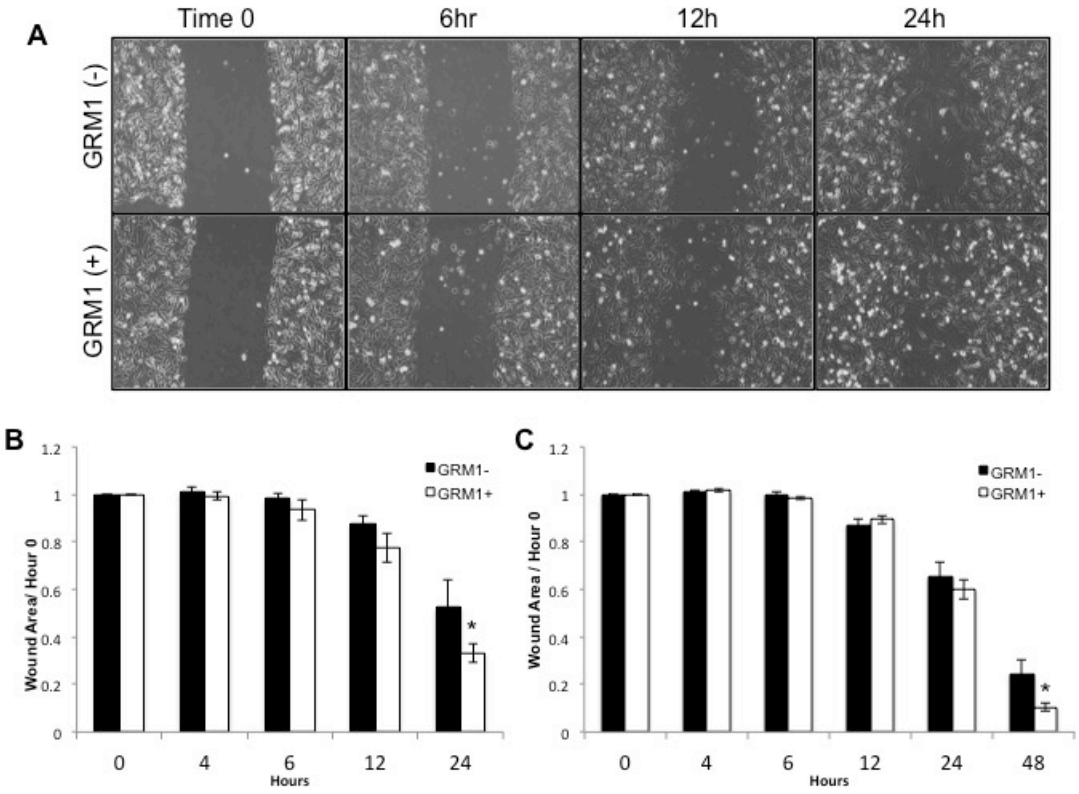

Figure 8: GRM1- cells exhibit increased mobility when exposed to GRM1+ cell derived exosomes

C81-61 melanoma cells (GRM1-) were incubated with conditioned media from either C81-61 (GRM1-) cells or C81-61 GRM1-6 (GRM1+) cells, a scratch was made in the confluent cell layer, and photographs were taken at various time points (A). Wound area was calculated using ImageJ, and normalized to the size of the original wound (Time 0). A significant reduction in wound size was observed in the cells incubated with exosomes derived from C81-61 GRM1-6 ($p=0.02$, $n=4$) (B). Wound healing assay was also performed using C81-61 cells incubated with purified exosomes from either C81-61 (GRM1-) cells or C81-61 GRM1-6 (GRM1+) cells. After 48 hours post-wound, a significant reduction was seen in the cells incubated with purified exosomes derived from C81-61 GRM1-6 (GRM1+) cells ($p=0.014$, $n=3$) (C).

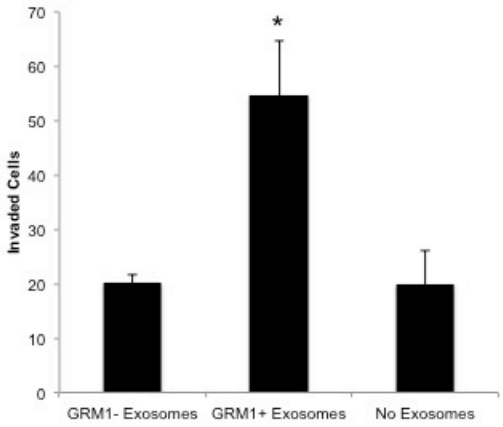

Figure 9: Exosomes released from GRM1+ cells induce invasion in GRM1- cells

Migration of C81-61 cells incubated with exosomes released from C81-61 cells (GRM1- exosomes), C81-61 GRM1-6 cells (GRM1+ exosomes) or no exosomes. Results of a representative experiment show the number of cells in 10 random fields. The number of cells invaded when incubated with exosomes from C81-61 GRM1-6 is significantly higher than those incubated with exosomes from C81-61 cells ($p=0.016$, $n=4$).

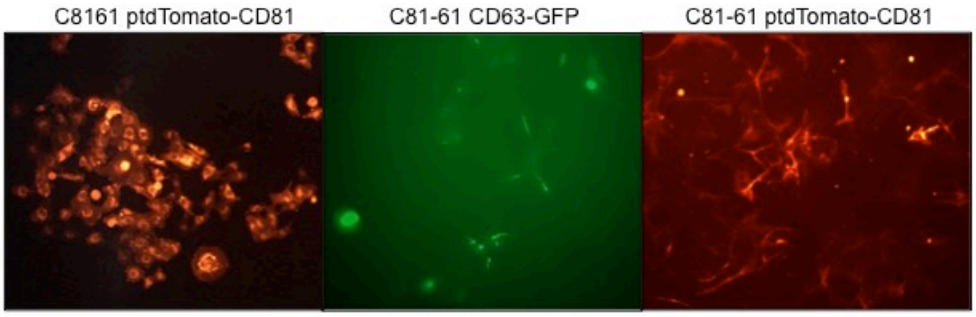

Figure 10: Cells have been stably transfected with either CD63-GFP or ptdTomato-CD81
The Keyence BZ-X710 florescent microscope was used to confirm the presence of GFP or ptdTomato florescent tags in stably transfected C81-61 ptdTomato-CD81, C8161 ptdTomato-CD81 and C81-61 CD63-GFP

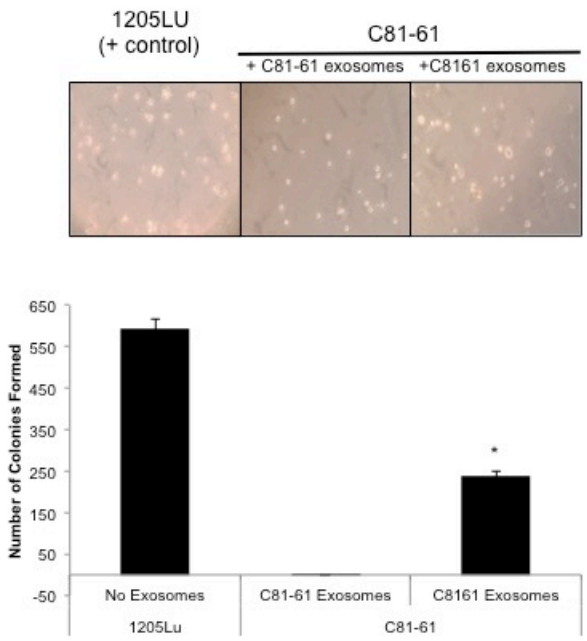

Figure 11: Exosomes from GRM1^{+} cells induce colony formation in non-tumorigenic, GRM1^{-} cells

Cells were photographed after 21 days of growth in soft agar and exosomes. 1205Lu serves as a positive control. C81-61 CD63-GFP cells were plated in media with 0.33% agarose and incubated with either C8161 ptdTomato-CD81 exosomes that show significant number of colony formation, or with C81-61 ptdTomato-CD81 exosomes that only show two colonies (n=4, t-test, p=0.0000005).

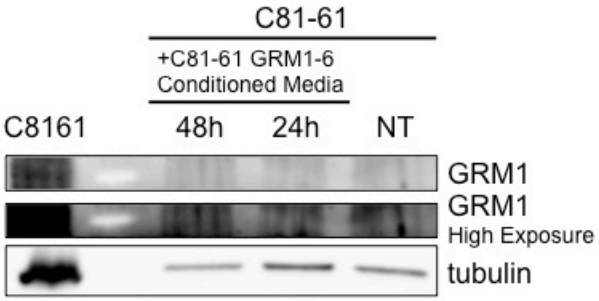

Figure 12. GRM1 protein is not transferred from exosomes to recipient cells
Western blot with GRM1 antibody of washed cell lysates of C81-61 cells incubated with conditioned media from C81-61 GRM1-6 cells.

GMNDR -	ACC ATA CAA AAC CAC AAT ATC C
GMNDD -	GTT GAG TGA TGA CAT CAT ACT C
HZOB2 -	CTC CCT GAC TCT CTC TCA TTG TCT TG

Table 2: TGS genotyping
Sequences of primers used to determine the genotype of TGS mice. GMNDR and GMNDD amplified the wild type copy of the GRM1 gene in the genome of the mouse. GMNDD and HZOB2 amplified a portion of the transgene, indicating the presence of the GRM1 gene mutation resulting in aberrant expression.

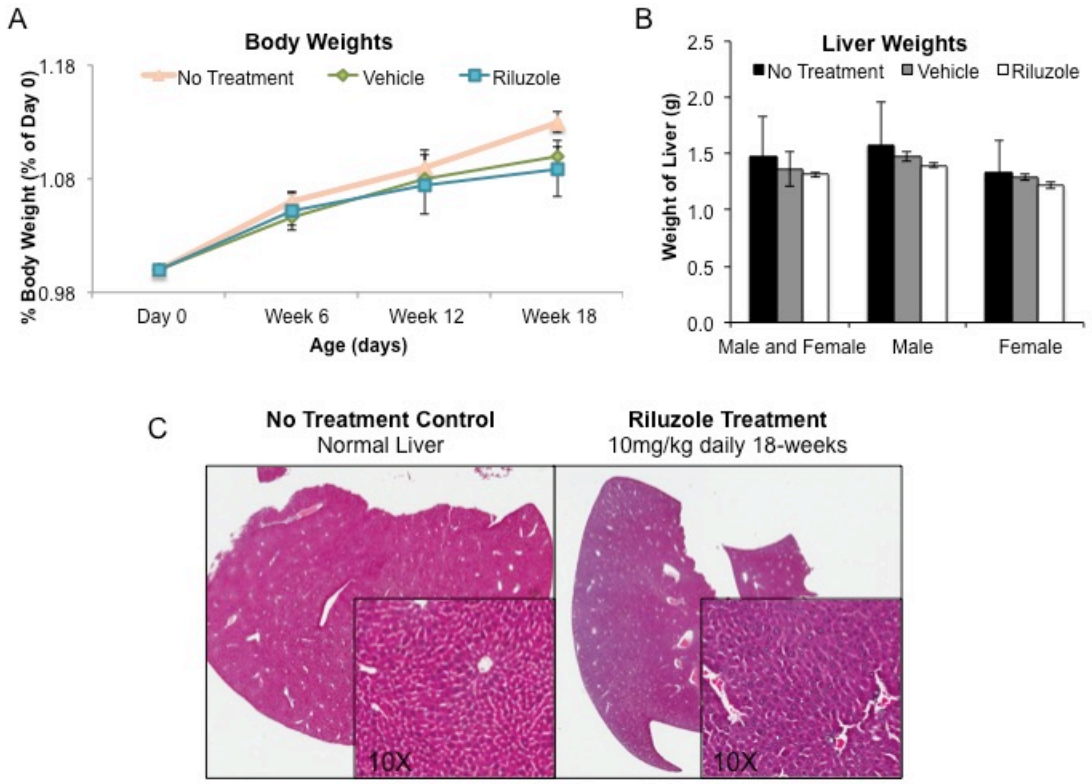

Figure 13: No apparent toxicity due to daily treatment with riluzole
Body weights were monitored throughout treatment with 10mg/kg riluzole and no significant differences in weight were observed as a result of treatment (A). At necropsy, livers were weighed and preserved for histology. No significant weight differences were observed with treatment (B), and no histological abnormalities indicating toxicities were observed (C).

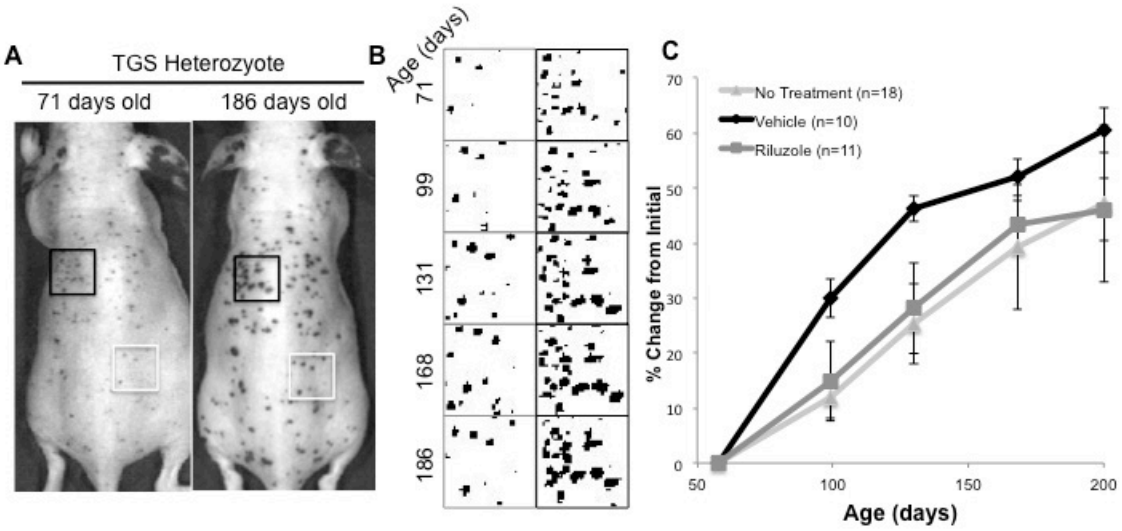

Figure 14: Riluzole treatment results in no change in tumor area growth
Images were taken of a TGS heterozygote at 71 days (Left) and 186 days old (right) (A). An example diagram of converted binary images of consistent chosen TGS lesion throughout treatment is shown (B). 5 individual skin lesions were selected and quantified. Values were graphed as percent change in lesion area (from initial) of TGS mice treated oral gavage daily with 10mg/kg riluzole, vehicle and no treatment controls (C).

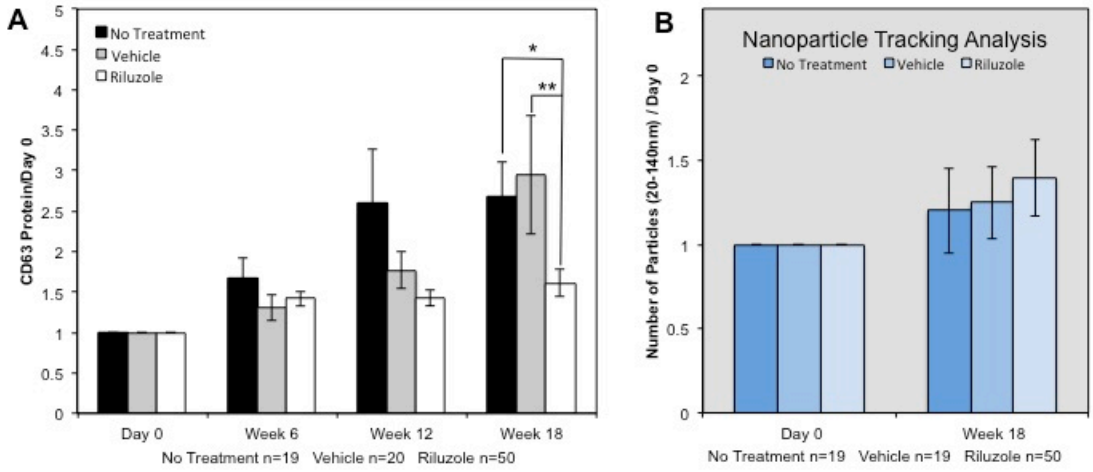

Figure 15: Riluzole treatment of TGS mice results in a reduction of CD63 protein in circulating exosomes

Protein lysates of plasma exosomes from untreated, vehicle treated and riluzole treated (15mg/kg) TGS mice were analyzed by western immunoblot at various timepoints for CD63 (A). A significant decrease in CD63 protein was observed after 18 weeks of riluzole treatment when compared to vehicle treatment ($p=0.0007$) or no treatment ($p=0.01$) controls. Nanoparticle tracking analysis shows no detectable differences in particle number in the exosome size range (20-140nm) with treatment compared to controls (E).

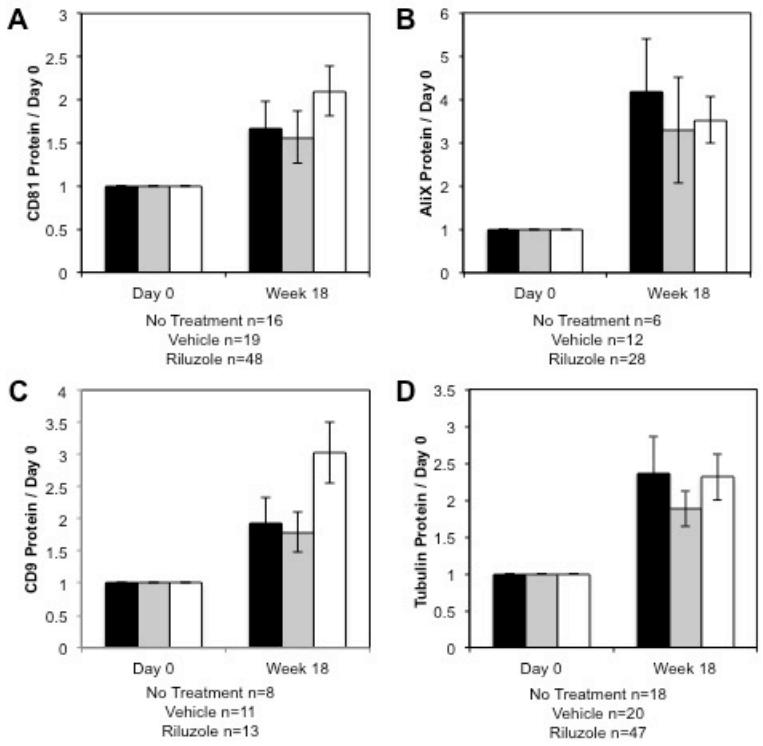

Figure 16: Alternative exosome protein markers show no change in plasma exosome lysates of TGS mice

Protein lysates of plasma exosomes from untreated, vehicle treated and riluzole treated (15mg/kg) TGS mice were analyzed by western immunoblot at various timepoints for (A) CD81, (B) AliX, (C) CD9 and (D) Tubulin. No significant change was seen in the exosome protein markers.

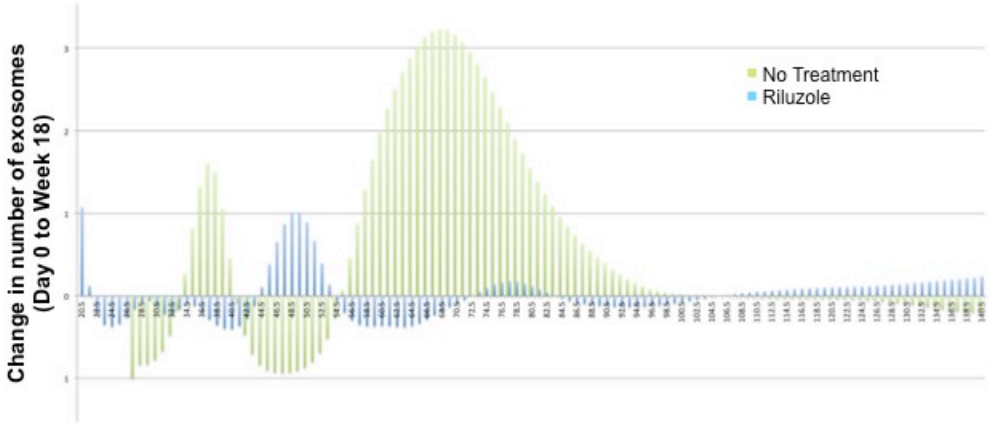

Figure 17: Change in size distribution of plasma exosomes with treatment. Nanosight analysis indicates a change in the size alterations of exosomes isolates from the plasma of TGS mice treated daily for 18 weeks when compared to the no treatment TGS control.

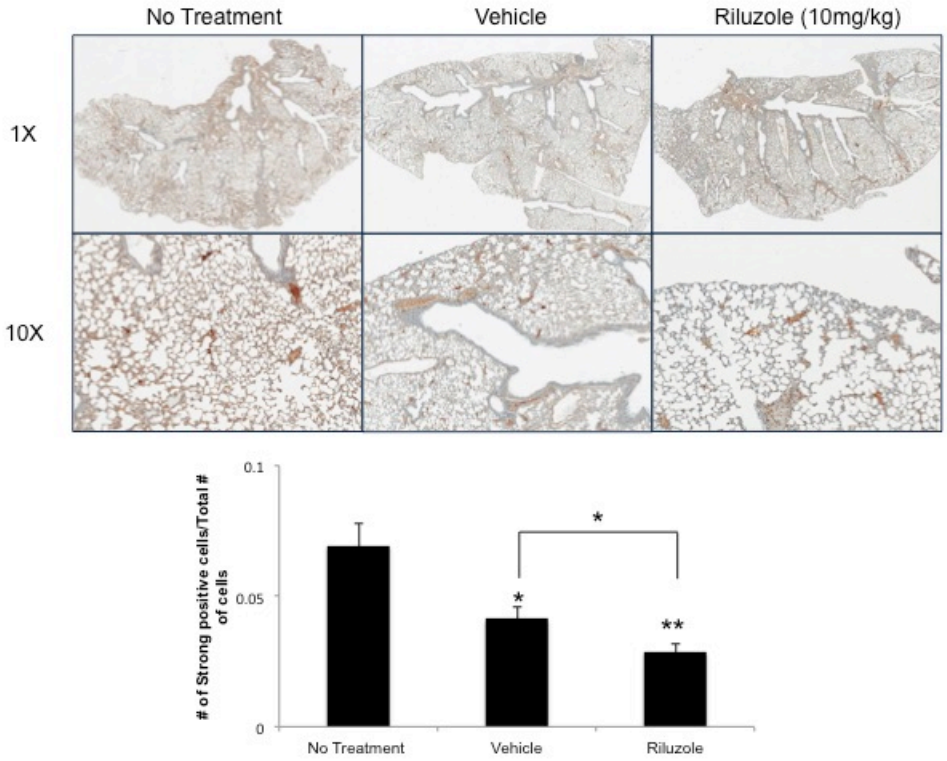

Figure 18: Reduction in fibronectin deposition with treatment.
Lungs from TGS animals treated with riluzole and vehicle were compared to untreated TGS. The lungs were fixed and incubated with an antibody to a marker of pre-metastatic niche formation, fibronectin. A significant reduction in fibronectin staining was seen in both vehicle (n=6, $p<0.05$) and riluzole (n=6, $p<0.000005$) treated samples when compared to no treatment. A significant reduction was observed between riluzole and vehicle (n=6, $p<0.05$).

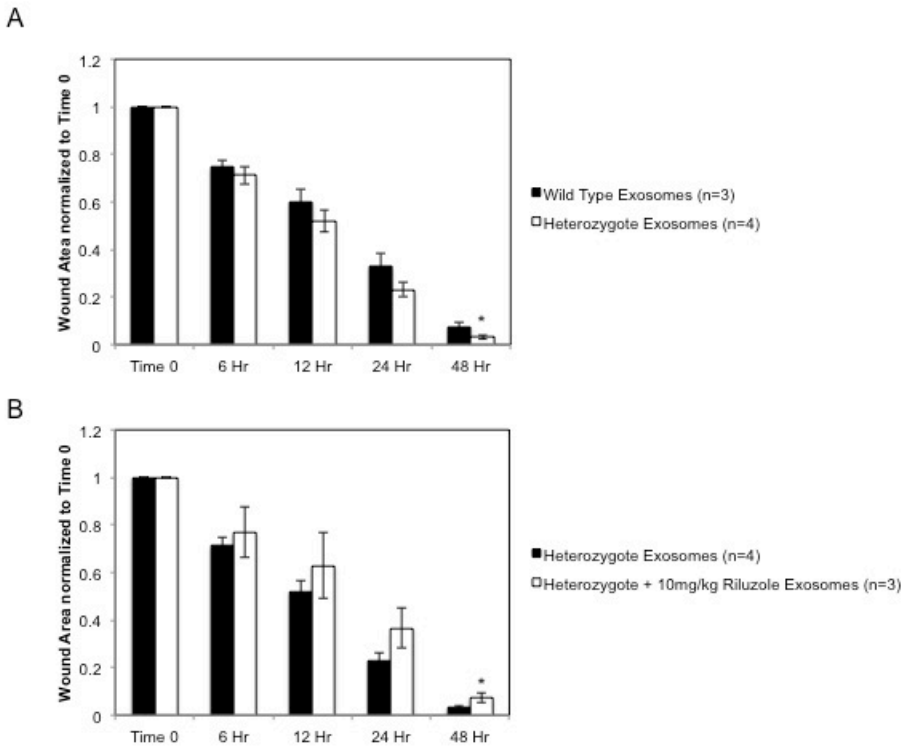

Figure 19: Exosomes isolated from heterozygous TGS mouse plasma induce migration in GRM1- cells

Migration assay performed on C81-61 ($GRM1^-$) cells pretreated with exosomes isolated from the blood plasma of TGS mice of Wild Type or Heterozygous genotypes at 200 days old. A reduction in wound size was seen in the C81-61 cells incubated with exosomes from heterozygous mice after 48 hours ($p = 0.08$) (A). Exosomes were isolated from plasma after 18 weeks of 10mg/kg riluzole treatment of heterozygous TGS mice. C81-61 cells showed an increase in wound size when incubated with exosomes from riluzole treated TGS heterozygotes ($p < 0.1$).